Canadian Technical Report of
Hydrography and Ocean Sciences 221

2002

Modelling System for Tides for the Northwest Atlantic Coastal Ocean

by

F. Dupont, C. G. Hannah, D. A. Greenberg, J. Y. Cherniawsky[1] and C. E. Naimie[2]

Coastal Ocean Science Section
Ocean Sciences Division
Maritimes Region
Fisheries and Oceans Canada

Bedford Institude of Oceanography
P.O. Box 1006, Dartmouth, N.S.
Canada B2Y 4A2

[1]Ocean Science and Productivy Division, Institute of Ocean Sciences Sidney, B.C., Canada

[2]Dartmouth College, Hanover, New Hamsphire, USA

Cat. No. Fs 97-18/221E ISSN 0711-6764

Correct citation for this publication:

Dupont, F., C. G. Hannah, D. A. Greenberg, J. Y. Cherniawsky and C. E. Naimie. 2002. Modelling System for Tides. Can. Tech. Rep. Hydrogr. Ocean Sci. 221: vii + 72 pp.

Table of Contents

List of Figures

List of Tables

Abstract

Dupont, F., C. G. Hannah, D. A. Greenberg, J. Y. Cherniawsky and C. E. Naimie. 2002. Modelling System for Tides. Can. Tech. Rep. Hydrogr. Ocean Sci. 221: vii + 72 pp.

We assimilated Topex-Poseidon tidal observations into a finite element model of the northwest Atlantic. The modelling system consists of running a forward time-stepping nonlinear model that predicts the tides and a linear inverse model that computes the elevation boundary conditions that minimize the difference between the selected observations and the model predictions. In the coastal zone, we achieve an accuracy of 4-5 cm for M2 and 2-3 cm for the other constituents (outside of the Gulf of Maine and Bay of Fundy). On the shelf and offshore the system is capable of an accuracy of 2 to 3 cm per constituent. A goal of 10 cm accuracy along the coast was ascribed to this system based on a vision of what is required for future applications. The analysis indicates that the 10 cm prediction error is being achieved in Labrador, Newfoundland, the Atlantic coast of Nova Scotia, parts of the Gulf of St. Lawrence and the offshore and shelf regions. The prediction errors are generally of the order of 6 cm offshore, and between 5 to 10 cm along the coast. The prediction error increases in the Gulf of Maine and reaches 60 cm in the Bay of Fundy. The addition of SA and SSA to the predictive system improves the prediction by 0-2 cm.

Résumé

Dupont, F., C. G. Hannah, D. A. Greenberg, J. Y. Cherniawsky and C. E. Naimie. 2002. Modelling System for Tides. Can. Tech. Rep. Hydrogr. Ocean Sci. 221: vii + 72 pp.

Nous avons assimilé des observations de marée du satellite Topex-Poseidon dans un modèle aux éléments finis de l'Atlantique Nord-Ouest. Le système de modélisation comprend un modèle non linéaire que l'on intégre en avant dans le temps et qui fait la prévision de marée et d'un modèle linéraire inverse harmonique qui calcule la condition frontière d'élévation qui minimise la différence entre une selection d'observations et la prévision du modèle. Dans les régions côtières, nous avons obtenu une précision de 4-5 cm pour M2 and 2-3 cm pour les autres constituantes (en dehors du golfe du Maine et de la baie de Fundy). Sur le plateau continental et en mer, le système est capable d'une précision de 2 à 3 cm par constituantes. Un niveau d'erreur de 10 cm est requis basé sur une estimation de la précision exigée pour des applications futures. L'analyse indique qu'un niveau d'erreur de 10 cm pour les prévisions est atteint dans les régions côtières du Labrador, Terre-Neuve, de la Nouvelle-Écosse, une partie du golfe du Saint Laurent et en mer. En mer, l'erreur de prévision est de 6 cm, et entre 5 et 10 cm le long des côtes. Cette erreur augmente dans le golfe du Maine et atteint 60 cm dans la baie de Fundy. L'addition de SA et SSA au système prédictif améliore le résultat de 0-2 cm.

1 Introduction

A tidal prediction system for the northwest Atlantic coastal ocean from Davis Strait to Cape Cod has been developed. The system integrates a high-resolution numerical tidal model with observational sea level datasets and creates spatially varying predictions of tidal elevation and currents for the whole region. The system is based on the finite element method with variable spatial resolution. This allows the upper Bay of Fundy and many inlets to be included in the regional model. Overall the spatial resolution of the model mesh varies from about 2 km to 50 km.

The simulations reported here assimilate tidal constituents derived from Topex-Poseidon (TP) altimetry. The TP data has broad spatial coverage and the self consistent time reference allows an independent check on the timing information in the archived coastal tide gauge data. This report focuses on the modelling of the five major tidal constituents (M2, N2, S2, K1, and O1). These constituents arise from the analysis of the coastal gauge data (see Appendix A). The model simulations are tested against all available coastal tide gauge data and offshore pressure data. The comparisons are done by looking at amplitude and phase errors for each constituent and by comparing the *rms* error in a 1 year time series. Our goal is to achieve prediction error levels less than 10 cm along the coast. This value comes from the Canadian Hydrographic Service (CHS) vision of what is required for future applications of tidal models. The difficulty is to achieve this number in the Gulf of Maine and Bay of Fundy system where the semi-diurnal tidal constituents are resonant.

The annual (SA) and semi-annual (SSA) variations in water level are not astronomical tides and so cannot be modelled by the tidal modelling system. Spatially explicit estimates of SA and SSA are created using optimal estimation and evaluated for inclusion in the tidal prediction system.

There have been many tidal models developed for portions of the Northwest Atlantic Ocean. Table 1 contains a partial list of publications related to such models. In additions, the tides in the Gulf of St. Lawrence are being modelled as part of the operational forecast model developed by Francois Saucier (IML) and the forecasts are available on the web at `www.osl.gc.ca`. All of these models are limited in terms of geographic coverage and many only consider 1 or 2 tidal constituents. Other tidal models have been developed as part of other projects but never published. For example, the ocean modelling group at Dalhousie University has done some work with a large-scale tidal models as part of their storm surge research but the tidal model results have not been published.

Han et al. (2000), Han (2000) and Xu et al. (2001) used TP data in their tidal models of the Newfoundland shelf. The inverse model used here is similar to that of Xu et al. (2001), the primary difference is that Xu et al. (2001) only consider linear dynamics and a single constituent whereas our modelling system constructs the non-linear inverse for multiple constituents. Han (2000) used the same 5 constituents as we do but derived his boundary conditions directly from TP data using optimal estimation. Han et al. (2000) only consider the M2 constituent and do the assimilation by inserting the TP data directly into the interior of the model using a nudging technique.

Gulf of Maine and Bay of Fundy	Greenberg (1979), Lynch and Naimie (1993);
Scotian Shelf	de Margerie and Lank (1986), Hannah et al. (2001); Han and Loder (2002)
Gulf of St. Lawrence	Lu et al. (2001);
St. Lawrence Estuary	Saucier and Chassé (2000);
Newfoundland Shelf	de Margerie and Lank (1986), Han (2000); Han et al. (2000), Xu et al. (2001).

Table 1: A partial list of published tidal models for portions of the Northwest Atlantic Ocean.

The present work is a new contribution for three reasons: 1) it is the first of regional studies applied to the Northwest Atlantic that links the large scale features of the tides to small scale features observed in semi-enclosed seas, 2) by focusing on the five major constituents, we expect to cover most of the observed variation in the elevation time series and 3) we construct the non-linear inverse for multiple constituents. This work is similar in scope to the study of Foreman et al. (2000) where they used TP data for the Northeast Pacific. Both studies use finite element models to make the bridge between the large oceanic scales to smaller coastal scales. In contrast, we used a fully nonlinear time-stepping model instead of their harmonic model for the forward model in the hope of better resolving the complex interactions between the different tidal constituents occurring in resonant regions. However they used 8 constituents compared to the 5 used in this study.

The report is divided as follows. The modelling system is described in Section 2 and the datasets used for comparison and assimilation are described in Section 3. The model solutions for the five major constituents and the two non astronomical tides are described in Section 4 where they are extensively compared with observations. We also discuss our attempt to model the datum Z0. In Section5, we quantify the predictive value of our assimilation system region by region and station by station. A final discussion and the conclusions are found in Section 6.

2 The modelling system

2.1 The models

The data assimilation system (Figure 1) consists of two numerical models and the utility programs that provide the structure that connects the two models and handles the data (Appendix B). The models are 1) a nonlinear time-stepping model that computes the water levels and currents from specified elevation boundary conditions and 2) a linear inverse model that computes the elevation boundary conditions that minimize the difference between the selected observations and the model predictions (Figure 1).

The steps in the assimilation procedure are:

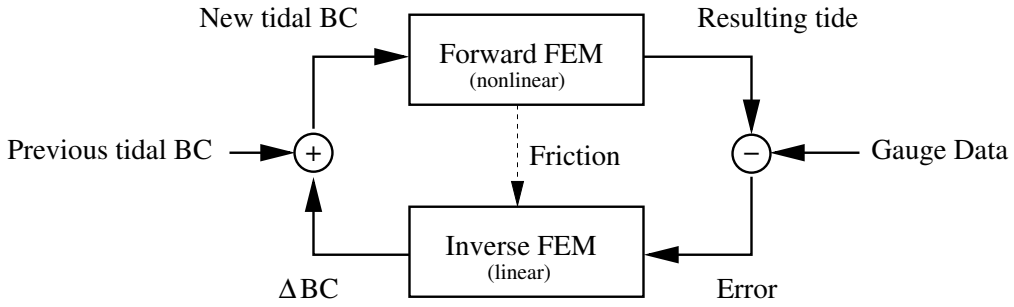

Figure 1: Diagram representing the assimilation system. BC stands for boundary condition and FEM for finite element model.

1. First a subset of the observations are selected to be part of the assimilation procedure. In this report this subset is the tidal constituents derived from the TP data and 2 coastal tide gauges in the St. Lawrence Estuary where there is no TP data.

2. These observations are fed to the inverse model which estimates the tidal boundary conditions that minimize the difference between the selected observations and the model predictions (subject to the linear dynamics of the inverse model).

3. These boundary conditions are then used to drive the forward model. A harmonic analysis extracts the tidal constituents at each node of the mesh from the model solution. The model harmonic fields are then interpolated to the observation locations.

4. The differences between the model constituents and the observed constituents are then used as input to the inverse model and the process is repeated until a stopping criterion is reached (steps 2-4 are an iteration loop).

5. The observations that were not used in the assimilation are used to test the quality of the model solutions.

The arrow labelled 'Friction' in Figure 1 indicates that the *rms* currents at every point in the model domain are calculated during the forward run and fed to the inverse model. These are used for a better approximation of the bottom friction in the inverse model.

The forward model (`MOG2D`) was written by David Greenberg (BIO) and Florent Lyard (CNES). It is a 2-d (depth-integrated) model based on the generalized wave equation (Lynch and Gray, 1979; Lynch and Werner, 1991) using spherical coordinates. For this application the tidal potential, the tidal self-attraction and loading (SAL) were included. The parameters for the former are part of the model and the parameters for the latter two were obtained from Richard Ray (Goddard-NASA, pers. comm., 2001) and Ray (1998). The model is run for a specified number of days at each iteration level using the fields saved from the previous iteration as initial conditions but using the new boundary conditions. For the first iteration, the model boundary conditions are ramped from zero to full values during a user specified period (4 days in this report).

The output of the forward model is analyzed in order to extract the different tidal constituents following the method of Foreman (1977). Since the observational data we used is already corrected for the nodal oscillations, the analysis of model output does not need to account for nodal corrections.

The inverse model (`Truxton`, Lynch et al., 1998) is a linear, harmonic FE model which, given some data and constrained by some parameters, reconstructs the implied boundary elevation at the open boundaries (not necessarily the true elevation). As part of this project, `Truxton` was modified to use either Cartesian or spherical coordinates and to allow for the assimilation of sea level and velocity data and both harmonic constituents and time series data all at the same time. For this application we used spherical coordinates and only assimilated harmonic sea level data. The model was modified in order to accept a 2-d field of the local *rms* velocity computed from the forward model for computing the bottom drag coefficient. In the forward model, the bottom friction is of quadratic form:

$$\mathbf{F}_b = C_d(u_0 + \sqrt{u^2 + v^2})\mathbf{u} \tag{1}$$

where $C_d = 0.0025$ (nondimensional), u_0 is the background velocity (10 cm/s for individual constituent assimilation and 1 cm/s when the 5 majors are assimilated together) and $\mathbf{u} = (u, v)$ is the velocity field. In `Truxton`, the bottom friction becomes:

$$\mathbf{F}_b = C_d(u_0 + u_{rms})\mathbf{u} \tag{2}$$

This allows `Truxton` to account for the spatially varying bottom drag that arises in the forward model.

`Truxton` has 3 parameters that control the inversion:

1. E_{rms} is the expected overall level of errors relative to the TP data;
2. w_0 represents the expected amplitude of the boundary elevations;
3. w_1 controls how steep the slope along the open boundary condition can be.

In this study, $E_{rms} = 0.03$ m, $w_0 = 1.0$ m^{-2} and $w_1 = 200$ deg^2/m^2 for all tidal constituents. In section 4, a sensitivity study is reported for E_{rms}. The inverse model seeks to minimize the following cost function:

$$F = E_{rms}^2 \boldsymbol{\zeta}^T \mathbf{W} \boldsymbol{\zeta} + \boldsymbol{\epsilon}^T \boldsymbol{\epsilon} \tag{3}$$

where $\boldsymbol{\zeta}^T \mathbf{W} \boldsymbol{\zeta} = \oint \left[w_0 \boldsymbol{\zeta}^2 + w_1 \left(\frac{\partial \boldsymbol{\zeta}}{\partial s} \right)^2 \right] ds$ represents a penalty term that forces the solution to be smoothed along the boundary, $\boldsymbol{\epsilon} = \mathbf{A}\boldsymbol{\zeta} - \eta$ is the error between the observations and the model solution. $\mathbf{W}$ represents the smoothing terms along the open boundaries and $\mathbf{A}$ represents the influence matrix of the open boundary elevation points at the location of the observations (.i.e., $\mathbf{A}$ represents the model dynamics). The minimization process is done by solving for

$$(E_{rms}^2 \mathbf{W} + \mathbf{A}^T \mathbf{A})\, \boldsymbol{\zeta} = \mathbf{A}^T \eta \tag{4}$$

where $\boldsymbol{\zeta}$ are the open boundary elevations and η are the observed elevations in the interior of the domain. The system is solved using a SVD decomposition (see also Xu, 1998, for more details).

2.2 The mesh

The model domain (Fig. 2) covers most of the northwest Atlantic from 35^o south to 67^o north and from 75^o west to 35^o west. It covers from Cape Cod to Greenland, part of Baffin Island, Northern Quebec, Labrador, Newfoundland and Nova Scotia. In the north, Davis Strait and Hudson Strait limit the mesh. The boundary on the east side was cut into several straight segments in order to avoid sea-mounts and potential related problems. Some small islands were included, mainly in the Gulf of Saint Lawrence (Madgalena Islands, Anticosti, Prince Edward Island), close to Newfoundland (St Pierre, Miquelon), Sable Island, Grand Manan in the Gulf of Maine and two close to Cape Cod. The Gulf of Maine was fully included, including the upper Bay of Fundy. The Saint Lawrence river is not entirely covered, the mesh stops close to the mouth of the Saguenay river. The bathymetry (Fig. 2) was obtained from a 430,000 point file (a collection of different surveys) covering most of the domain. Some extra bathymetry data was used for the gulf and estuary of the Saint Lawrence (Joël Chassié, pers. comm. 2001). The mesh was obtained using the mesh generation package of Chaffey and Greenberg (manuscript in preparation). The package automatically refines the resolution in regions of shallow water and steep bathymetry. The final mesh has 17055 nodes and 30839 elements (Fig. 3) and requires a 20 seconds time step. The forward model can simulate 8 days in less than 4 hours on a 1 GHz AMD Athlon PC. The open boundaries are the south-eastern Atlantic boundary, Davis Strait in the north, Hudson Strait and the Saint Lawrence river in the west. Care was taken in order to design open boundaries that intersect the coastline at 90 degrees. This is believed to help the coastal waves to better propagate out of the model. The absence of Frobisher Bay and Ungava Bay which tend to resonate with the M2 tide may affect the accuracy of our modelling system close to the Hudson Strait.

3 Data and error measures

3.1 Data

The primary data for input into the assimilation component of the modelling system was the tidal harmonics computed at TP cross-over points as described by Cherniawsky et al. (2001). The alongtrack TP data were first subjected to standard geophysical corrections at the Goddard Space Flight Center, NASA (Koblinsky et al., 1998), except for the ocean and load tides. GSFC data were then interpolated to exact cross-over locations between

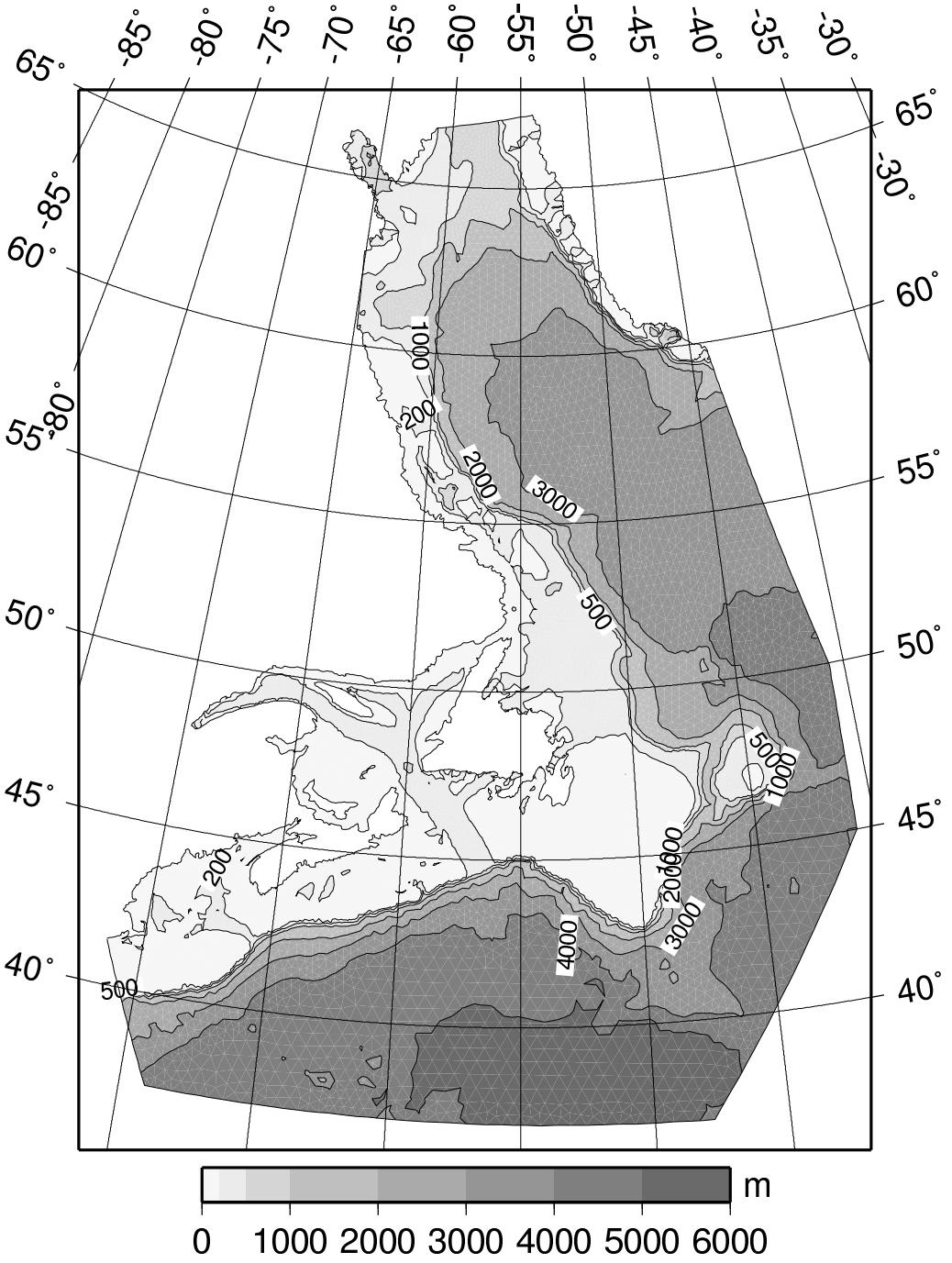

Figure 2: Bathymetry showing the computational domain.

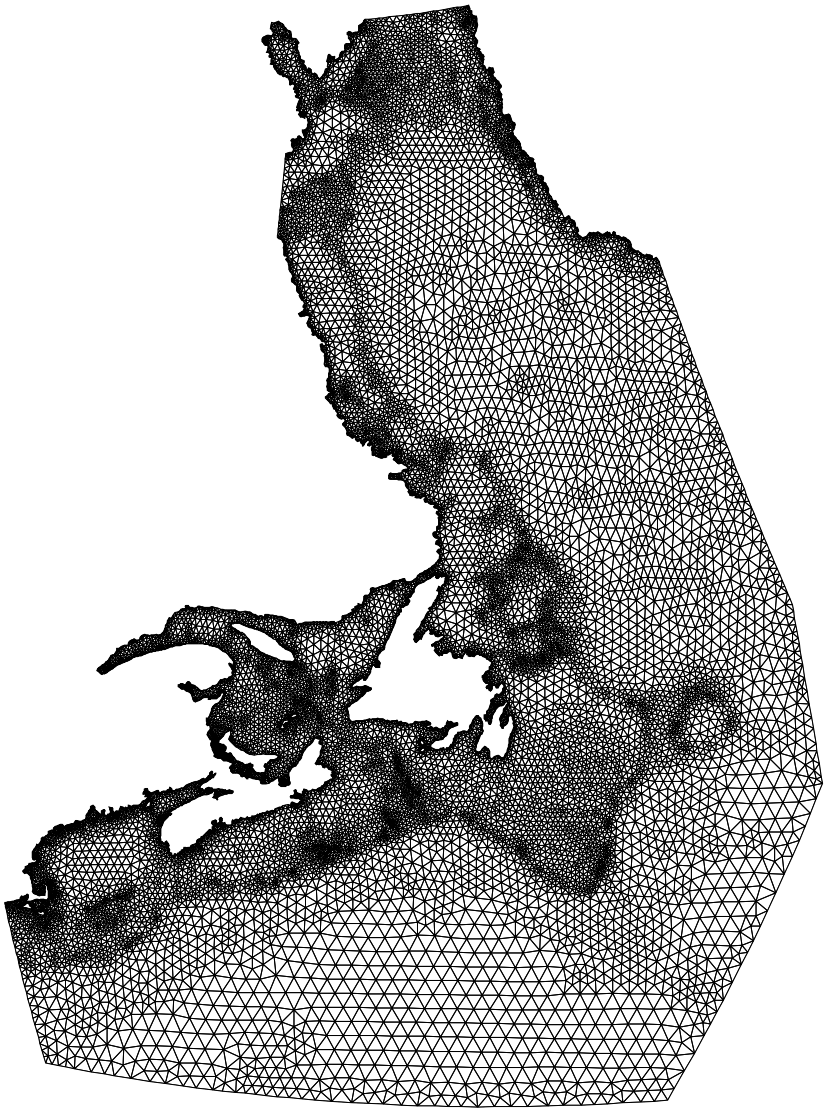

Figure 3: The finite element mesh with 17055 nodes and 30839 elements.

ascending and descending tracks. Data at cross-overs were preferred because of their higher level of accuracy, as they contain twice as much data compared to the alongtrack locations. The tidal data were computed from harmonic analysis of 19 constituents (including Z0, SA, and SSA) of almost seven years (Sep. 1992 - July 1999) of cross-over data. Average errors in constituent amplitudes, estimated as described in Cherniawsky et al. (2001), are less than 1 cm. These errors range from about 0.3 cm in quiescent ocean areas to 3 cm in the Gulf Stream, where some energy leaks to analyzed tidal frequencies from very strong (up to 200 cm) and broad-band (synoptic to interannual) geophysical signals. The TP data has broad coverage over the shelf and deep ocean which provides the large scale constraints on the tidal dynamics. This data was decimated to 50 km resolution in the Northern Labrador Sea where the cross-over points are densely packed. This prevents the Labrador Sea data from dominating the error minimization in the assimilation scheme. Two coastal tide gauges in the Saint Lawrence estuary were added to the input data set to constrain the open boundary condition there. The input data locations are marked in Figure 4.

The observational data for testing the accuracy of the modelling system were compiled from several sources.

- The bulk of the coastal tide gauge data and offshore pressure gauge data came from the electronic data base maintained by the Marine Environmental Data Service (MEDS). We call this the 'Blue set', named for the 'Blue Book' which is the official CHS tidal constituent database (Fig. 4c).

- The data for Boston and Bar Harbor was extracted from an unofficial 1981 dataset from MEDS and added to the 'Blue' set (Fig. 4c).

- A set of northern coastal stations, Baffin Island, Greenland and the northern tip on Labrador was extracted from the 'Blue Book' and denoted North Coast (Fig. 4c).

- Nine stations located along the western Greenland coast (Fig. 4d) were extracted from the Danish tidal office (Farvandsvæsenet, 2000). This dataset contains only four constituents (M2, S2, K1 and O1). The absence of N2 suggests that the length of the record used for analysis was short.

The 'Blue' set was divided into 7 subsets based on geography: Offshore (Fig. 4b and Tab. 2), Labrador, Newfoundland, Gulf of Saint Lawrence, Nova Scotia, Gulf of Maine and Bay of Fundy. These subsets are used to assess the quality of the model solutions in different regions of the model domain. There is some overlap between the subsets. Another subset was based on a set of 15 coastal stations for which the level of confidence is very high (Fig. 5 and Tab. 3). This list was provided by Charles O'Reilly (CHS, pers. comm., 2001). These stations are mainly located in the Gulf of Saint Lawrence, the Gulf of Maine, some along the Newfoundland shore and one along the Labrador shore. This subset is referred as the 'Super Station' set. All the data sets were used for estimating the error of the model and for finding stations where the level of confidence in the data might be low.

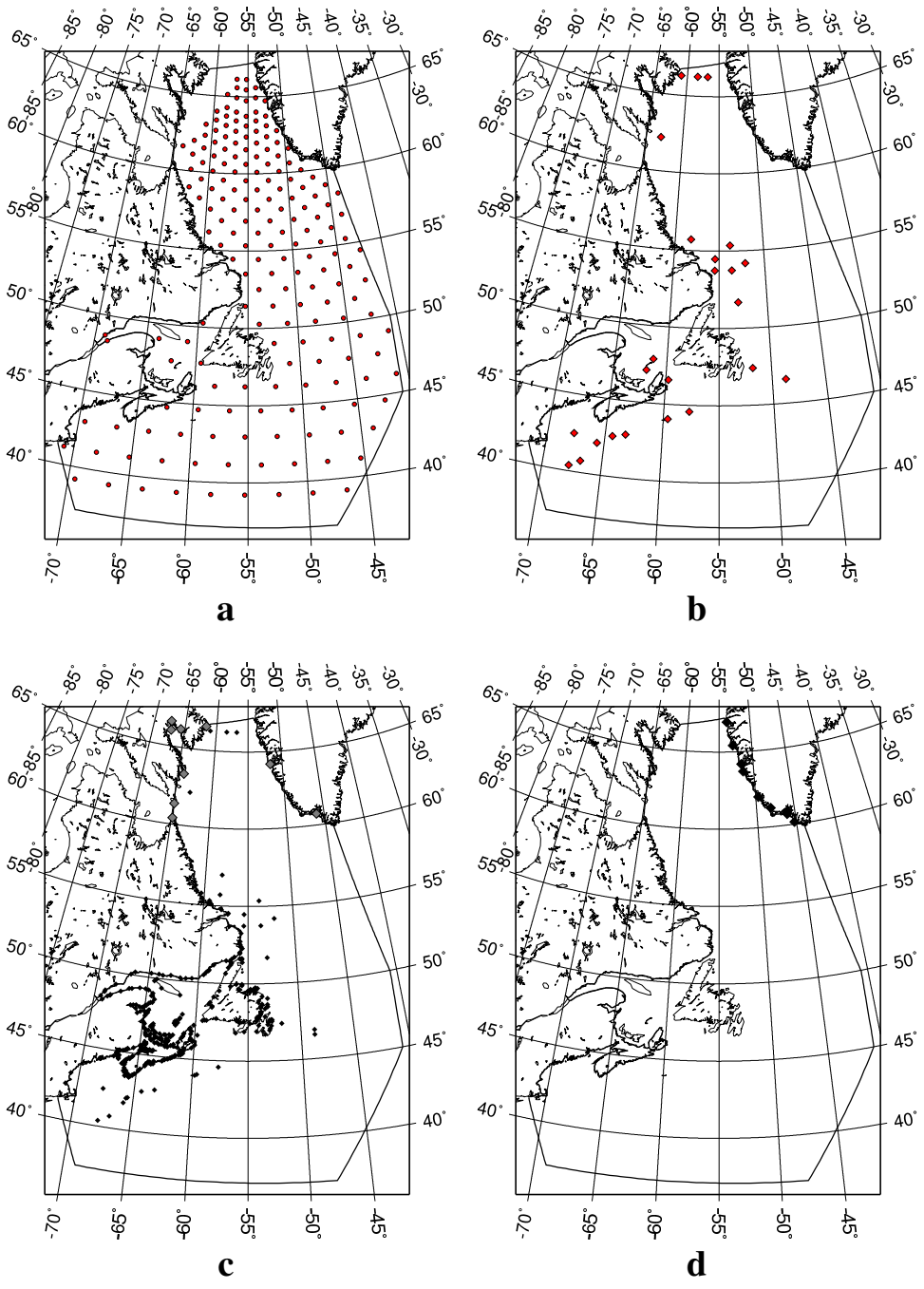

Figure 4: Locations of the data. (a) TP crossover points plus two coastal stations in the Saint Lawrence river selected for assimilation, (b) the Offshore stations, (c) the 'Blue' set including the N. Coast stations in lighter diamonds and (d) the Greenland data.

40551	SABLE ISLAND DRILL SITE
40555	BANQUEREAU BANK
40889	HIBERNIA (780-1080)
40900	AVALON CHANNEL
41182	HAMILTON BANK 796
41227	HAMILTON BANK 334
41232	HAMILTON BANK 789
41256	HAMILTON BANK 790
41368	HAMILTON BANK 795
41400	MAKKOVIK BANK NORTH
41403	HAMILTON BANK
41960	MILLERAND
41987	ILE BRION, MAGDALEN
44081	HEJKA DRILL SITE
50001	FUNDY (OFFSHORE 23)
50002	FUNDY (OFFSHORE 4)
50003	FUNDY (OFFSHORE 6)
50005	FUNDY (OFFSHORE 22B)
50007	FUNDY (OFFSHORE 21)
50008	FUNDY (OFFSHORE 1)
50608	CABOT STRAIT
64000	DAVIS STRAIT
64005	DAVIS STRAIT
64010	DAVIS STRAIT

Table 2: Name and MEDS code of the 24 off-shore stations used for validating the assimilation system.

A final data set was derived by using optimal interpolation to map the TP tidal constituents to the model grid. The optimal interpolation was done using `OAX5`, developed at BIO by Ross Hendry and Ian He (pers. comm., 1996). The horizontal correlation scales were chosen to be isotropic and vary with latitude from 160 km at the southern boundary to 80 km at the northern boundary. This latitudinal variation mimics the latitudinal variation of the density of the TP cross-over points. The data used in the optimal interpolation is the same as that used in the assimilation component plus 385 selected coastal data so the comparison uses few independent data. However the methodology used is completely different so that it does provide a useful comparison data set. Also the optimal interpolation is very inexpensive relative to the assimilation modelling system and it is useful to know whether the dynamical assimilation works better than simple interpolation.

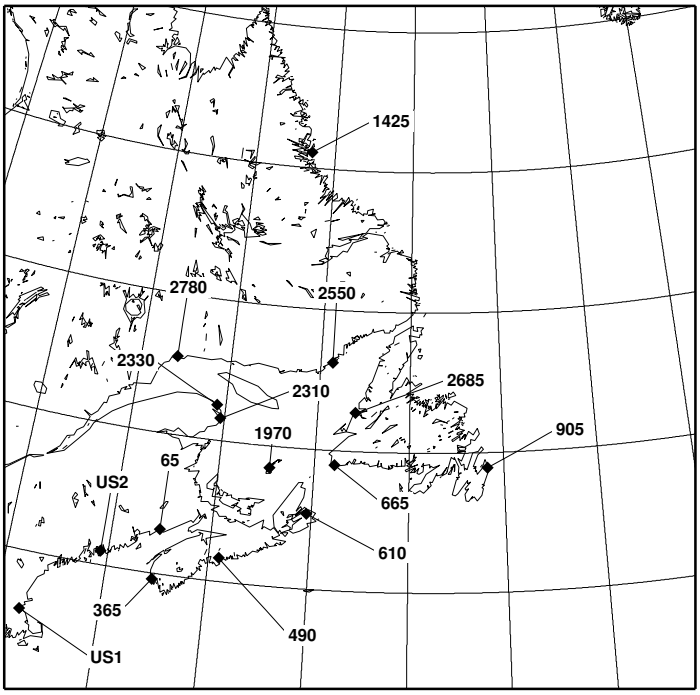

Figure 5: Location of the Super Stations.

65	Saint John
365	Yarmouth
490	Halifax
610	Sidney
665	Port-aux-Basques
905	St John's
1425	Ford Harbour
1970	Cap-aux-Meules
2310	Pointe-St-Pierre
2330	Rivière-au-Renard
2550	Harrington-Harbour
2685	Lark Harbour
2780	Sept-Îles
US1	Boston
US2	Bar Harbor

Table 3: Name and MEDS code of the Super Stations.

3.2 Error measures

The error in a tidal constituent at an observation point was computed by interpolating the model solution for that constituent to the observation point. For some applications we report the complex difference (observed - modelled) and, for some others, we report the difference of the amplitude and the phase. In each application we state which one of these two methods is used. Error statistics for a particular tidal constituent for each of the data subsets also use one of these two error measures.

The tidal prediction error was estimated as follows. Tidal synthesis was used to compute 1 year time-series of tidal elevation at a location for both the observed constituents and the modelled constituents. The root-mean-square (*rms*) error was computed from the difference of the two time series. This *rms* error is referred as the prediction error at a particular station to avoid confusion with other use of *rms* computations. Error statistics for a particular data subset were computed based the prediction error at each location. The details of which constituents were used in the synthesis of the time series is reported.

In order to derive *rms* errors for the tidal currents, we computed the tidal currents at 200 time intervals over a tidal period for both the observations (averaged over depth) and the model solution. The difference between the instantaneous observation and model current is used to compute the *rms* error of the tidal currents. The relative *rms* error is computed by dividing the *rms* error by the length of the major axis of the observed tidal current ellipse.

4 The results

The modelling focussed on the five major tidal constituents that dominate the tide in most regions: M2, N2, S2, K1 and O1. Modelling these constituents should provide a reasonable test of the modelling system.

4.1 The five major tidal constituents assimilated separately

As a first step, the five tidal constituents were computed separately. In each case the solution stopped improving (model error relative to the TP data stopped decreasing) after 5 iterations of the modelling loop shown in Fig. 1. The comparison with the observations was done after the 7th iteration. The values reported in Table 4 are the *rms* of the amplitudes of the errors computed across the different data sets. As described in the previous section, the error was computed by interpolating the modelled constituents to the observation locations and computing the difference in the complex plane between the observed and modelled tidal constituents. The model error relative to TP is less than 3 cm for M2 and between 1 and 2 cm for the remaining four constituents. Except for M2, the error against the Offshore subset is usually larger (since it was not used in the assimilation) by about 1 cm. For M2, the error relative to the Offshore subset is about 0.3 cm less than the error relative to TP. We have no explanation for why the error relative to the Offshore subset is lower than the

error relative to TP for M2. A station by station comparison against the 'Super Stations' is presented in Table 5. M2, O1, K1 are generally in overall agreement but the amplitudes of the modelled S2 and N2 tend to be overestimated in the Gulf of Maine and the Bay of Fundy. This is partly due to the under-estimation of the bottom friction in the forward model due to the absence of the largest constituent (M2).

We tried different values for the assimilation parameter E_{rms} when M2 and K1 were assimilated separately (Fig. 6). E_{rms} is an estimate of the inherent misfit between the observational data and the dynamical models. It also relates to the energy level at the open boundaries since lowering E_{rms} forces the model to add smaller scale structures along the open boundaries (the 'Bdy/10' curves in Fig. 6). For M2 and after 7 iterations, the Offshore *rms* error tends to be minimized for E_{rms} about 0.01 to 0.04 m/s. Our chosen value falls in that range. The model *rms* error relative to TP never falls below 2 cm. For K1, there is no clear minimum relative to the Offshore data, suggesting that the inverse model was able to extract the dynamical part of the signal for a high value of E_{rms} and that lowering E_{rms} failed to improve that part. The magnitude of the M2 boundary values is larger than K1 (and by extension the remaining three tidal constituents). This suggests that the choice of w_0 should depend on the constituent. We did not pursue this. Finally, the fact the *rms* error relative to TP does not fall below 1 or 2 cm suggests that this is the level of accuracy at which our modelling system can assimilate the TP data.

4.2 The five major constituents assimilated simultaneously

Modelling all the constituents simultaneously has the advantage of allowing for the nonlinear interactions between the constituents, especially through the bottom friction. A drawback is that the model needs to be run longer in order to separate the different constituents in the tidal analysis. In these solutions the most serious problem is due to the aliasing between M2 and N2 which are only separated by 0.544 degrees/h in the frequency domain. We found that stable results required model runs of at least 32 days (compared with 4 days for the single constituent runs). As a result the simultaneous constituent run (also referred

Tide	*rms* error compared to TP data (cm)	*rms* error compared to off-shore data (cm)
M2	2.84	2.47
N2	1.61	3.10
S2	1.46	2.85
O1	1.48	2.50
K1	1.25	2.41

Table 4: The *rms* error after 7 iterations for the different tidal constituent run assimilated separately. This error is computed as the *rms* of the error in the complex plane between the observed and modelled constituents.

Stat #	M2 error		N2 error		S2 error		K1 error		O1 error	
	cm	deg	cm	deg	cm	deg	cm	deg	cm	deg
65	-4.0	-2.0	-25.3	20.3	-30.8	9.5	0.1	5.2	-0.6	2.0
365	-5.5	1.0	-7.9	18.3	-10.4	6.5	-0.3	1.7	-1.1	0.6
490	0.9	2.4	3.0	-8.2	2.7	-5.8	-1.7	1.6	-1.4	5.0
610	-1.7	0.7	-0.2	12.8	-1.0	15.1	1.4	-3.5	0.6	-3.1
665	-1.6	1.9	0.1	-0.8	0.5	2.5	1.2	9.1	0.2	5.0
905	-1.9	3.5	-0.1	4.8	-0.9	1.3	0.7	-7.1	1.7	-4.1
1425	3.2	3.2	-0.1	-0.1	0.9	0.5	-2.0	3.4	1.0	9.1
1970	-1.4	-1.1	-0.6	-13.3	0.5	-4.2	0.5	-2.8	-1.1	4.1
2310	0.9	-0.2	-0.3	-3.9	0.1	2.7	3.0	-3.3	0.3	0.4
2330	0.5	-3.3	0.6	-7.1	0.1	0.4	1.4	-4.3	0.2	-3.2
2550	-1.6	-0.6	0.4	-6.1	3.2	0.3	1.5	2.3	-0.6	1.7
2685	-0.9	0.3	0.3	-7.0	3.0	1.0	1.6	-0.1	0.3	3.0
2780	0.8	0.9	-0.9	-4.6	1.3	0.6	1.0	-2.9	-0.6	0.4
US1	0.0	4.2	-4.3	15.6	-3.3	-6.6	0.7	3.9	-1.1	1.8
US2	-4.3	0.6	-8.0	9.8	-9.6	-5.6	0.4	4.2	-0.4	-1.0
Mean	-1.1	0.8	-2.9	2.0	-2.9	1.2	0.6	0.5	-0.2	1.4
Abs	1.9	1.7	3.4	8.8	4.5	4.2	1.1	3.7	0.7	3.0
rms	2.4	2.1	6.9	10.6	8.5	5.8	1.3	4.3	0.8	3.7

Table 5: Elevation error for the different tidal constituents assimilated separately at the location of the Super Stations. Shown at the bottom of the table are the mean deviation or bias (Mean), the mean of the absolute error (Abs) and the *rms* error. The amplitude errors are positive if the observed amplitude is greater than the modelled amplitude. The phase errors are positive if the observed phase lag is greater than the modelled lag.

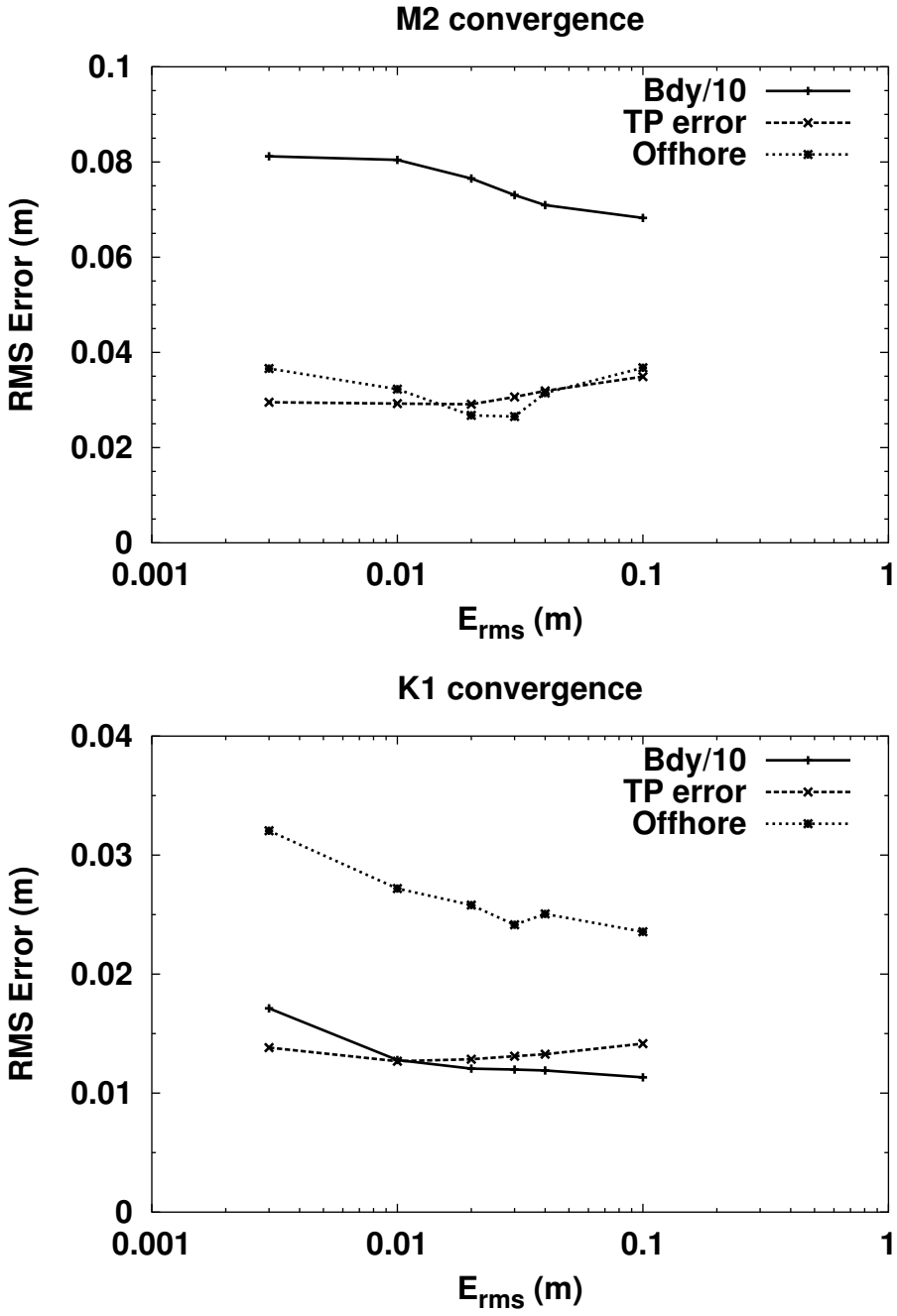

Figure 6: Influence of the E_{rms} parameter in `Truxton` after 7 iterations on the *rms* error relative to TP and Offshore for M2 and K1 assimilated separately. The *rms* boundary elevation (divided by 10 in order to fit in this graph and labelled Bdy/10) shows the increase in elevation induced at the open boundaries by lowering the value of E_{rms}.

as the multi-constituent run) takes between two to three times more time to run than five single constituent runs.

Figure 7 shows the amplitude and phase for the five constituents. The solution is in broad agreement with the global Oregon State University (OSU) Topex/Poseidon solution (Egbert et al., 1994; Egbert and Erofeeva, 2002) in the interior of the domain (the OSU solution is downloadable from `www.oce.orst.edu/po/research/tide`.) The semi-diurnal solutions are characterized by an amphidromic system along the eastern open boundary and an amplification of the tide in the northern part of the domain and in the Gulf of Maine, M2 being the largest. The diurnal solutions are characterized by an amphidromic system on the Scotian Shelf and east of the Baffin Island. However, our solution quality degrades closer to the southern and the eastern open boundaries. There, some spurious oscillations are present. They are the most severe for O1 with extension of 500 km or more and amplitude error of 5 cm. They tend to be less severe for N2, S2 and K1 with extension of less than 100 km and amplitude of a few centimeters. They are barely visible on the M2 solution. These spurious oscillations are an indication that we allow for larger variations than in reality along the open boundaries in order to better match the TP data in the interior. In the future this can be improved by using more smoothing along the boundary or using one of the global models to supplement the TP data along the boundary.

Table 6 shows the score of the modelling system solution against the different subsets of the data. The changes compared to the individual constituent runs are minor expect in Gulf of Maine and Bay of Fundy where N2 and S2 are much improved at the Super Stations (stations 65, 465, US1 and US2 of Table 7). This is related to the fact that the large friction due to the M2 tide in that particular region damps the other semi-diurnal tides. However, there is no major gain by including the diurnal constituents (O1 and K1) in the multi-constituent run. For M2, an important improvement was observed in the Labrador Sea where the overall level of errors compared to the TP data drops from over 3 cm to less than 2 cm (Table 6). When the *rms* error is computed against the Offshore set, the agreement is better for N2, S2 and K1 and a bit worse for M2 and O1 (5 mm of loss for both, compare Table 6 to Table 4). Compared to the Super Stations, all constituents show smaller errors except for K1. The overall *rms* error computed against the TP data shows error level of 1-2 cm. The *rms* error relative to the offshore pressure gauges is 2-3 cm per constituent, about a 1 cm increase over the TP data. This error relative to the offshore tide gauges represents the model's ability to dynamically interpolate the TP data over the model domain. The errors relative to the coastal tide gauges cannot be expected to be better than this. We note that the M2 constituent generally has the largest error because it has the largest amplitude.

For M2 the *rms* error relative to the Super Stations is 6.8 cm, a 4 cm increase over the offshore tide gauges. A large part of this error is due to a 4 degree phase error at Saint John which results in a 21 cm error (relative to a 3 m amplitude). When Saint John is excluded from the Super Stations, the *rms* error for M2 is reduced to 4.3 cm. The errors in the other constituents remain at the 1-2 cm level.

A comprehensive investigation of the agreement between the model and the data is carried out in Section 5.2. Here we discuss some of the patterns evident in Table 6. There is

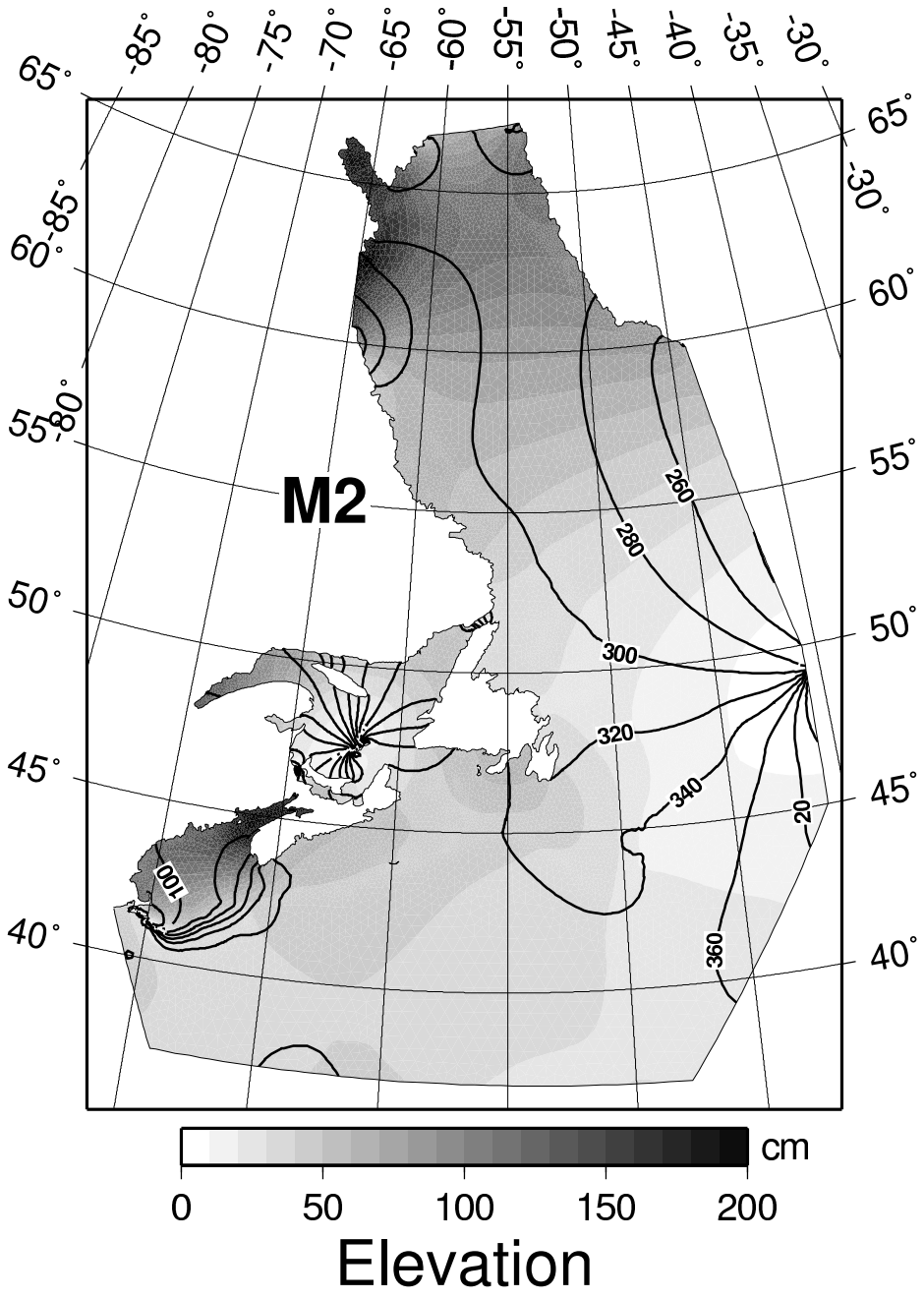

Figure 7: Solution for five tidal constituents obtained from the multi-constituent run. The contours are iso-phase lines given every 20 degrees and the elevation is given according to the scale.

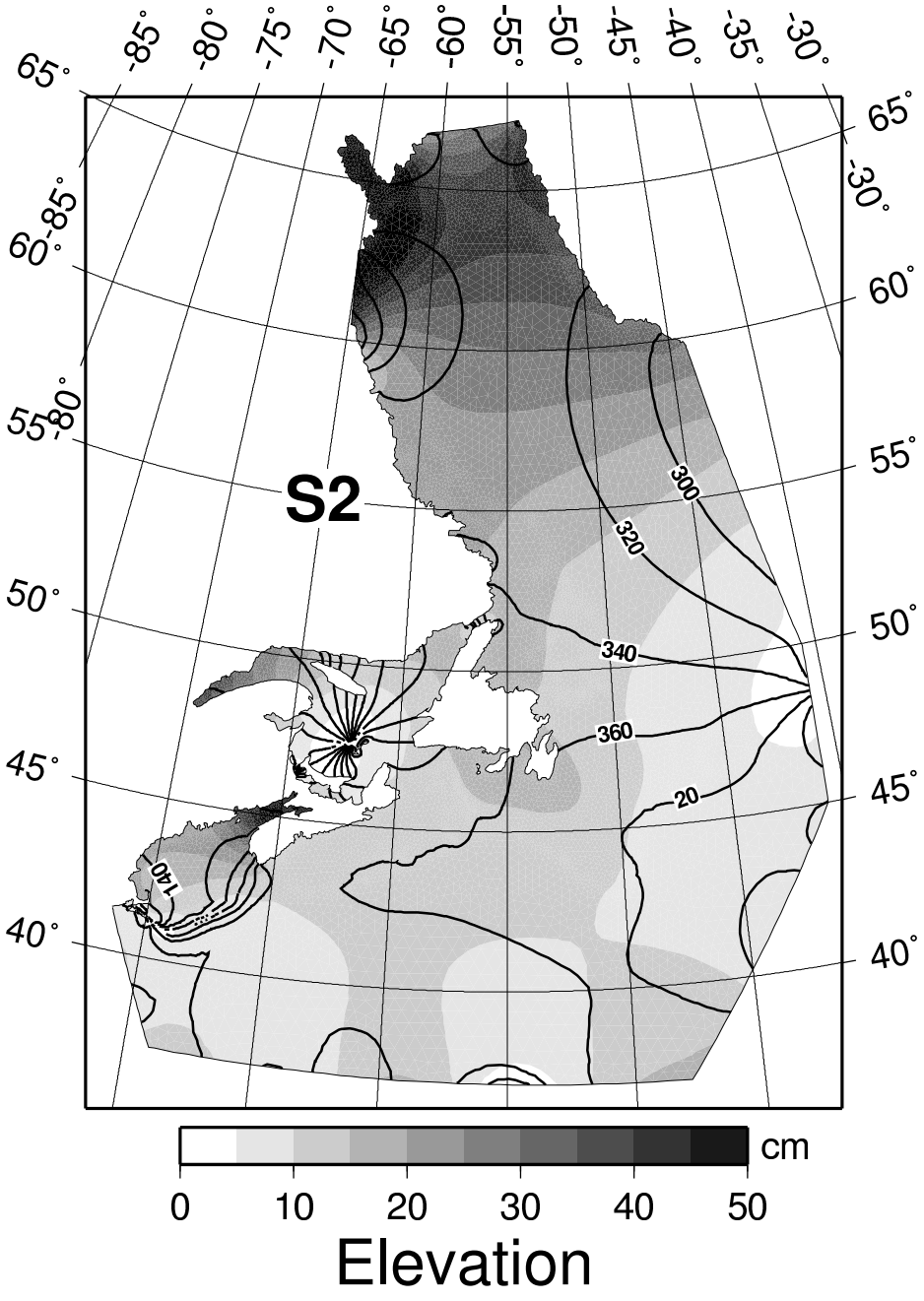

Figure 7 continued.

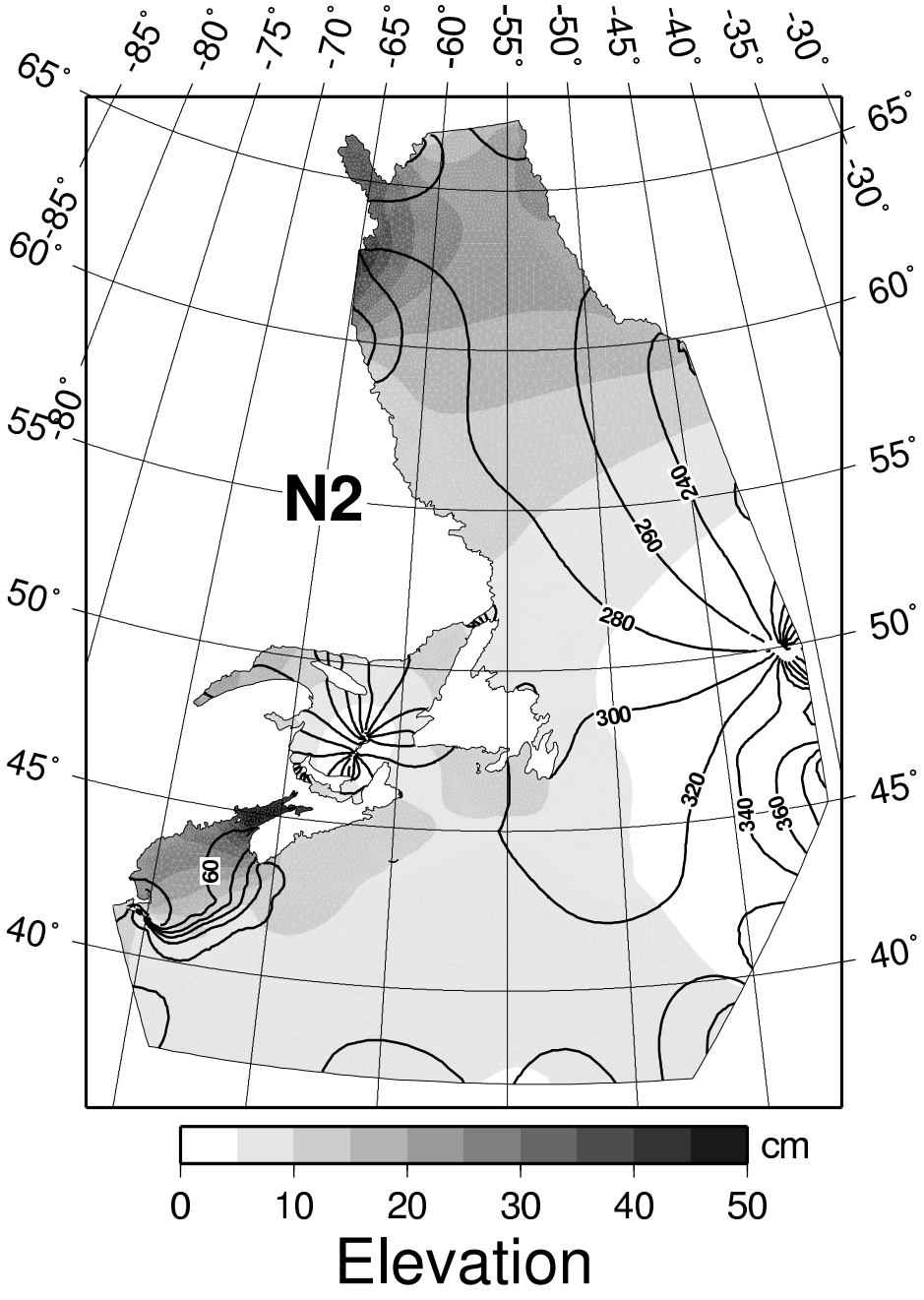

Figure 7 continued.

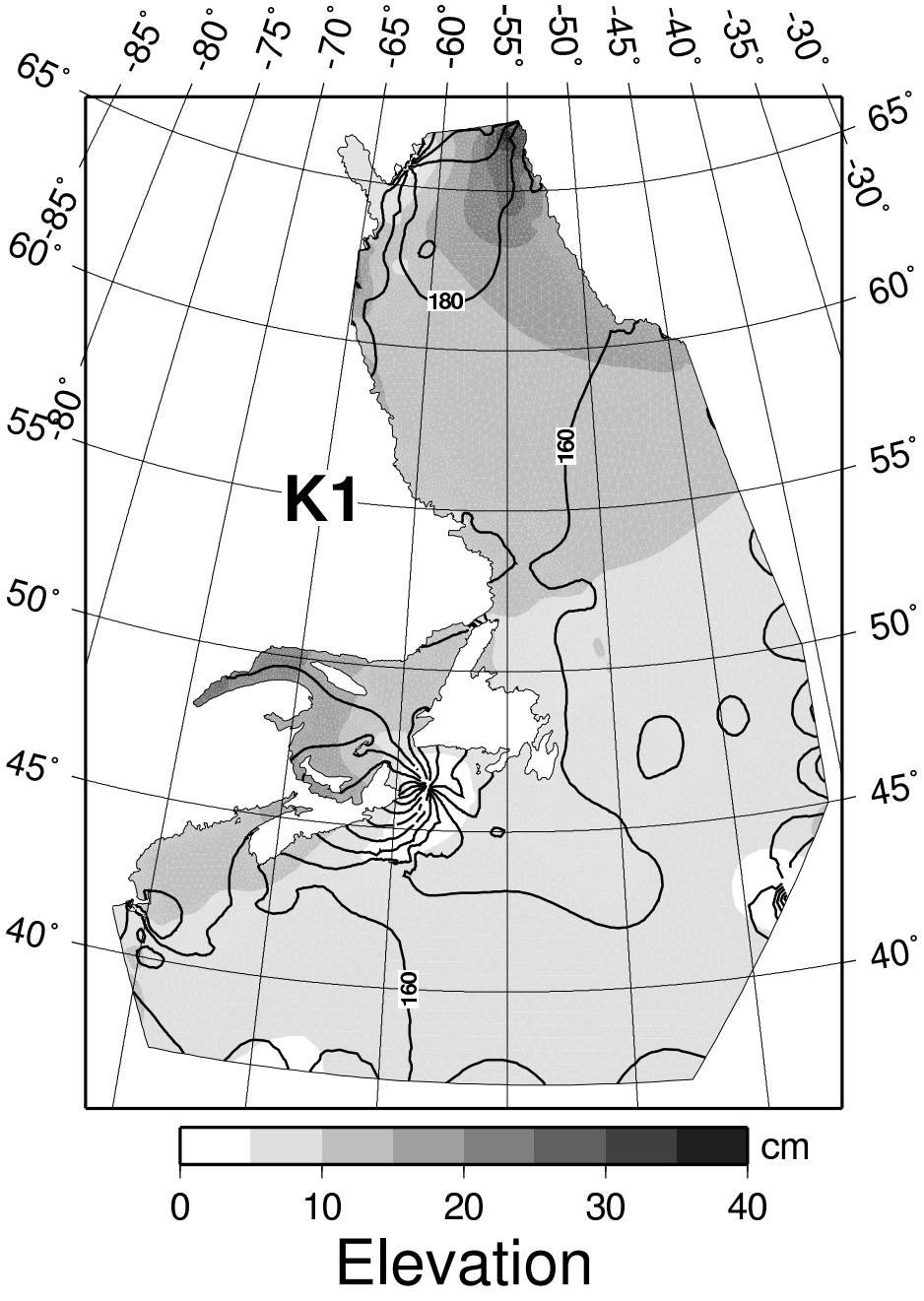

Figure 7 continued.

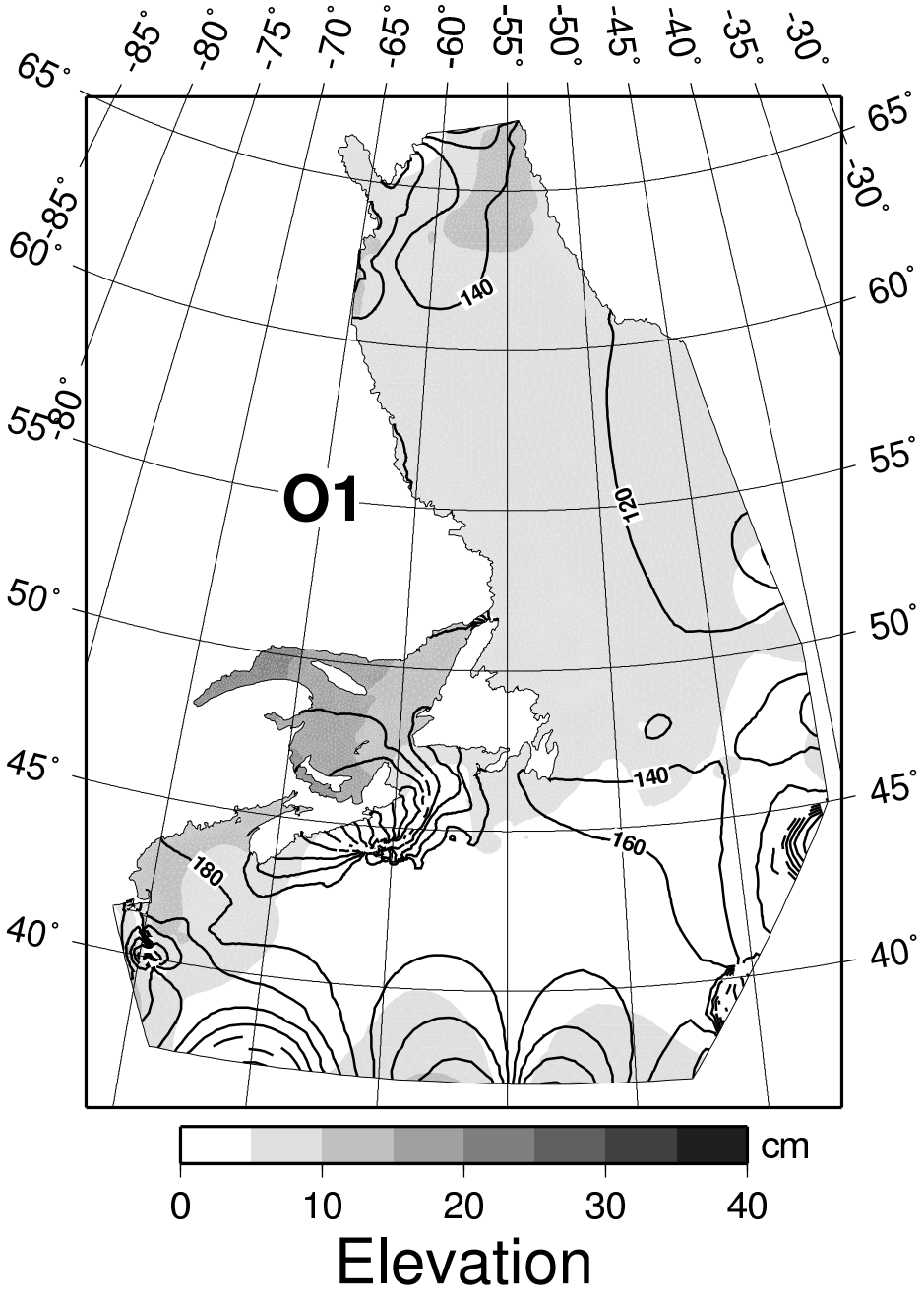

Figure 7 continued.

rms error (cm)	M2	N2	S2	K1	O1
TP	1.77	0.91	1.17	1.37	1.37
Offshore	2.74	2.08	1.69	2.00	1.44
Super St.	6.84	2.35	1.34	1.60	0.94
All Blue	29.0	8.02	6.44	2.94	2.40
N. Coast	35.8	11.1	14.5	5.42	5.74
Labrador	7.88	6.10	5.51	4.77	3.55
Newfoundland	4.96	2.02	2.90	1.82	1.68
St Lawr.	10.8	5.65	3.47	2.77	2.58
N-Scotia	15.4	3.90	4.44	2.78	2.08
G. Maine	23.6	8.56	7.47	2.00	1.50
B. Fundy	84.1	19.6	15.4	4.03	2.63
Greenland	10.3	–	4.27	2.60	1.92

Table 6: The *rms* elevation error after 7 iterations for the different tidal constituent assimilated together.

Stat #	M2 error		N2 error		S2 error		K1 error		O1 error	
	cm	deg	cm	deg	cm	deg	cm	deg	cm	deg
65	3.3	3.9	-0.4	-4.7	-0.6	-1.5	0.3	6.7	0.5	0.9
365	-2.1	1.6	-0.5	-4.4	-0.9	-2.0	0.5	7.1	0.7	2.8
490	0.7	0.2	0.0	0.1	-0.0	-0.4	-1.1	0.9	-0.6	5.2
610	-0.4	0.5	0.4	11.9	-0.4	11.8	0.9	0.2	-0.5	-3.6
665	-0.2	-1.1	0.5	-4.0	0.6	-1.6	0.3	10.3	-0.3	2.5
905	0.1	3.3	0.4	5.5	-0.8	1.2	0.4	0.5	1.1	-1.8
1425	3.8	2.5	0.3	-1.3	0.9	0.8	-3.3	0.5	0.0	7.4
1970	-1.1	-2.9	1.3	-10.9	-0.1	-8.6	0.9	-0.5	-0.5	0.5
2310	0.2	3.0	-0.1	17.9	0.4	3.7	1.6	-2.5	-0.6	-2.5
2330	0.5	-0.5	2.3	8.5	0.9	1.4	0.1	-3.1	-0.6	-5.7
2550	-1.3	-1.0	-0.2	-8.6	1.8	-4.0	0.9	2.4	-0.7	-2.1
2685	-0.7	0.2	-0.4	-8.6	1.5	-3.1	0.5	0.1	-0.2	-0.1
2780	-1.3	1.7	3.3	3.0	2.0	1.2	-0.7	-1.7	-0.9	-2.1
US1	0.1	4.6	0.3	2.4	0.8	1.6	-0.1	9.6	-0.4	5.3
US2	-3.2	2.9	1.7	-4.7	0.5	-2.4	0.3	8.1	0.5	0.6
Mean	-0.1	1.3	0.6	0.1	0.4	-0.1	0.1	2.6	-0.2	0.5
Abs	1.2	2.0	0.8	6.4	0.8	3.0	0.7	3.6	0.5	2.9
rms	1.7	2.4	1.2	7.9	1.0	4.3	1.1	5.1	0.6	3.6

Table 7: The elevation error for the different tidal constituents assimilated together at the Super Stations.

clearly a problem in the N. Coast and Greenland sets. The errors for all the constituents are much larger than for the Super Stations. The errors for the Newfoundland stations are comparable to the Super Stations (with Saint John, NB removed), but the Labrador errors are larger. The difference can be explained by the discrepancy at four stations. When these are removed the Labrador M2 *rms* error drops to 4.5 cm, consistent with the Super Stations.

The relatively large M2 error for the Gulf of Saint Lawrence cannot be explained by a few stations. The error is dominated by systematic phase errors in Northumberland Strait, which given the relatively coarse resolution in the Strait, suggests the need for more resolution.

For Nova Scotia, the Gulf of Maine and the Bay of Fundy the large errors relative to the Super Stations are primarily due to the semi-diurnals. The growing absolute error is due in part to the increased amplitude of M2, N2, S2 in the Bay of Fundy and Gulf of Maine. For Nova Scotia, the large M2 *rms* error is due to one bad station (if removed, the *rms* error drops to 4.5 cm). In the Gulf of Maine, the largest errors were found around Grand Manan Island, close to Digby and along western Nova Scotia. It is likely that the model underresolves some of the complex bathymetry features there. The model also fails for lack of resolution in the upper part of the Bay of Fundy, although the solution is surprisingly good at Saint John.

In the coastal zone, the modelling system is therefore capable of an accuracy of 4-5 cm for M2 and 2-3 cm for the other constituents (outside of the Gulf of Maine and Bay of Fundy) and an accuracy of 2 to 3 cm per constituent on the shelf and offshore.

4.3 Optimal interpolation approach

We also evaluated the solution obtained using optimal interpolation (as introduced in Section 3.1). Table 8 shows the *rms* error for the five constituents relative to the different data sets. The *rms* errors for M2 are poorer using this approach than those of the assimilation system. However, the *rms* errors tend to be lower for the other constituents. Due to the choice of correlation scales, it is likely that the optimal interpolation approach fails where the solution displays rapid changes (e,g., the Gulf of Maine and Fundy regions and the Gulf of Saint Lawrence). However the error is more evenly spread in those region using optimal interpolation than the model. This explains the poorer result of the optimal interpolation for the Super Stations but the better result in the Bay of Fundy regions. The other limitation of the optimal interpolation approach relates to the way the search for neighbour points is done. The method does not account for the presence of islands and peninsulas and therefore counts as close neighbours points that are distant by sea-route. Finally, the fact that the optimal interpolation scores poorly for the M2 Greenland data set (as the model does) suggest that this data may not be very reliable. The role of the complex bathymetry around Greenland may account partly for the large observed discrepancy. Another possible explanation is that there is some problem with the TP data in the northern part of the domain. This remains to be investigated.

rms error (cm)	M2	N2	S2	K1	O1
TP	2.88	0.87	0.95	0.88	0.86
Offshore	3.82	1.41	1.49	1.81	1.00
Super St.	25.3	5.58	4.59	1.96	1.37
All Blue	28.1	7.65	5.77	2.80	2.49
N. Coast	19.0	5.78	9.77	2.65	2.58
Labrador	11.1	5.05	4.61	3.32	3.09
Newfoundland	8.02	2.21	2.93	1.67	1.81
St Lawr.	23.0	5.11	4.20	3.14	2.90
N-Scotia	19.4	4.25	4.29	2.62	1.80
G. Maine	25.8	8.75	7.66	1.61	1.42
B. Fundy	67.8	18.9	12.0	3.71	3.05
Greenland	13.8	–	5.82	4.73	1.85

Table 8: The *rms* elevation error for the optimal interpolation scheme.

4.4 Comparison of currents with observations

Since the model also calculates tidal currents, the comparison of those against observations provides another source of independent verification. We extracted 14 stations out of the 222 available from our database (Drozdowski et al., 2002). Their locations are shown in Figure 8. In Figure 9, we plotted the velocity ellipses of the model and the averaged depth observations station by station and separately for each of the five major constituents. Table 9 shows the *rms* error and relative error for the tidal currents. In general, the model is better at estimating the semi-diurnal tidal currents than the diurnal ones. In terms of *rms* error, the model seems to do poorly for M2. This in fact reflects that M2 is the largest constituent in terms of amplitude of tidal currents. The largest relative errors are found at two Newfoundland stations (NFLD19, NFLD21) where the relative error is over 100% for almost all constituents. Another problematic station is Sable Island (SIB6) where the M2 relative error is over 70% whereas it is only 40% at ESS4, a nearby station. The agreement over the Georges Bank (GBFS3) is excellent despite the very large currents there for all semi-diurnal constituents. Over Browns Bank (C1), the agreement is good for all constituents. The quality of the model estimate degrades closer to Boston (C.PORP) but somewhat recovers in the Bay of Fundy (BED61). Hannah et al. (2001) found poor agreement in M2 tidal currents close to Sable Island. Xu et al. (2001) experienced similar difficulties over the Grand Banks when the open boundary elevation is specified directly from TP data (but less when the interior TP data is assimilated.) According to Xu et al. (2001), assimilating the observed tidal currents as well as the elevations improves significantly the velocity solution. They suggest that the velocity, being related to the elevation gradient, provides a finer scale structure to the solution. These large velocity errors seem however to be localized to a few places, suggesting that we may not resolve sufficiently the

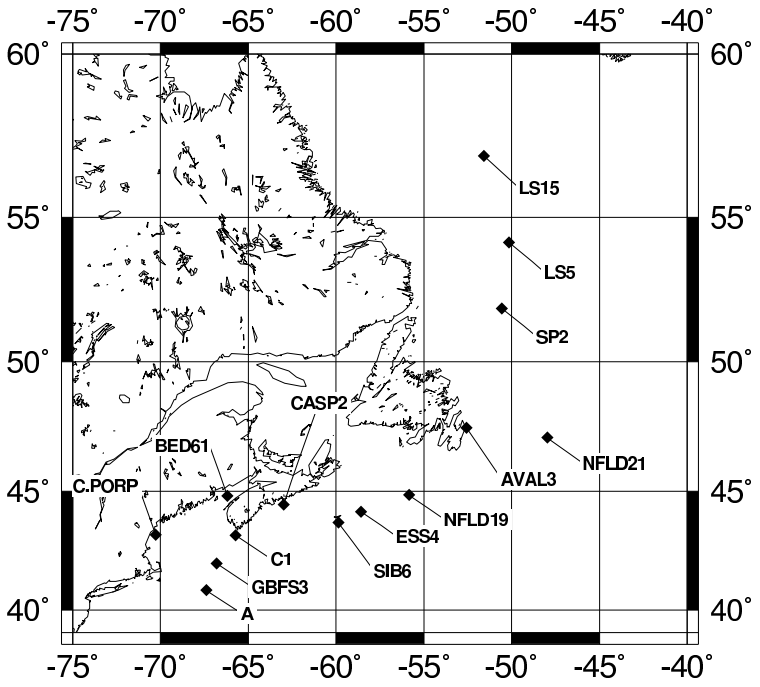

Figure 8: Map of the stations selected for comparison of the tidal currents.

rms error	M2 error		N2 error		S2 error		K1 error		O1 error	
	cm/s	%	cm/s	%	cm/s	%	cm/s	%	cm/s	%
LS15	0.87	**26.8**	0.20	**28.3**	0.16	**13.3**	0.10	**24.8**	0.03	**16.3**
LS5	0.74	**24.4**	0.11	**14.3**	0.20	**19.5**	0.25	**67.2**	0.07	**26.5**
SP2	1.03	**36.7**	0.24	**41.2**	0.29	**27.8**	2.09	**376.**	0.97	**312.**
AVAL3	0.94	**11.0**	0.76	**42.6**	1.02	**78.8**	0.88	**117.**	0.50	**38.6**
NFLD21	4.48	**101.**	1.56	**121.**	1.91	**119.**	3.86	**91.4**	4.12	**211.**
NFLD19	4.26	**251.**	1.11	**139.**	1.31	**249.**	3.02	**733.**	2.57	**746.**
ESS4	4.14	**41.8**	0.23	**10.6**	1.55	**67.2**	8.33	**206.**	6.76	**166.**
SIB6	3.69	**73.9**	0.54	**44.9**	0.54	**29.1**	2.54	**35.8**	4.03	**82.5**
CASP2	0.65	**24.0**	0.26	**42.6**	0.16	**47.2**	1.34	**47.0**	0.45	**13.5**
C1	11.0	**17.5**	2.39	**18.4**	2.02	**16.9**	1.07	**16.9**	1.41	**19.3**
GBFS3	11.6	**13.8**	2.21	**12.4**	1.04	**7.87**	4.20	**60.7**	4.86	**176.**
A	4.75	**13.6**	0.23	**3.06**	0.62	**12.4**	4.98	**128.**	7.93	**466.**
C.PORP	1.25	**28.6**	0.29	**34.3**	0.84	**102.**	0.05	**10.2**	0.06	**14.7**
BED61	23.8	**28.4**	4.65	**27.8**	3.45	**26.7**	0.48	**28.3**	0.32	**25.3**

Table 9: The *rms* error and relative error for the tidal currents.

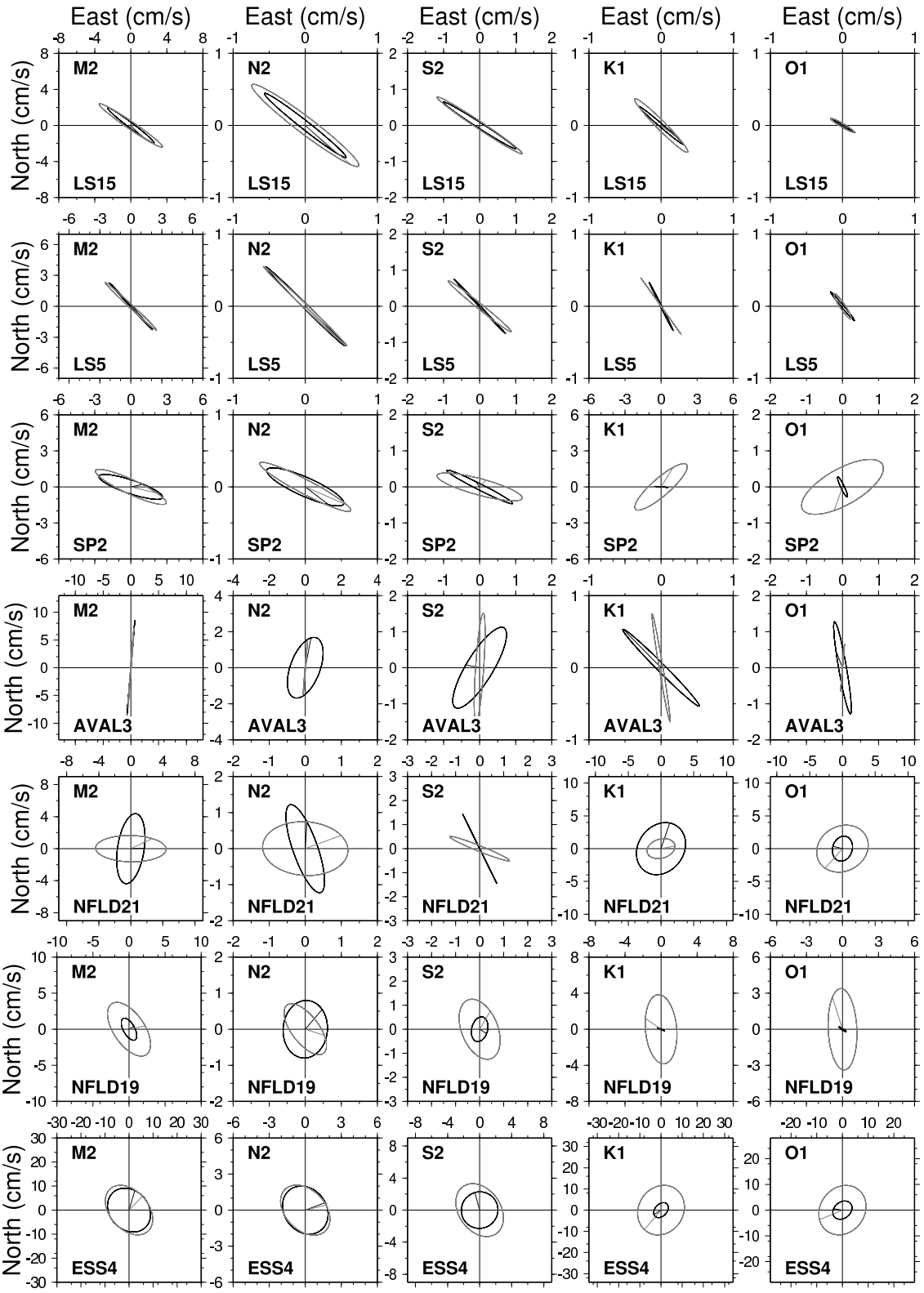

Figure 9: Comparison with velocity data. The dark ellipses are the averaged depth analyzed observations and the light grey ones are the model estimate at the same location. Units are cm/s.

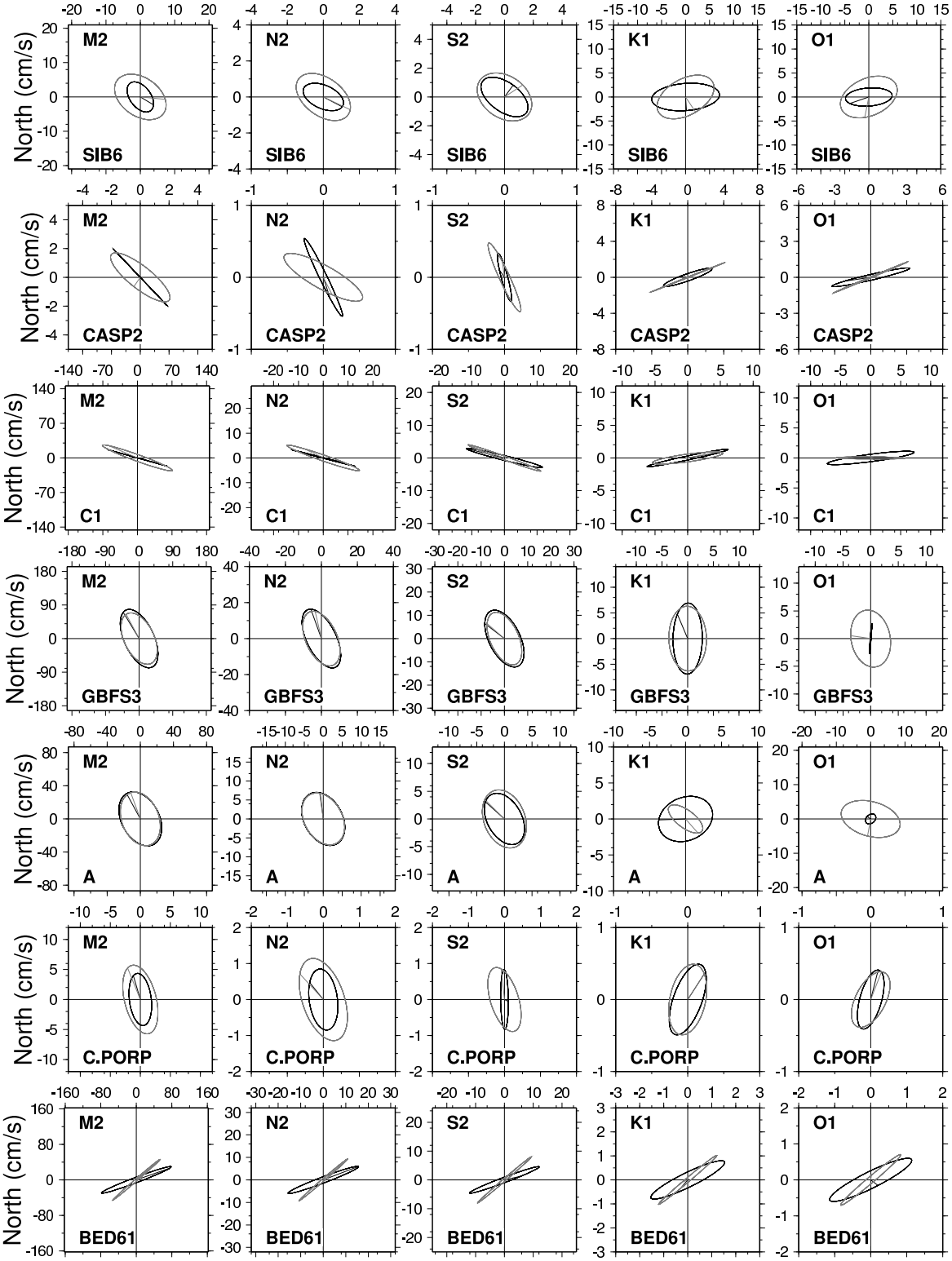

Figure 9 continued

shelf or other local dynamics. Hence, the comparison of the model tidal currents against a few observations is overall encouraging since the velocities were not part of the assimilated data.

4.5 Non-astronomical constituents

The quest for 10 cm accuracy with respect to CHS tidal prediction requires estimating several non-tidal constituents (Appendix A). Here we consider the annual (SA) and semi-annual (SSA) harmonics and the datum (Z0).

SA and SSA are not astronomical tides, they are due to seasonal cycles in wind stress, water temperature, salinity and the large scale circulation. As such, they cannot be modelled by our tidal model. We can make progress by mapping the TP estimates of SA and SSA onto our model grid (Figure 10) using linear interpolation (see Section 3.1 and 4.3). Because the number of TP observations on the shelf is limited, we included respectively 43 and 49 'Blue' stations for SA and SSA. The horizontal correlation scale varies from 160 km at the southern boundary of the model domain to 80 km at Davis Strait and the relative error was set to 10%. This coarse length scale means that this is a crude approximation to the seasonal cycle of the water levels on the shelf and near the coast. Nevertheless we find that the results are reasonable with misfits with respect to both the original TP data and the Super Stations of the order of 1-2 cm for both SA and SSA (Table 10). The amplitudes and phases for SA have reasonable spatial structure. However, the amplitude is very large in the Gulf Stream region where there is likely an aliasing problem with the Gulf Stream rings and meanderings. SSA tends to have small scale phase variations, possibly because it is primarily the residual from fitting a sine wave to an annual cycle that may not be strictly sinusoidal. As a result SSA may be subject to more spatial noise than SA. Robust estimates of SA and SSA require more years of satellite data, since the seasonal cycle does not have the same amplitude and phase every year. Note that we modified the TP data at one location, east of Newfoundland where the phase seems to be wrong by 180 degrees for SA.

The tidal constituents describe the oscillations of the sea surface about mean sea level. By convention, water depths on charts and tidal heights are given with respect to a different vertical reference, called chart datum or Z0. Chart datum, as defined by the International Hydrographic Organization in 1926, is 'a plane so low that the tide will but seldom fall below it.' In Canada the definition goes by the name lower low water. The Americans use a different datum, based on mean lower low water. The important point is that Z0 at a location is a function of the local tidal amplitudes; Z0 is larger where the tides are larger and smaller where the tides are smaller. However there is no standard formula for computing Z0 from the tidal amplitudes. As a consequence linking the tidal model results with the tidal predictions provided by CHS requires a model version of Z0 that varies in space in a way that is consistent with the Z0 used to produce the tide tables. Here we investigate whether there is a simple functional relationship between the tidal constituents at a gauge and the official Z0 at that location. Figure 11 shows that, based on the gauge data, there

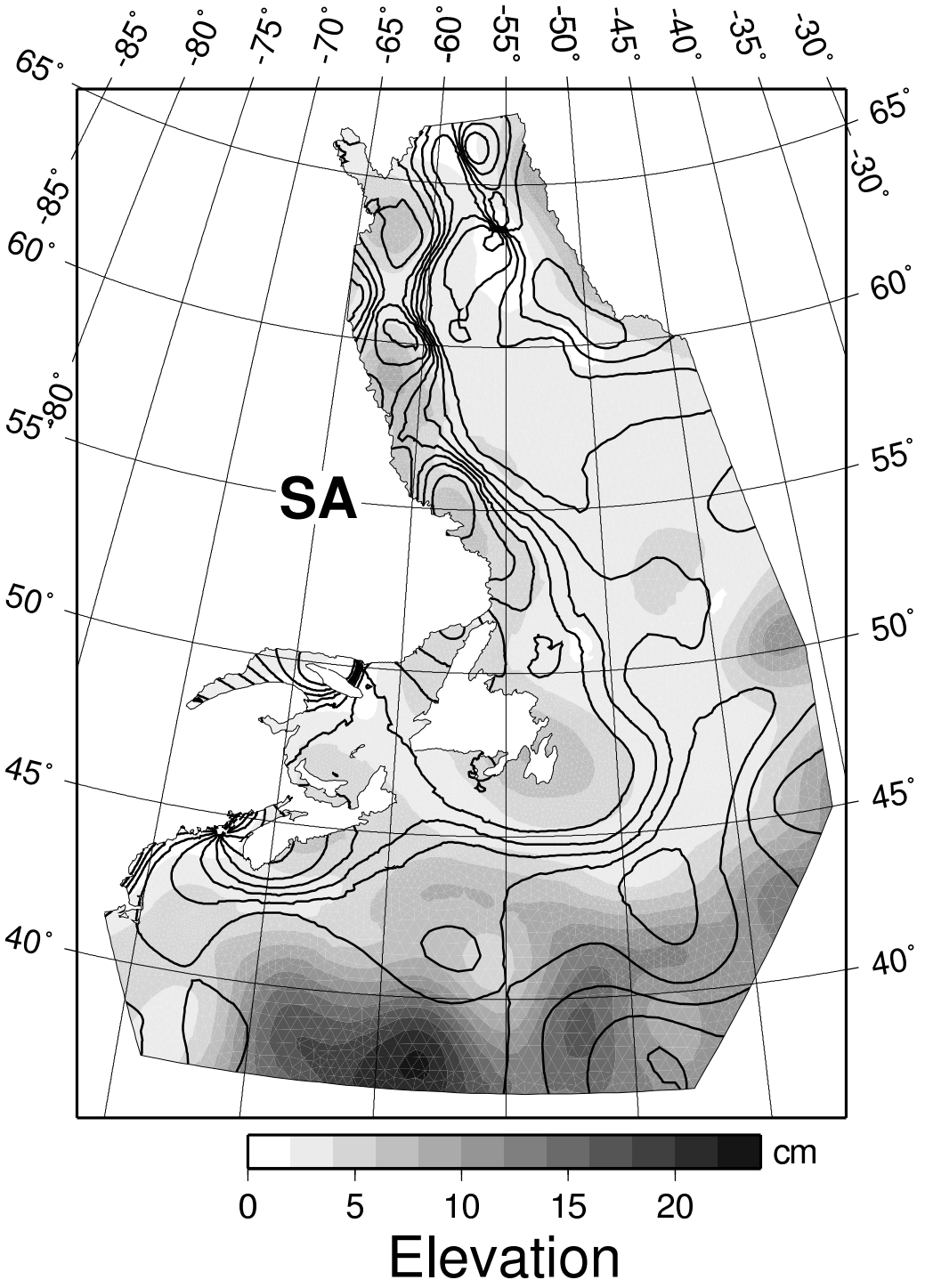

Figure 10: Solution for the SA and SSA constituents obtained using the optimal interpolation technique.

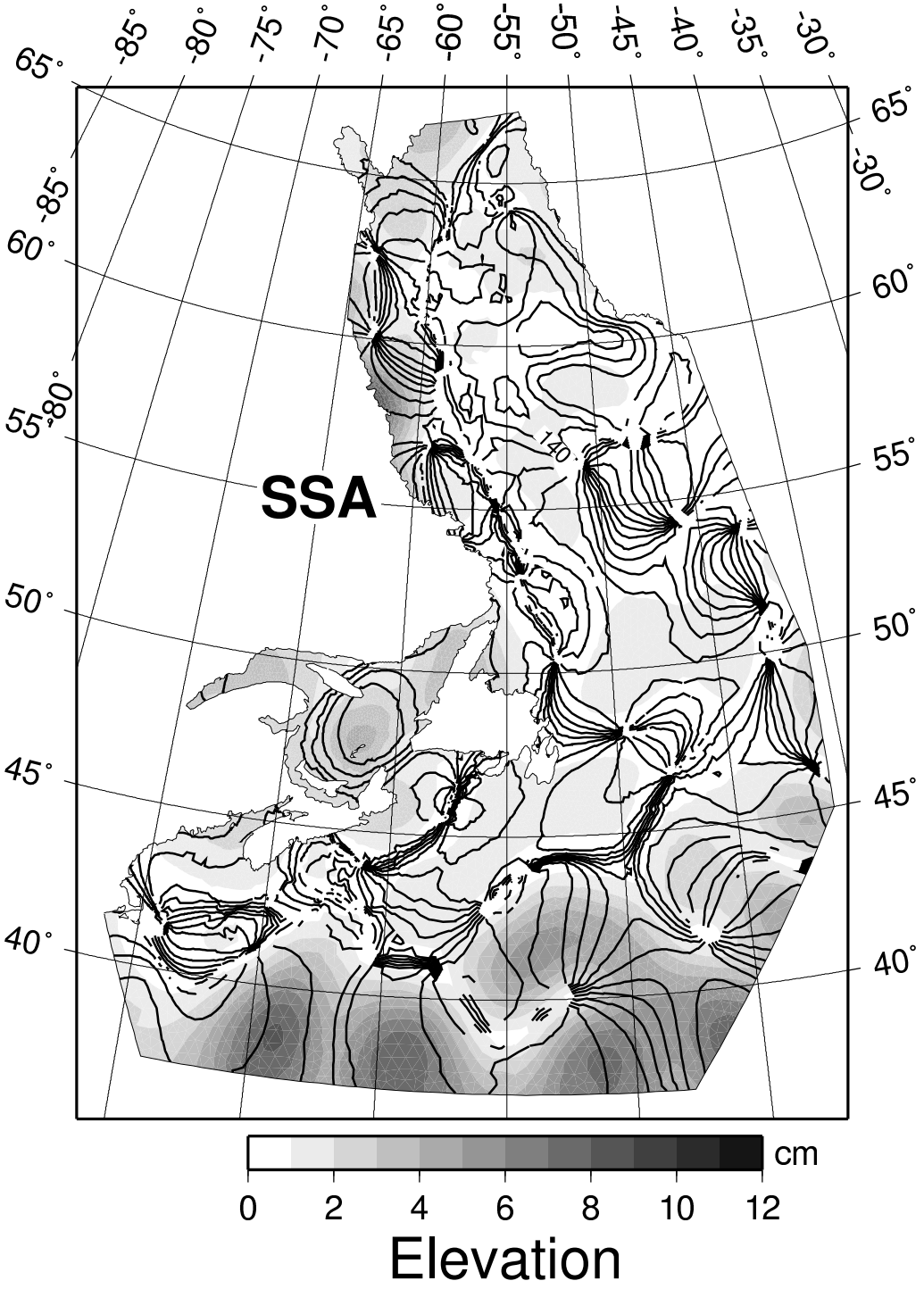

Figure 10 continued.

rms error (cm)	SA	SSA
TP	2.01	1.15
Offshore	9.26	4.15
Super St.	2.10	1.40
N. Coast	5.76	0.93
All Blue	3.58	2.04
Newfoundland	2.03	0.98
St Lawr.	2.26	1.53
N-Scotia	11.4	3.89
B. Fundy	1.76	3.25

Table 10: The *rms* error elevation for SA and SSA using the optimal interpolation.

is a strong relationship between Z0 and the sum of the amplitude of all the constituents (without Z0) and between Z0 and the sum of the amplitudes of the five major constituents. However, the residuals are very large relative to the target error of 10 cm for our modelling system. If only stations where the sum of amplitude is less than 2 m are considered (not shown) then Z0 is well modelled as 0.85 times the sum of the amplitudes of the five major constituents, as suggested by Fred Stephenson (IOS, pers. comm., 2001). However the *rms* residuals remain large (17 cm). A model of Z0 as a function of location is an important area for future development if this system is to be used for water level prediction by CHS.

5 Prediction error

We here concentrate on the solution from the multi-constituent run. The prediction error is computed for each station following the procedure introduced in Section 3.2. We use two different ways of reconstructing the time series that goes into the computation of the prediction error. One uses only the five major constituents (5 *vs.* 5) and the second uses all available constituents for the observations but only the five major constituents of the model (5 *vs.* all). The latter leads to a larger error since it incorporates more variability from the observations but is also closer to what the user would observe as a prediction error. Finally, when SA and SSA are available for both the model and the observations, we computed an error based on seven constituents for the model (the five major plus SA and SSA) against all constituents from observations (7 *vs.* all).

5.1 General results

Table 11 summarizes the prediction error for the different regions. Each number corresponds to the *rms* of all the prediction errors in the region. In this table the problematic

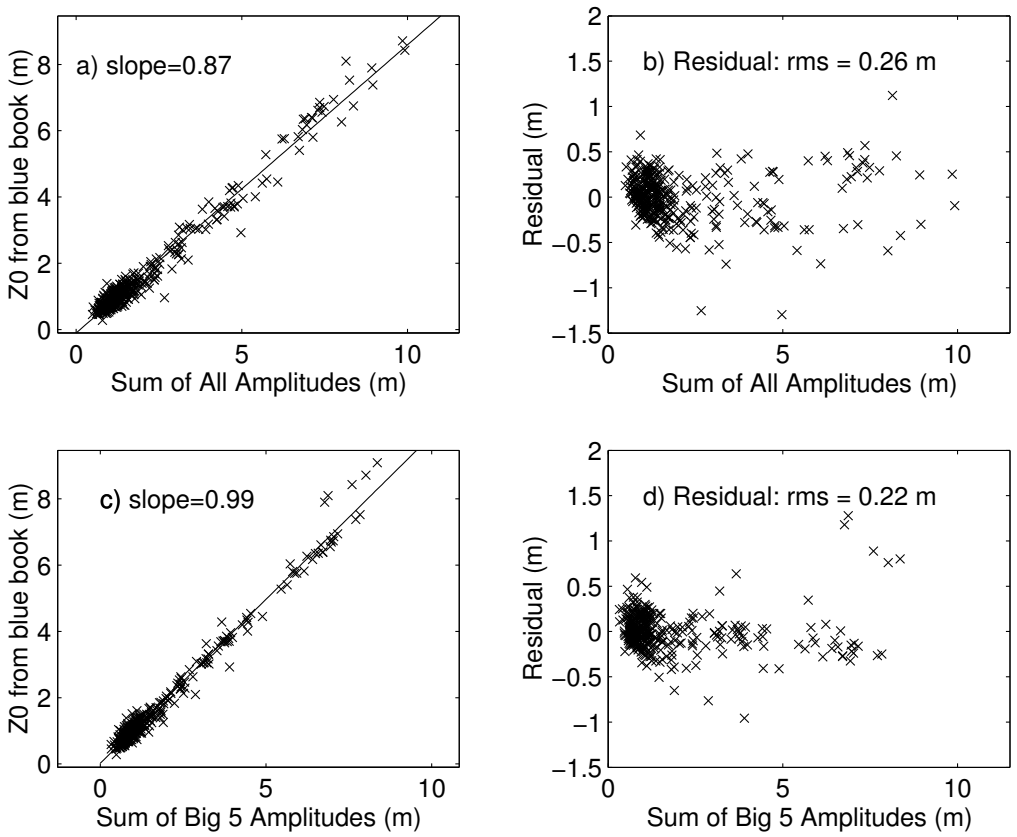

Figure 11: Z0 compared against the other constituents of the 'Blue' set. (a) Z0 against the sum of all constituents. (b) The residual of fitting a straight line in (a) is plotted against the sum of all constituents. (c) same as (a) except the five major constituents are used. (d) residual same as (b) except the five major constituents are used

region	*rms* error (cm)	
	5 *vs.* 5	5 *vs.* all
Offshore	3.5	5.9
Super St.	3.8	8.6
All Blue	22.6	25.4
N. Coast	29.7	34.5
Labrador	6.0	10.5
Newfoundland	4.7	8.0
St Lawr.	9.5	11.9
N-Scotia	4.6	7.6
G. Maine	19.1	23.2
B. Fundy	64.2	69.8

Table 11: The *rms* of the prediction error for the different data sets after removing problematic stations. The numbers on the left are based on time series computed using the 5 major constituents (5 *vs.* 5). On the right, all the other constituents were included for reconstructing the observed time series but the model time series still uses the 5 major ones (5 *vs.* all).

stations mentioned earlier have been removed (Saint John for the Super Station, four for Labrador, one for Nova Scotia). In general, the numbers follow the hierarchy established in Table 6 between the different regions. Depending on the region, the difference between the numbers given in the two columns can be large or small. A relatively large (small) difference indicates that there is a large (small) variance in the unmodelled portion of the tidal spectrum. The difference is large for the Super Stations and seems to be significant in the Labrador and Newfoundland regions. From this table, the prediction error should be about 6 cm offshore, and between 5 to 10 cm along the coast. In the Bay of Fundy, however, the error increases to 60 cm.

In Section 4.5, we computed some non-tidal constituents. Due to the limited number of stations for which SA and SSA were obtained from observations, it is difficult to compare region by region the effect of including these two constituents in the model. We therefore limited the comparison to a subset of the Super Stations for which SA and SSA were analyzed (Table 12). The third and fourth column of Table 12 shows the results for '5 *vs.* 5' and '5 *vs.* all'. The increase of 3-10 cm between column 3 and 4 is a result of how much signal remains to be modelled. The 10 cm difference at Saint John is due to the unmodelled minor semi-diurnal constituents. Finally, when SA and SSA are included in the reconstruction of the modelled time series (7 *vs.* all), the prediction error decreases by 0.2-2 cm, the largest improvement being observed at Ford Harbour. At Rivière-au-Renard, the inclusion of SA and SSA did not improve the prediction error. There, the prediction error increases by 0.2 cm. This shows that including the modelled SA and SSA improves the prediction by 1 or 2 cm at most.

Stat	name	prediction error (cm)		
		5 *vs.* 5	5 *vs.* all	7 *vs.* all
65	Saint John	15.8	26.3	26.1
365	Yarmouth	4.6	12.0	11.8
665	Port-aux-Basques	1.4	4.6	4.2
1425	Ford Harbour	4.2	10.8	8.3
2310	Pointe-St-Pierre	2.6	7.3	6.6
2330	Rivière-au-Renard	2.6	7.4	7.6
2550	Harrington-harbour	2.4	7.2	6.1
2685	Lark Harbour	1.8	7.7	5.6
2780	Sept-Îles	3.7	10.4	9.6

Table 12: Prediction elevation error for the 'Super Stations' that include SA and SSA. The second and third columns correspond to our two ways of computing the prediction error (5 *vs.* 5 and 5 *vs.* all). In the last column, the 5 major constituents plus SA and SSA were included in reconstructing the model time series (7 *vs.* all).

5.2 A region by region study of the accuracy of the solution

This section summarizes the region by region analysis of the model errors. The reader is referred to Appendix C for the maps locating the stations and for a detailed study of the discrepancy between the observations and the model solution station by station. Some of the stations lie relatively far inside shallow channels and show therefore large discrepancy with the model solution. We tried to avoid this problem by removing stations that were visually too far inland. We also removed the stations that were not analyzed for one of the considered tidal constituents (which is usually related to a short record).When the model solution agrees with surrounding stations except one, we raise doubts concerning the quality of the data there. In general, the agreement is good for M2 but poorer for N2, S2, K1 and O1.

The North Coast region is somewhat deceptive. Although the multi-constituent run is successful at matching the TP data in the interior, it seems unable to match the coastal gauge data along Baffin Island, Greenland and the Hudson Strait. This raises suspicion about the accuracy of either the TP data or the model in this region. While the model is still accurate for Station 3515 along Southwest Greenland, the level of accuracy degrades northward with errors above 20 cm at most stations. The model does not reproduce correctly the resonant interaction in Cumberland Sound for M2 (too large at Station 4031 by 9 cm and too little at Station 4040 and 4045 by about 30 cm). Close to the Hudson Strait, the model underestimates M2 at Station 4070 by 15 cm but overestimates it at Station 4170 and 4265 by over 30 cm. As already mentioned in Section 4, part of the problem may be the absence of the resonant regions beyond the entrance of Hudson strait (Frobisher Bay and Ungava Bay). Another difficulty may be related to the seasonal ice coverage. On the other side of the Labrador Sea along the Greenland coast, the agreement is not always very good. Sta-

tion G22 shows a large difference in amplitude for M2 although the closest station, G11, is in agreement. Station G22 is duplicated in the N. Coast data by Station 3575 which shows the same discrepancy. Station G19 shows a large phase discrepancy for S2. Since the optimal interpolation technique shows the same matching problem in the North Coast region, we investigated if there was a systematic problem between the TP and the gauge data there. Figure 12 and Figure 13 show respectively the amplitude difference for M2 between the observations (TP, Blue, N. Coast, Greenland) and the optimal interpolation technique and the model solution. Most of the amplitude error along the North Coast appears random, in the sense that the error plots do not show any spatial structure. This invalidates the assumption that the TP data may be inaccurate in the northern part of the domain. Therefore, the discrepancy between the two numerical approaches and the coastal gauges data reflects either a lack of information relevant to the model (bathymetry variations, bottom friction or lack of TP points in this region) or a low quality of the data itself (as suggested by the absence of N2 from the Greenland data).

For the Labrador region, the agreement is usually good for all constituents except at Stations 1267, 1400, 1485, 1490 and 41453. The M2 values reported by Wright et al. (1988) in the same area as Station 41453 are in better agreement with the model. Station 1490 lies close to Hudson Strait where the M2 tide is large (above 1 m) and where the solution is changing rapidly. This area also corresponds to a region where the coverage of the TP data becomes suddenly sparse. Further investigation is required to understand what are the weaknesses of our solution there.

For the Newfoundland area, one Station only shows large phase deviation (more than a hour) for all constituents (Station 1048). Station 810 and 818 show some phase difference with the model solution although Station 815 which lies in between is in agreement.

The main problem in the Gulf of Saint Lawrence is the model solution in Northumberland Strait with large departures from the observations. This might be related to poor resolution in the strait and unrealistic bottom friction. In general, there seems to be a 10 degrees phase difference between the model and the observations there. There is also some departure of the solution close to the western open boundary (at the mouth of the Saguenay river). The stations used in the assimilation system (2880 and 2995) differ in amplitude by 10 cm for M2 despite their close locations. The M2 model solution (run separately) lies in between whereas the M2 multi-constituent solution favours Station 2880. It is however difficult to argue that the model has the true solution due to the unresolved complexity of the estuary there.

Along the Atlantic Scotian shore, large differences are visible at Station 405 and 408 although Station 410 and 415 are closer to agreement. One off-shore Station (40562) is in very large disagreement in phase for all constituents although the amplitude seems to be correct (possibly a time problem).

In the eastern part of the Gulf of Maine (Grand Manan Island, Digby, western Nova Scotia), the model seems to over-estimate the semi-diurnal tides. Large discrepancies in amplitude are visible for almost all stations. At Yarmouth, the difference is about 4.5 cm for M2

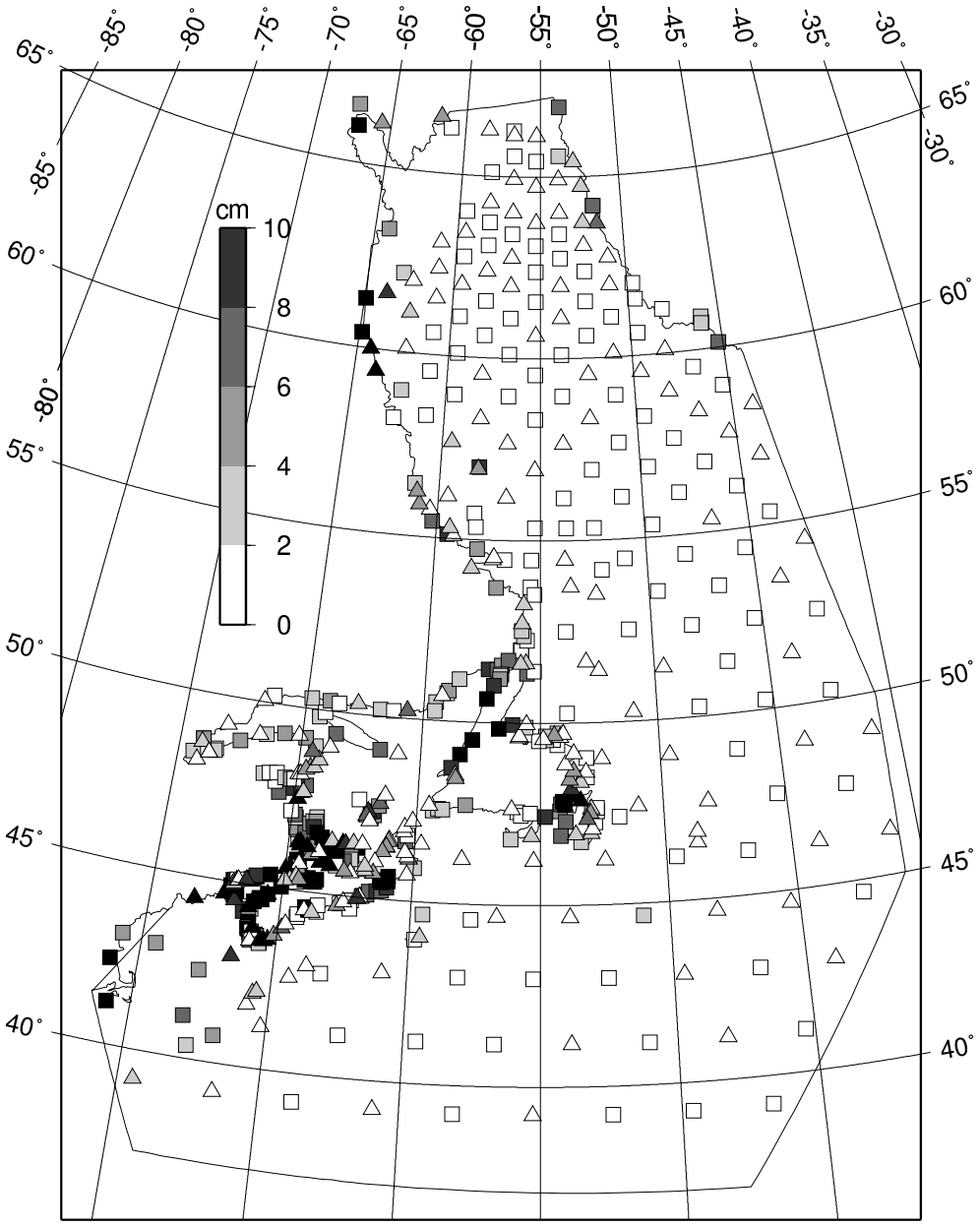

Figure 12: Map of the amplitude difference between the observations (TP, Blue, N. Coast, Greenland) and the optimal interpolation solution for M2. A square (a triangle) is plotted when the optimal interpolation underestimates (overestimates) the tidal amplitude. The symbol is then shaded in accordance with the scale on the left.

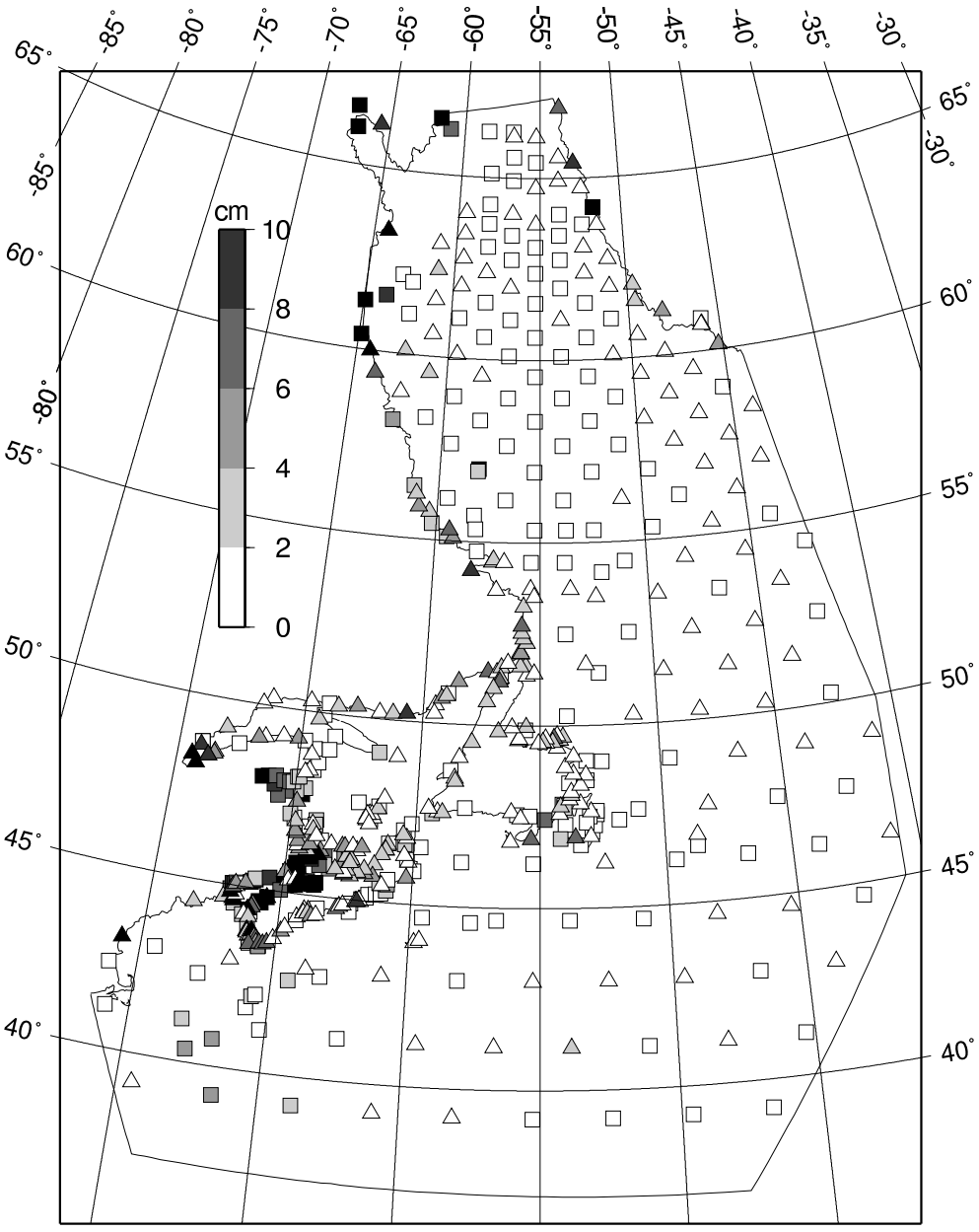

Figure 13: Same as for Fig. 12 but using the model solution.

but goes up to 33 cm at Station 335 for instance. However, closer to Saint John, the M2 amplitude is more realistic. In the Bay of Fundy, the model clearly over-estimates the semi-diurnal tides and there is a large shift in phase. This may be related to unrealistic bottom friction or to nonlinear interactions with missing constituents. Station 40320 may be mislocated (same location as Station 320). This station shows large amplitude differences for all constituents although the phases seem to be in agreement. Finally, we noted that it is in these two regions that the improvement of assimilating all the tidal constituents together is most visible.

We also computed a prediction error at each station using '5 *vs.* 5' and '5 *vs.* all' as defined above. These two *rms* errors are included in the tables given in Appendix as the two last columns except for the Greenland region. The overall level or errors tends to be larger using this test. Deviations in amplitude or phase are easily picked up by this test although they are mainly related to discrepancies in the leading constituents (usually M2). Most of the stations already noted as problematic showed up. When all the constituents are included in the reconstructed time series based on the observations, the *rms* difference can increase by about 10 cm, although this is observed at locations where the agreement between the observations and the model is not very good. At locations where the agreement is usually better, the addition of the other constituents leads to an increase of 2 to 3 cm in *rms* error. In general, this comes from the agreement being poorer in regions of higher tides. Another source of discrepancy is the fortnight tides (MM and MSF) and the annual or semi-annual tides (SA and SSA) which appear surprisingly large at some stations (Stations 1052, 2880 and 41256). At Station 1520, Q1 is of the same order as M2, which comes also as a surprise. In the Gulf of Maine and the Bay of Fundy, because the semi-diurnal frequencies lie close to the resonance frequency, some of the semi-diurnal constituents that are not included in the modelled constituents account for a large difference between the two *rms* errors.

We finally studied the relation between the record length of the observations and the discrepancy with the model at these stations. Figure 14 shows the normalized error as the ratio of the *rms* time series difference (5 *vs.* 5) over the *rms* of the observed time series as a function of the record length. The data is plotted as individual points and is also sorted into bins of at least 10 data points in increasing value of the record length. A curve runs through the median error of each bin. Apart from a peak around 30 and 45 days, the curve is rather flat with an averaged normalized error around 10%. The peaks may be due to aliasing problems with the fortnight and monthly constituents.

6 Discussion and conclusion

In the coastal zone, the tidal modelling system described here is capable of an accuracy of 4-5 cm for M2 and 2-3 cm for the other constituents (outside of the Gulf of Maine and Bay of Fundy). On the shelf and offshore the system is capable of the an accuracy of 2 to 3 cm per constituent. The analysis indicates that the goal of 10 cm tidal prediction error can be reached, again outside of the Gulf of Maine and Bay of Fundy and some of the M2

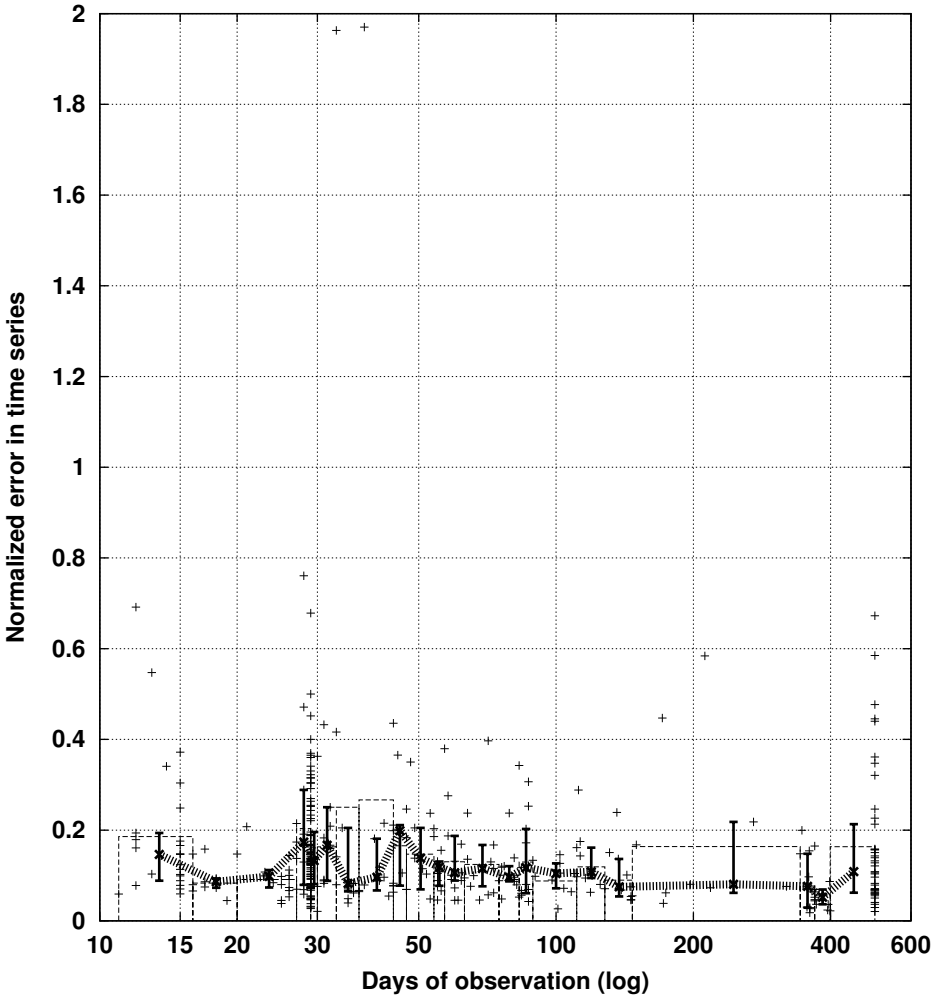

Figure 14: The normalized error (the ratio of the *rms* time series difference over the *rms* of the observed time series) as a function of the record length. The small crosses (+) are the individual data points. The data was binned according to the length of the record with at least 10 points in each bin. The width and height of the dashed rectangles represent the width and mean error in each bin. For each bin the 'x' shows the median error and the vertical line shows the 25^{th} and 75^{th} percentile. The thick dashed line runs through the median errors. Record of length greater than or equal to 500 days were assigned a length of 500 days.

resonant bays in the north. In the areas where the M2 tide gets large it is unlikely that the 10 cm accuracy will be achieved and another error metric will be required here, perhaps a relative error of 10-20%.

The analysis indicates that the 10 cm prediction error is being achieved in Labrador, Newfoundland, the Atlantic coast of Nova Scotia, parts of the Gulf of St. Lawrence and the offshore and shelf regions. Further analysis is required to understand whether the stations identified as 'pathological' are actually in error or whether there is a modelling problem. Further analysis is also required to address whether some of the large MM, MSF, SA and SSA constituents in the observations are real. The prediction errors might also be improved by using tidal inference to include some of the unmodelled tidal constituents.

Overall the prediction errors are of the order of 5 to 10 cm, generally of the order of 6 cm offshore, and between 5 to 10 cm along the coast. The prediction error increases in the Gulf of Maine and reaches 60 cm in the Bay of Fundy. We therefore expect to reach our goal of 10 cm error for the predictive system outside of Gulf of Maine, Bay of Fundy, parts of the Gulf of St. Lawrence and the northern parts of the model domain. We note that the error is larger than our given goal at some locations. The addition of SA and SSA to the predictive system improves the prediction by 0-2 cm.

The model solutions in the Gulf of St. Lawrence needs to be improved near Northumberland Strait where the M2 has phase errors of about 10 degrees (about 20 minutes). All of the semi-diurnal constituents have an amphidrome in the southern Gulf and so the solution is sensitive to both resolution and bottom friction. The solution in the estuary also needs to be improved.

Improving the prediction error in the Bay of Fundy will likely require higher resolution, improved bathymetry and modelling of the minor semi-diurnals that get amplified (e.g. K2, L2, MU2, NU2, LDA2 and 2N2; see also Appendix A). The lower limit for the prediction error in the Bay of Fundy is likely greater than 10 cm, but where it lies between 10 cm and 60 cm is not obvious.

The solutions are poor in the northern part of the domain. The source of the problem is not clear. The spatial coverage of the TP data does not extend to Hudson Strait, David Strait and the Baffin Island. This may be crucially lacking to the modelling system since these regions are very dynamically active. The coastal data may be of poor quality, there may be some local factors that were not taken into account in the modelling system or the optimal interpolation approach, or perhaps the seasonal ice coverage is playing a role. However, it seems that the dynamics of the model is not the source of the problem. One possibility is that we are missing crucial information about the small scale bathymetry/friction along western Greenland as well as the presence of the resonant regions beyond the Hudson Strait. We investigated the quality of the TP data in the northern part of the domain but did not find any systematic discrepancy between the TP data and the coastal data.

The optimal estimation approach does a very good job of mapping the TP data onto the model grid. According to the error metrics, it actually does better than the dynamical model in most regions except for M2. We choose to use the dynamical model because it can deal

naturally with small-scale structure, tidal resonance and nonlinear interactions and can be extended to include wind and pressure forcing in order to provide real time prediction of water levels. Nevertheless the optimal estimation solution provides a good benchmark for measuring the success of future improvements to the dynamical model. The fact that the optimal estimation does better than the dynamical model relative to the North Coast gauges indicates that there is room for improvement in the dynamical model.

In terms of relative cost between the tides assimilated separately and simultaneously, the five-constituent run is more expensive than five separate runs but is more accurate due the representation of nonlinear interactions between tidal components (either direct or indirect through bottom friction enhancement, the latter being the more important).

We attempted to improve the model solutions by including some Super Station data in the input data for the assimilation. This did not yield a clear improvement and was not included in this report. The version of `Truxton` used here weights all the observations with the same error. Therefore in the assimilation, the Super Station data was overwhelmed by the amount of TP data. Recent developments in `Truxton` include the ability to weight the observations individually, which we could take advantage of in the future.

There are several avenues for improvements to the modelling system. A more extensive study of the sensitivity of the solutions to the inversion parameters E_{rms}, w_0 and w_1 should be done. In addition, the new capabilities of `Truxton` could be used to: 1) improve the tidal currents by including some current data as part of the data input to the assimilation scheme and 2) weight the observations by their estimated accuracy and so allow the Super Stations more weight than the TP data. The system could also be improved by using more accurate bathymetry in the northern regions and the Bay of Fundy and possibly by including the resonant regions which lie presently beyond the Hudson Strait in the mesh (although the bathymetry data is rather scarce there).

Acknowledgements

We thank John Loder for his vision and his leading role in acquiring the resources for this project. Many thanks goes to Florent Lyard from CNES in Toulouse, France, for providing the latest versions of the forward finite element model, MOG2D, as well as providing Genesis, an excellent package for creating and editing triangular meshes. We also used the mesh generating package of Jason Chaffey and David Greenberg from BIO. Charles O'Reilly and Glen King, from the Canadian Hydrographic Service, provided us with the analyzed harmonic constituents observed along the Canadian Atlantic coast and in the Gulf of Saint Lawrence. Richard Ray from Goddard-NASA kindly provided the tidal self-attraction and loading constituents for the major constituents. We thank our two reviewers Charles Tang and Zhigang Xu for their helpful and significant comments. Shawn Oakey did a great job at incorporating the assimilation solution into a web-designed interface for public use (`www.mar.dfo-mpo.gc.ca/science/ocean/coastal_hydrodynamics/WebTide/webtide.html`). This work was supported in part by the DFO Strategic Science Fund and the Canadian Hydrographic Service.

References

Chaffey, J., and D. Greenberg, manuscript in preparation: A semi-automated finite element mesh generation routine. Tech. rep., BIO, Departement of Fisheries and Oceans, Bedford Institute of Oceanography, P.O. Box 1006, Dartmouth, NS, Canada, B2Y-4A2.

Cherniawsky, J., M. G. G. Foreman, W. R. Crawford, and R. F. Henry, 2001: Ocean tides from Topex/Poseidon sea level data. *J. Atmos. Oceanic Tech.*, **18**, 649–664.

de Margerie, S., and K. Lank, 1986: Tidal circulation of the Scotian Shelf and Grand Banks. Tech. rep., Contractor report for the Department of Fisheries and Oceans, ASA Consulting, Dartmouth, Nova Scotia.

Drozdowski, A., C. G. Hannah, and J. W. Loder, 2002: The Northwest Atlantic tidal current database. Tech. rep., BIO, Departement of Fisheries and Oceans, Bedford Institute of Oceanography, P.O. Box 1006, Dartmouth, NS, Canada, B2Y-4A2.

Egbert, G. D., A. F. Bennet, and M. G. G. Foreman, 1994: Topex/Poseidon tides estimated using a global inverse model. *J. Geophys. Res.*, **99**, 24 821–24 852.

Egbert, G. D., and S. Erofeeva, 2002: Efficient inverse modeling of barotropic ocean tides. *J. Atmos Oceanic Tech.*, **19**, 183–204.

Farvandsvæsenet, 2000: *Tidevandstabeller 2001 for grønlandske farvande*. Farvandsvæsenet.

Foreman, M. G. G., W. E. Crawford, J. Y. Cherniawsky, R. F. Henry, and M. R. Tarbotton, 2000: A high-resolution assimilating tidal model for the Northeast Pacific Ocean. *J. Geophys. Res.*, **105**, 28 629–28 651.

Foreman, M. M. G., 1977: Manual for tidal heights analysis and prediction. Tech. Rep. 77-10, Pacific Marine Science, Institute of Ocean Sciences, Patricia Bay.

Greenberg, D. A., 1979: A numerical model investigation of tidal phenomena in the Bay of Fundy and Gulf of Maine. *Marine Geodesy*, **2**, 161–187.

Han, G., 2000: Three-dimensional modeling of tidal currents and mixing quantities over the Newfoundland Shelf. *J. Geophys. Res.*, **105**, 11 407–11 422.

Han, G., R. Hendry, and M. Ikeda, 2000: Assimilating Topex/Poseidon derived tides in a primitive equation model over the Newfoundland Shelf. *Contin. Shelf Res.*, **20**, 84–108.

Han, G., and J. Loder, 2002: Modeling tidal currents and seasonal-mean circulation in the Scotian Gully region. *Submitted to the Proceedings of the 7th International Conference on Estuarine and Coastal*, ASCE.

Hannah, C. G., J. Shore, J. W. Loder, and C. E. Naimie, 2001: Seasonal circulation on the western and central Scotian Shelf. *J. Phys. Oceanogr.*, **31**, 591–615.

Koblinsky, C. J., R. Ray, B. D. Beckley, Y.-M. Wang, L. Tsaoussi, A. Brenner, and R. Williamson, 1998: NASA Ocean Pathfinder Project, Report 1: Data processing handbook. Tech. Rep. NASA/TP-1998-208605, NASA, GSFC, Greenbelt, Maryland.

Lu, Y., K. R. Thompson, and D. G. Wright, 2001: Tidal currents and mixing in the Gulf of St. Lawrence: An application of the incremental approach to data assimilation. *Can. J. Fish. Aquat. Sci.*, **58**, 723–735.

Lynch, D., C. E. Naimie, and C. G. Hannah, 1998: Hindcasting the Georges Bank circulation, Part I: Detiding. *Continental Self Research*, **18**, 607–639.

Lynch, D., and F. Werner, 1991: 3-D hydrodynamics in finite elements. Part II: Non-linear time-stepping model. *Int. J. for Num. Methods in Fluids*, **12**, 507–533.

Lynch, D. R., and W. G. Gray, 1979: A wave equation model for finite element tidal computations. *Comput. Fluids*, **7**, 201–228.

Lynch, D. R., and C. E. Naimie, 1993: The M2 tide and its residual on the outer banks of the Gulf of Maine. *J. Phys. Oceanogr.*, **23**, 2222–2253.

Ray, R., 1998: Ocean self-attraction and loading in numerical tidal models. *Marine Geodesy*, **21**, 181–192.

Saucier, F., and J. Chassé, 2000: Tidal circulation and buoyancy effects in the St. Lawrence Estuary. *Atmosphere-Ocean*, **38**, 1–52.

Wright, D. G., J. Lazier, and W. Armstrong, 1988: Moored current and pressure data from the Labrador/Newfoundland Shelf. Tech. rep., BIO, Departement of Fisheries and Oceans, Bedford Institute of Oceanography, P.O. Box 1006, Dartmouth, NS, Canada, B2Y-4A2.

Xu, Z., 1998: A direct inverse method for inferring open boundary conditions of a finite-element linear harmonic ocean circulation model. *J. Atmos. Oceanic Tech.*, **15**, 1379–1399.

Xu, Z., R. Hendry, and J. Loder, 2001: Application of a direct inverse data assimilation method to the M2 tide on the Newfoundland and southern Labrador Shelves. *J. Atmos. Oceanic Tech.*, **18**, 665–690.

Appendix

A Tidal constituents sorted by amplitude for the 6 main regions

Table 13 is derived from the analysis of the 'Blue' dataset (the coastal gauge data). For each region, the mean amplitude for each constituent was computed and sorted in decreasing order. The number of stations for which a given constituent was analyzed is reported in the second column. The five major constituents (M2, N2, S2, K1 and O1) come out as being the main ones. SA (the annual constituent) is often found very close in amplitude (between 3 to 8 cm) to the five major constituents.

Labrador		
name	cm	nb stat
M2	58.7	35
S2	22.2	35
N2	13.5	35
K1	11.8	35
O1	7.4	35
SA	6.6	13
K2	6.1	33
SSA	4.4	13
MU2	3.7	24
P1	3.7	33
MM	2.9	25
MSF	2.7	27
NU2	2.4	20
L2	2.2	26
MF	2.0	13
2SM2	1.9	7
2N2	1.9	19
Q1	1.5	26
NO1	1.5	23
T2	1.4	14
H2	1.2	13
J1	1.0	19
EPS2	1.0	19

Newfoundland		
name	cm	nb stat
M2	41.4	63
S2	15.4	63
N2	8.7	63
K1	8.1	63
O1	6.7	63
SA	5.8	4
K2	4.3	63
MSF	3.8	43
MM	3.4	33
P1	2.6	63
MU2	2.1	40
NU2	1.6	37
2SM2	1.6	9
M4	1.6	63
L2	1.5	37
MF	1.3	7
2N2	1.3	26
MSN2	1.1	14
Q1	1.1	45
MS4	1.0	61
M3	1.0	46

Saint Lawrence		
name	cm	nb stat
M2	45.8	139
K1	17.7	139
O1	17.3	139
S2	13.1	139
N2	10.0	139
P1	5.8	136
SA	4.3	18
K2	3.6	136
SSA	3.1	20
MSF	3.1	66
Q1	3.1	120
MM	2.9	65
MF	2.5	24
NU2	2.1	48
MU2	2.0	119
RHO1	2.0	18
L2	1.9	70
NO1	1.4	65
H1	1.3	7
2N2	1.3	35
M4	1.3	134
S1	1.2	15
J1	1.2	86
H2	1.1	8
T2	1.1	15

Table 13: Amplitude for individual constituents from observations

Atl. Nova Scotia		
name	cm	nb stat
M2	57.7	57
N2	12.7	57
S2	12.5	57
K1	9.0	57
SA	8.7	3
O1	5.5	57
SSA	3.9	7
MM	3.7	35
K2	3.5	49
MSF	3.5	37
P1	2.9	49
M4	2.7	56
NU2	2.7	24
L2	2.1	35
MF	1.8	12
MU2	1.8	44
2N2	1.5	14
MN4	1.3	35
MS4	1.2	55
S1	1.0	3

Gulf of Maine		
name	cm	nb stat
M2	195.3	45
N2	41.2	45
S2	31.3	45
K1	14.5	45
L2	11.2	31
O1	10.8	45
NU2	10.1	26
K2	8.7	44
2N2	6.1	22
P1	4.7	42
MM	4.4	28
M4	3.5	42
MSF	3.3	31
MF	3.0	6
SA	3.0	2
M6	3.0	33
H1	2.6	1
MSN2	2.3	11
MU2	2.1	27
LDA2	2.0	4
Q1	1.9	33
2MN6	1.7	30
ETA2	1.7	19
EPS2	1.7	19
OQ2	1.7	11
T2	1.7	2
MN4	1.4	30
SSA	1.3	2
2MS6	1.3	31
2SM2	1.2	10
NO1	1.2	23
H2	1.2	1
MS4	1.1	42

Bay of Fundy		
name	cm	nb stat
M2	426.8	36
N2	86.3	36
S2	64.6	36
L2	39.6	16
K2	17.7	33
NU2	17.2	10
K1	17.1	36
MU2	12.3	15
O1	12.2	36
LDA2	9.5	7
M4	8.3	36
2N2	7.9	9
OP2	6.7	5
MKS2	6.6	7
M6	6.4	18
P1	5.7	33
H1	4.9	1
MM	4.6	16
2MN6	3.9	16
SSA	3.8	3
MSF	3.7	18
MSN2	3.6	16
OQ2	3.4	15
EPS2	3.4	8
T2	3.3	3
MS4	3.0	35
MN4	2.8	16
2MS6	2.8	18
H2	2.5	1
Q1	2.2	19
2SM2	2.0	13
MF	2.0	13
SA	1.5	2
NO1	1.5	11
ETA2	1.3	8
MO3	1.1	15
MSM	1.1	1
2MK6	1.1	7
M10	1.1	3
MSN6	1.0	5
S1	1.0	3

Table 13 continued

B The C utility programs

The C utility programs created specifically for this application are:

- `anal_tide` for computing the different tidal constituents (the harmonic solutions) from the time iterated solution of the forward model using a least square method that maximizes the energy represented by the given constituents. This program is a modified version of the program provided by Florent Lyard. It accounts for the phase being computed relative to Greenwich time (i.e., an absolute reference time).
- `inter` for interpolating the harmonic solution at gauge locations.
- `compare` for computing the difference in complex space between the observation data and the model solution.
- `extrac` for extracting the boundary information from a harmonic solution of the `Truxton` model.
- `add_diff` for adding the new incremental boundary elevation to the previous open boundary elevation in complex space. The new file then drives the forward model.

C Station by station comparison

We broke up the domain under study into 8 different regions (N. Coast, Labrador, Western Greenland, Newfoundland, Gulf of Saint Lawrence, Atlantic Nova Scotia, the Gulf of Maine and the Bay of Fundy.) Tables are produced for each region showing the discrepancy between the tidal constituents obtained from the tidal gauge stations and the model solution for the multi-constituent run in terms of amplitude and phase. At the end of each table, a summary is given in terms of mean error (bias), the mean of the absolute error and the *rms* error for the amplitude and phase separately. When present, the last two columns represent the *rms* difference between the model and the station reconstructed time series. The first column corresponds to the time series reconstructed using only the five major constituents (M2, N2, S2, K1, O1) and the second column, when present, corresponds to the time series reconstructed using all constituents modelled and analyzed from the observations. Since only the five major constituents where computed, the values in the second column are likely to be larger than those in the first column.

C.1 North Coast region

Stat #	M2 error		N2 error		S2 error		K1 error		O1 error		time *rms*	
	cm	deg	cm	deg	cm	deg	cm	deg	cm	deg	cm	cm
3515	-1.4	5.0	-1.2	6.0	1.5	2.9	-1.1	-0.4	0.3	-0.1	6.2	9.0
3575	17.2	3.3	3.2	2.9	12.5	3.9	1.2	6.3	0.9	3.4	16.7	19.5
3995	22.5	6.9	2.3	-9.3	-1.8	14.7	0.4	-2.4	0.6	29.3	18.4	19.1
4031	-8.7	10.5	14.5	-25.2	-6.0	16.8	1.9	111.8	13.0	32.3	36.6	57.1
4040	31.4	11.3	-3.3	21.4	8.7	11.0	0.8	-36.8	-3.7	11.3	41.6	43.6
4045	36.8	-3.6	8.3	-3.1	-1.5	-15.5	1.8	4.6	-3.4	74.2	32.6	34.8
4070	-14.3	6.5	-5.5	5.5	-5.4	4.8	4.0	-10.6	0.2	-15.2	20.4	21.4
4170	50.3	6.8	9.8	2.4	15.6	8.6	-4.0	2.5	-2.4	17.2	43.5	46.2
4265	36.1	-1.4	5.4	-6.2	13.2	1.4	-0.9	1.8	-1.4	-16.0	28.7	30.6
Mean	18.9	5.0	3.7	-0.6	4.1	5.4	0.5	8.5	0.5	15.2	27.2	31.3
Abs	23.8	6.1	5.7	9.1	7.0	8.8	1.7	19.7	2.6	22.1	27.2	31.3
rms	27.3	6.9	6.8	12.1	8.5	10.4	2.1	39.5	4.4	30.4	29.7	34.5

C.2 Labrador

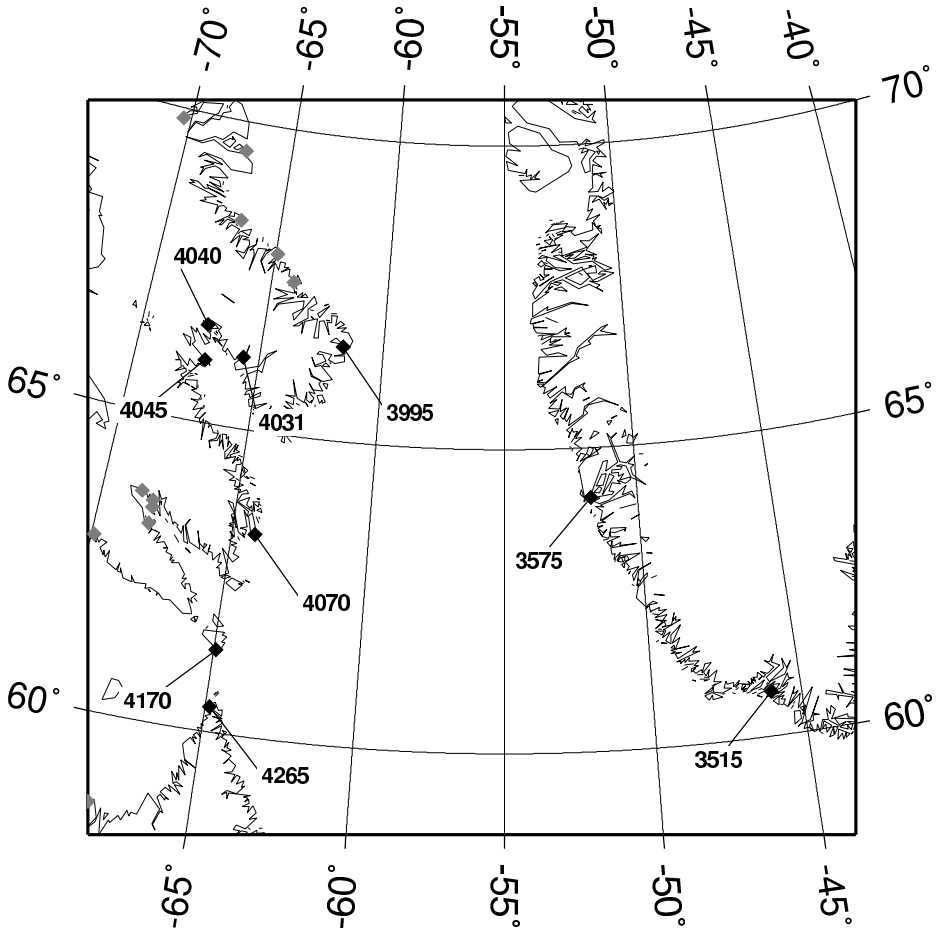

Figure 15: North Coast

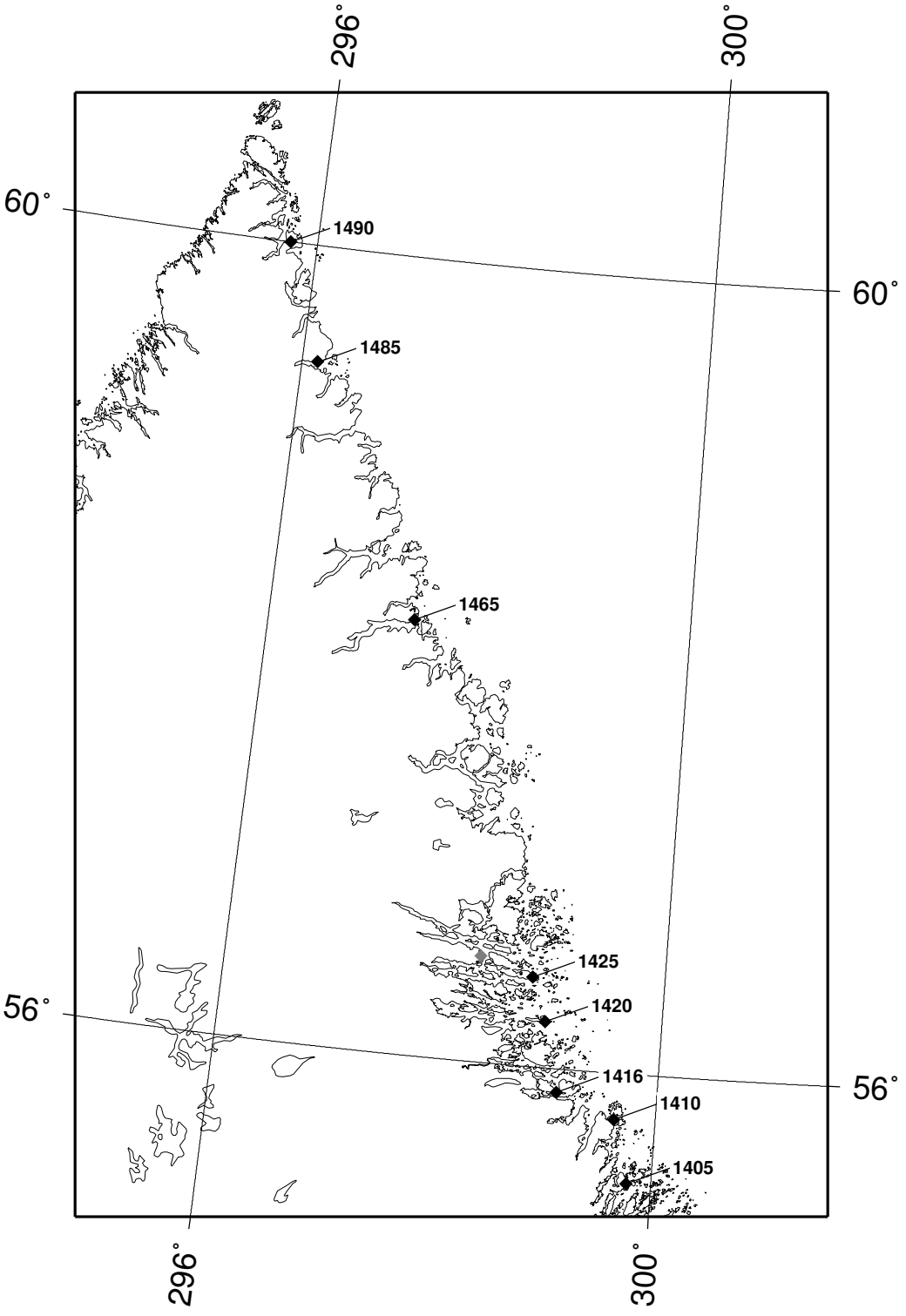

Figure 16: Labrador - North

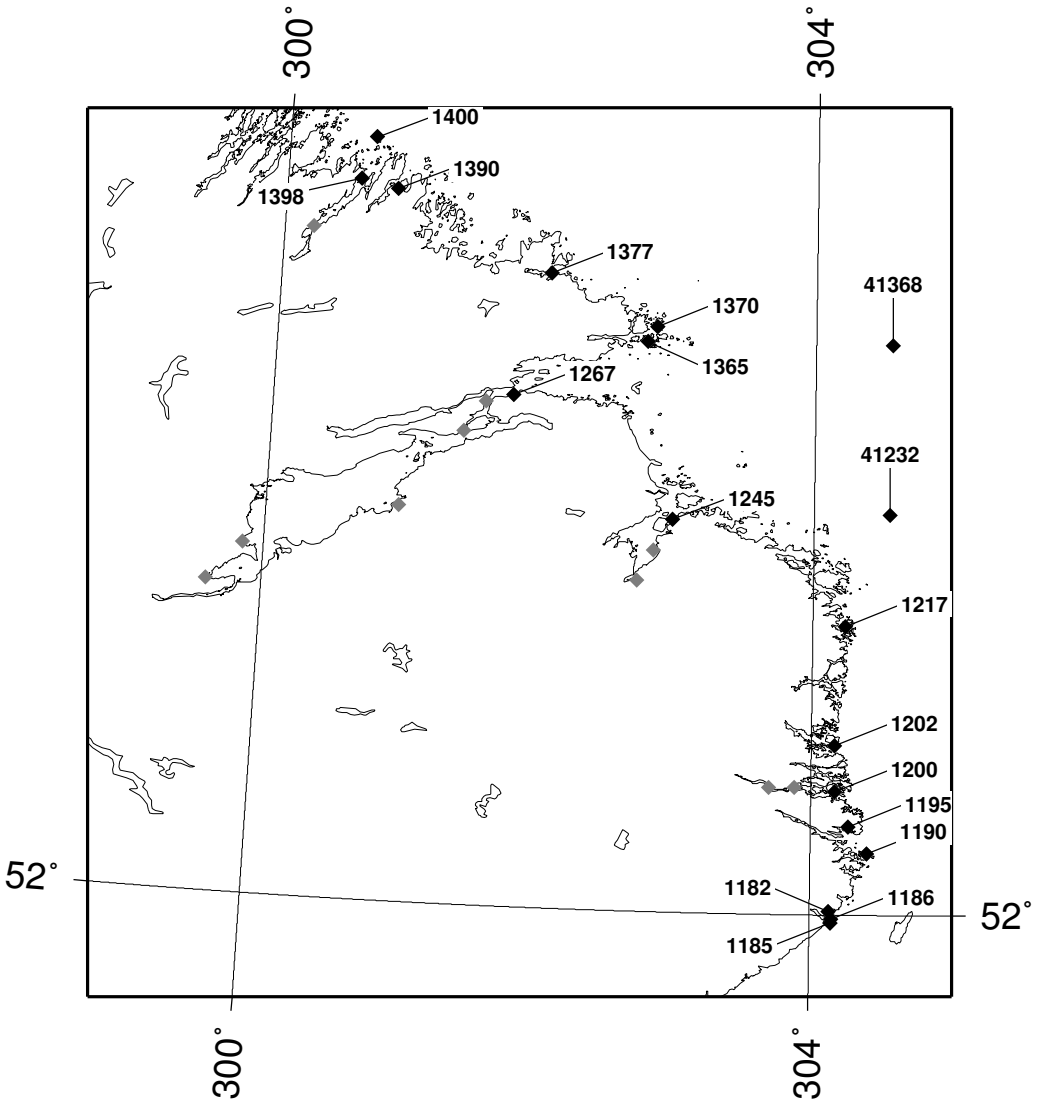

Figure 17: Labrador - South

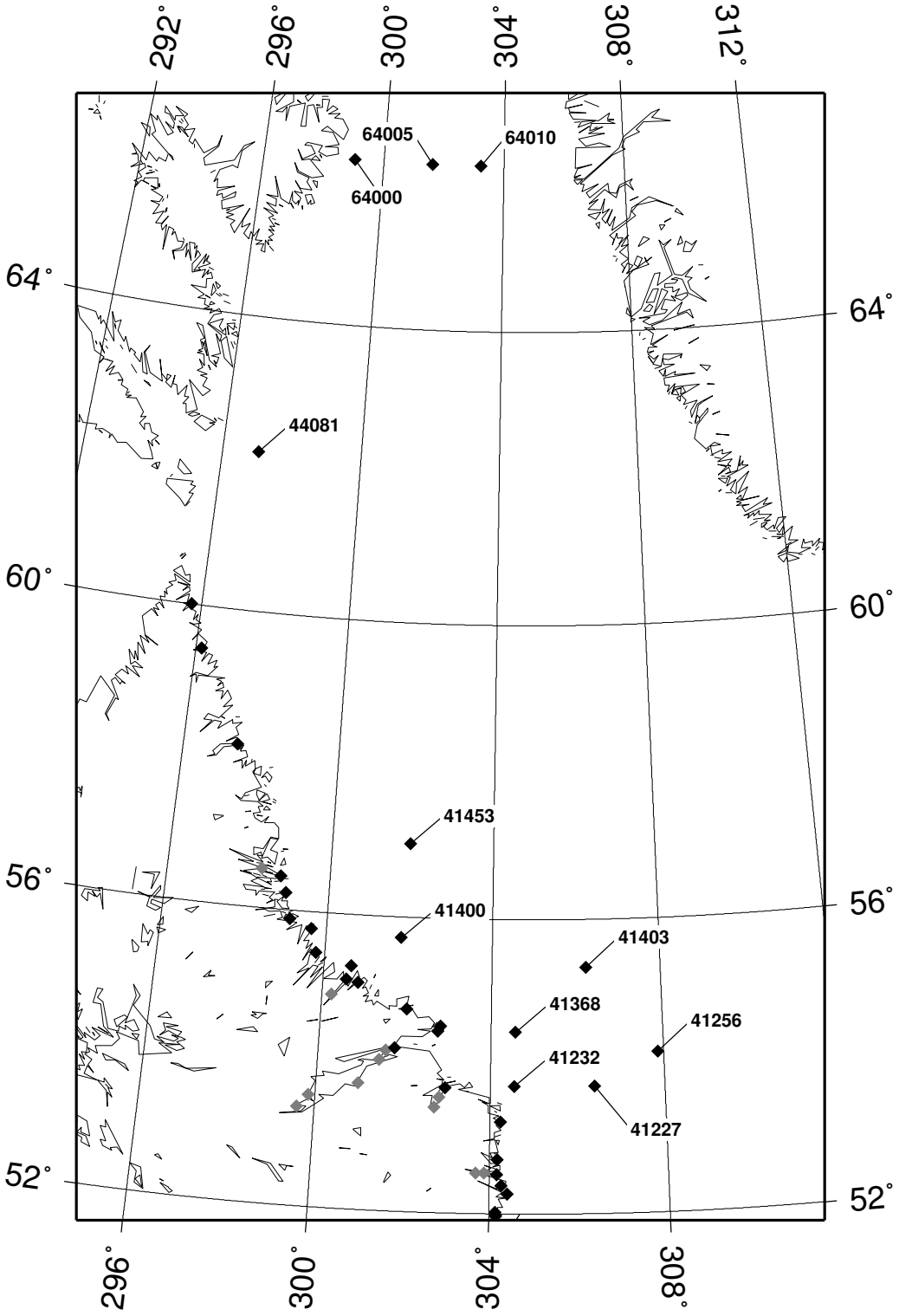

Figure 18: Labrador - Offshore

Stat #	M2 error		N2 error		S2 error		K1 error		O1 error		time *rms*	
	cm	deg	cm	deg	cm	deg	cm	deg	cm	deg	cm	cm
1182	-3.2	-8.2	-1.2	-9.2	-1.7	-0.9	-2.5	-3.7	-2.0	-8.6	5.1	9.3
1185	-4.0	1.9	-1.1	7.0	-1.0	-1.5	-0.5	9.3	-1.4	-1.3	3.6	6.5
1186	-4.3	0.9	-1.2	-5.1	-2.2	0.4	-1.1	4.1	-0.5	0.7	3.8	8.3
1190	-2.8	-9.6	-1.1	-16.0	-1.4	-3.5	-3.0	0.5	-1.7	0.2	5.8	6.6
1195	-2.2	-1.9	-0.7	-2.2	-0.4	-1.7	1.4	5.2	0.1	4.6	2.3	4.6
1200	-2.1	-5.6	-0.6	-9.0	-2.7	-15.6	2.5	13.2	-0.5	-17.6	5.6	7.0
1202	-6.1	-4.7	0.4	5.4	-3.2	-8.8	0.7	-5.3	-1.0	-12.8	5.9	7.7
1217	-3.1	1.0	-0.0	0.1	0.8	-5.2	-1.5	4.3	-0.3	3.5	2.9	7.3
1245	-1.6	4.9	-1.5	1.8	-1.5	9.2	0.1	22.6	-0.5	-9.1	5.3	7.0
1267	-9.7	21.0	0.2	-57.8	-5.1	86.4	0.5	135.1	-1.6	-80.2	30.2	31.3
1365	-3.3	-0.6	0.1	-2.3	-1.9	-0.4	-0.8	9.1	-1.4	5.3	3.2	5.0
1370	-3.0	-0.4	2.3	-12.0	-1.4	-0.4	-0.3	7.0	0.7	-7.5	3.8	5.2
1377	1.1	1.5	-0.9	-1.8	0.5	-4.3	0.6	10.0	-0.3	4.2	2.3	7.5
1390	-5.8	1.4	-1.1	-176.9	-2.4	3.6	-1.2	7.7	-0.3	16.5	20.2	20.6
1398	3.9	3.1	-10.9	102.7	1.9	17.8	-0.5	15.6	-1.1	7.3	13.1	20.3
1400	-7.2	20.1	4.0	-14.1	1.8	7.5	12.1	2.8	17.8	0.2	20.9	32.5
1405	2.0	3.5	-0.2	-0.1	0.4	1.5	-1.9	-3.1	-0.1	8.4	3.6	10.7
1410	-2.9	2.9	1.9	5.0	-1.7	-1.1	-2.2	1.2	-1.3	3.3	4.1	7.7
1416	-5.7	8.6	0.5	18.4	-2.2	2.4	-2.0	5.1	-0.2	4.3	8.9	12.1
1420	-3.8	-0.1	-0.0	1.5	0.5	-0.9	-2.3	-1.8	-0.1	10.2	3.3	11.9
1425	3.8	2.5	0.3	-1.3	0.9	0.8	-3.3	0.5	0.0	7.4	4.2	10.8
1465	4.2	-2.0	1.6	-4.8	0.9	-3.3	-2.0	14.0	1.1	6.6	4.7	14.7
1485	-6.8	-3.2	0.0	-5.3	-3.2	-5.1	0.1	14.6	1.4	0.5	6.6	10.7
1490	-12.6	6.4	5.9	1.0	-4.4	6.9	5.8	17.2	0.4	-24.5	34.4	35.0
41227	-0.2	-0.1	0.6	-3.8	-0.0	-2.0	-0.5	0.0	-0.3	-0.0	0.8	5.9
41232	-0.5	-0.4	-0.1	-1.2	-0.2	-2.8	-0.6	-0.5	-0.5	-2.1	1.0	6.2
41256	0.5	-1.1	0.0	-1.1	0.2	-3.0	-0.6	-1.0	-0.2	-0.9	1.0	20.3
41368	0.2	0.9	1.1	0.8	-0.1	-1.3	-0.7	0.1	-0.3	-1.4	1.2	5.8
41400	0.8	1.0	-0.1	8.1	-0.8	-1.2	-1.1	-4.9	-1.5	-2.3	2.2	4.9
41403	0.7	-1.5	0.4	-2.4	0.3	-3.1	-0.8	0.3	-0.1	-2.5	1.5	8.3
41453	15.8	1.6	3.7	0.8	5.3	-0.2	2.1	3.3	1.7	-1.4	12.7	15.0
44081	1.0	-2.3	4.6	6.0	-0.2	-4.7	0.8	-0.5	0.7	-8.2	7.2	12.9
64000	6.4	-0.3	2.4	-1.4	0.8	2.4	-1.0	41.8	-1.9	49.6	6.2	10.3
64005	0.1	0.4	-0.3	-2.6	0.8	1.7	-1.1	-2.9	-0.4	-9.2	1.6	8.7
64010	1.6	1.4	-0.5	0.6	1.6	1.5	-1.0	4.4	-0.8	1.0	2.9	10.2
Mean	-1.4	1.2	0.2	-4.9	-0.6	2.0	-0.2	9.3	0.1	-1.6	6.9	11.7
Abs	3.7	3.6	1.4	14.0	1.5	6.1	1.6	10.6	1.2	9.2	6.9	11.7
rms	5.0	6.0	2.5	36.5	2.0	15.6	2.6	25.2	3.1	17.8	10.4	14.0

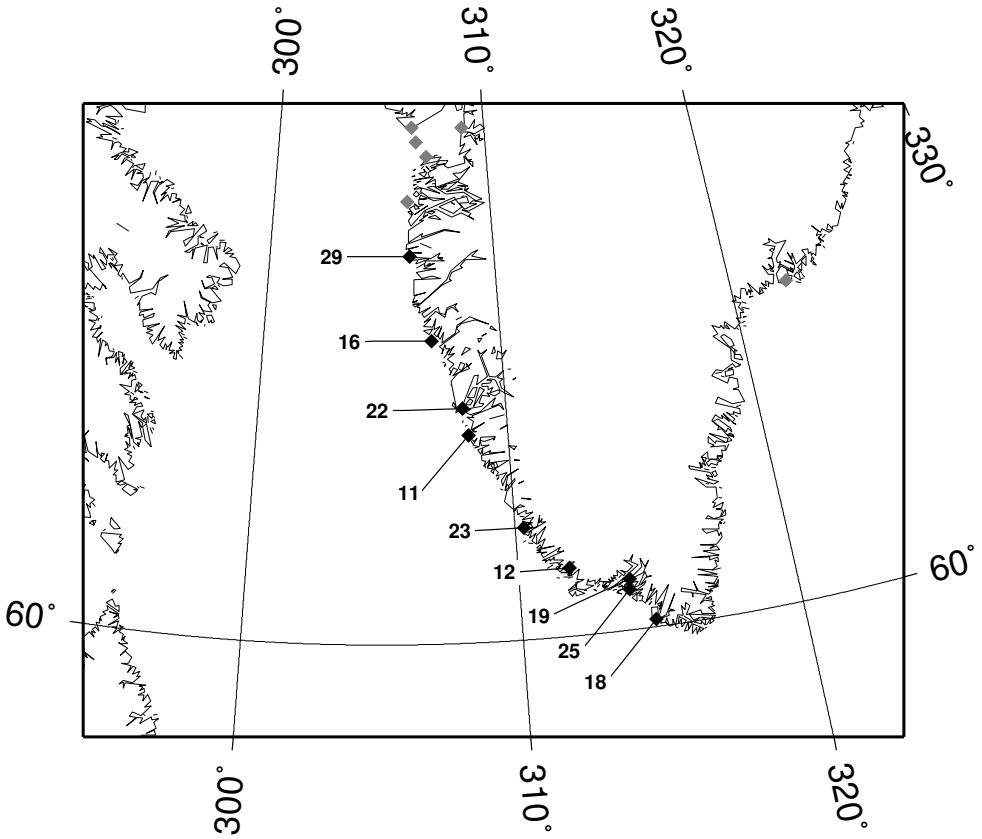

Figure 19: Greenland stations

C.3 Greenland

Stat #	M2 error		S2 error		K1 error		O1 error	
	cm	deg	cm	deg	cm	d eg	cm	deg
G11	-1.8	1.8	-3.2	0.3	-0.7	2.3	0.3	12.9
G12	-4.3	2.6	-0.8	2.7	-1.0	0.8	1.5	-1.1
G16	-9.2	5.5	-4.9	1.9	1.7	9.6	0.7	-0.2
G18	-5.0	-5.7	2.9	-3.8	-0.6	-1.8	3.1	3.5
G19	0.2	-4.4	1.8	-10.4	1.9	-6.6	3.1	-2.2
G22	16.5	1.3	6.5	2.9	0.0	3.3	0.0	3.4
G23	-2.8	-5.7	-1.5	-3.4	-2.5	-3.7	0.5	-7.4
G25	-0.2	4.0	0.5	2.9	-0.8	-0.4	0.1	1.9
G29	-7.9	-1.8	-1.9	-3.1	-1.7	8.2	-0.7	7.6
Mean	-1.6	-0.3	-0.1	-1.1	-0.4	1.3	1.0	2.1
Abs	4.9	3.6	2.4	3.5	1.1	4.1	1.1	4.5
rms	6.7	4.0	3.0	4.4	1.3	5.1	1.5	5.9

C.4 Newfoundland

Stat #	M2 error		N2 error		S2 error		K1 error		O1 error		time *rms*	
	cm	deg	cm	deg	cm	deg	cm	deg	cm	deg	cm	cm
663	3.1	3.5	2.4	25.0	1.1	3.2	1.8	-2.6	0.4	-8.5	4.7	8.8
665	-0.2	-1.1	0.5	-4.0	0.6	-1.6	0.3	10.3	-0.3	2.5	1.4	4.6
666	-3.3	-6.2	1.9	1.8	-4.0	-23.0	1.1	9.5	-0.4	1.1	6.3	8.8
672	0.9	1.8	0.1	0.1	-0.5	2.9	0.3	7.1	0.1	1.5	1.6	6.0
690	-1.4	-3.2	-1.8	-0.2	0.1	-0.5	-0.3	-11.5	-0.5	-7.7	3.1	4.7
710	1.5	0.8	0.7	-1.2	0.7	-4.5	1.0	16.4	1.3	-5.7	2.4	4.3
720	-0.3	0.3	0.3	3.2	0.9	-2.6	-0.3	6.5	-0.7	11.2	1.5	4.8
724	0.6	-0.4	-4.3	5.9	0.9	8.8	-0.1	5.3	0.2	-8.4	4.0	10.3
745	-0.1	-1.6	-2.4	19.5	0.1	-1.8	-0.2	11.7	0.5	0.6	3.6	5.3
755	-6.2	-1.8	0.7	0.4	-5.9	-6.3	4.3	5.9	0.1	25.9	7.3	9.0
795	-1.7	-4.1	-0.4	2.8	-0.8	-5.1	1.8	5.8	0.7	9.5	4.3	7.3
805	-2.3	4.9	0.8	4.9	-0.6	5.0	3.6	-3.2	4.9	11.5	6.2	8.5
810	2.8	11.8	0.6	3.8	-2.5	8.8	1.2	8.1	1.0	12.9	11.3	14.0
815	0.8	-0.8	2.4	-3.9	-1.8	0.8	0.4	3.3	0.0	-4.4	2.5	8.9
818	2.5	-13.1	-0.6	-20.4	-2.4	-17.1	1.0	-7.1	0.8	4.6	13.1	15.3
830	7.4	-4.6	1.6	-8.0	8.2	-12.1	-1.0	13.9	-0.7	-1.4	9.8	11.6
835	1.2	0.7	0.6	1.0	0.2	-2.1	0.4	8.0	1.0	1.8	1.6	10.1
845	3.5	-4.6	0.8	-8.6	5.7	-7.8	-1.6	3.7	0.1	6.6	6.8	8.5
860	-6.8	-1.9	-2.2	21.3	-2.5	-27.3	-0.9	39.1	0.5	-7.6	9.1	22.5
880	1.4	3.2	-0.6	4.7	-1.0	-1.1	0.7	3.3	0.9	0.5	2.8	6.0
890	-0.2	-2.6	1.0	10.6	-1.4	-6.9	1.2	2.9	0.6	-0.7	2.7	5.6
893	1.0	-0.6	0.2	8.3	-1.3	-0.2	-0.0	2.4	1.0	-0.9	1.6	4.6
898	1.3	-0.8	-0.0	7.1	-1.2	0.2	0.1	1.8	1.2	0.4	1.7	4.6
905	0.1	3.3	0.4	5.5	-0.8	1.2	0.4	0.5	1.1	-1.8	1.9	8.0
907	0.5	-1.4	0.3	5.9	-1.1	0.2	-0.1	0.4	0.9	-2.3	1.3	4.3
915	-0.9	-0.6	1.4	3.7	-0.7	-3.7	0.1	-3.5	0.2	0.6	1.6	8.5
920	0.5	1.6	0.9	-0.7	-1.6	0.9	0.5	1.2	1.6	-0.9	1.8	6.4
925	1.5	2.3	0.8	3.3	-0.6	-3.1	0.2	6.2	1.0	-4.1	2.0	5.7
955	-0.9	3.1	-0.3	-2.5	-2.1	2.3	0.1	-8.1	0.5	-2.2	2.3	6.2
970	-0.9	-3.8	0.2	-0.6	-1.0	2.2	0.1	-4.5	0.1	-14.2	2.1	4.9
973	-2.2	7.3	-0.0	12.3	-1.3	5.3	-0.8	-2.9	-0.1	2.6	3.7	5.2
977	-1.7	4.0	0.1	7.2	-0.4	2.8	0.2	-10.2	0.5	-1.7	2.4	5.1
981	-1.8	-1.8	-0.8	-4.9	-1.2	-3.9	-0.6	1.2	0.6	0.4	2.1	6.6
985	0.1	-5.0	-1.2	-5.9	-1.6	-3.0	-0.4	-15.2	-1.5	42.9	3.7	4.5
990	-1.2	-1.4	0.4	7.6	-2.4	4.3	0.0	0.0	0.9	-11.5	2.4	4.9
1003	0.7	0.9	0.5	2.4	-2.0	-4.0	-0.9	-0.2	0.1	8.5	1.9	4.5
1015	-1.9	0.8	-0.5	3.3	-2.6	6.1	-0.3	-0.7	0.1	-11.3	2.7	7.1
1025	-0.2	0.5	-0.8	29.2	-1.3	0.8	0.4	-4.5	1.5	-3.9	2.5	8.1

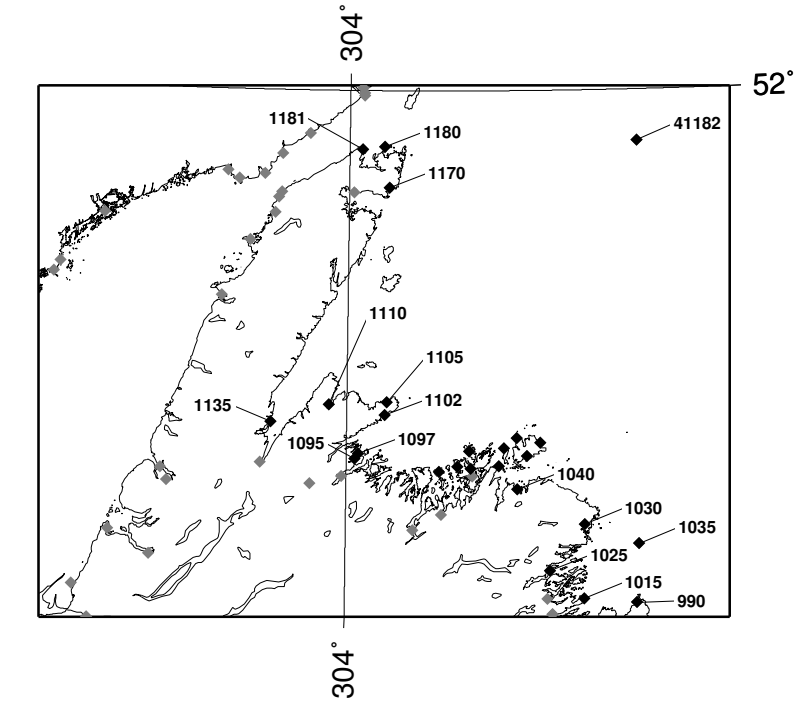

Figure 20: Newfoundland - North

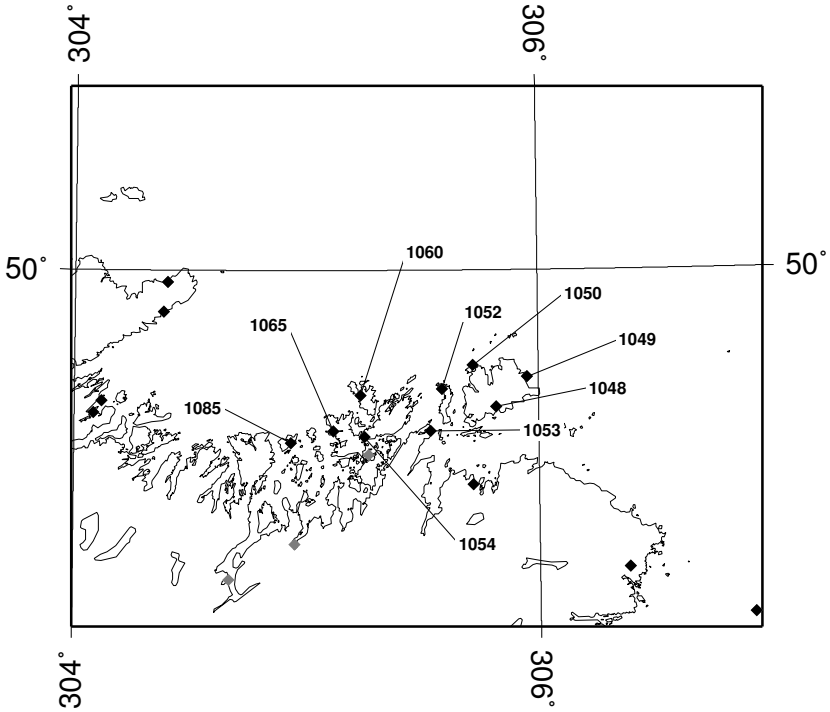

Figure 21: Newfoundland - North (close up)

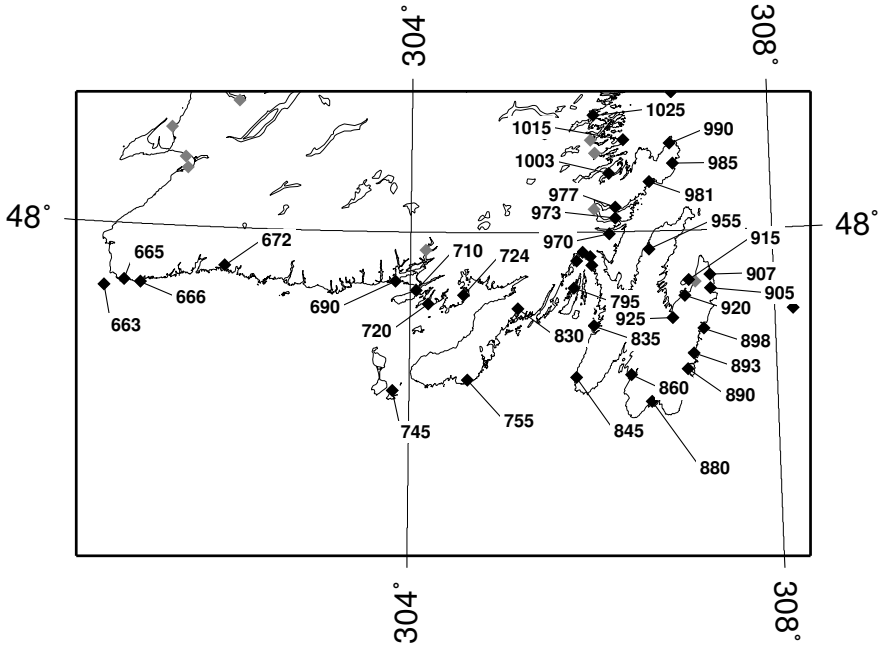

Figure 22: Newfoundland - South

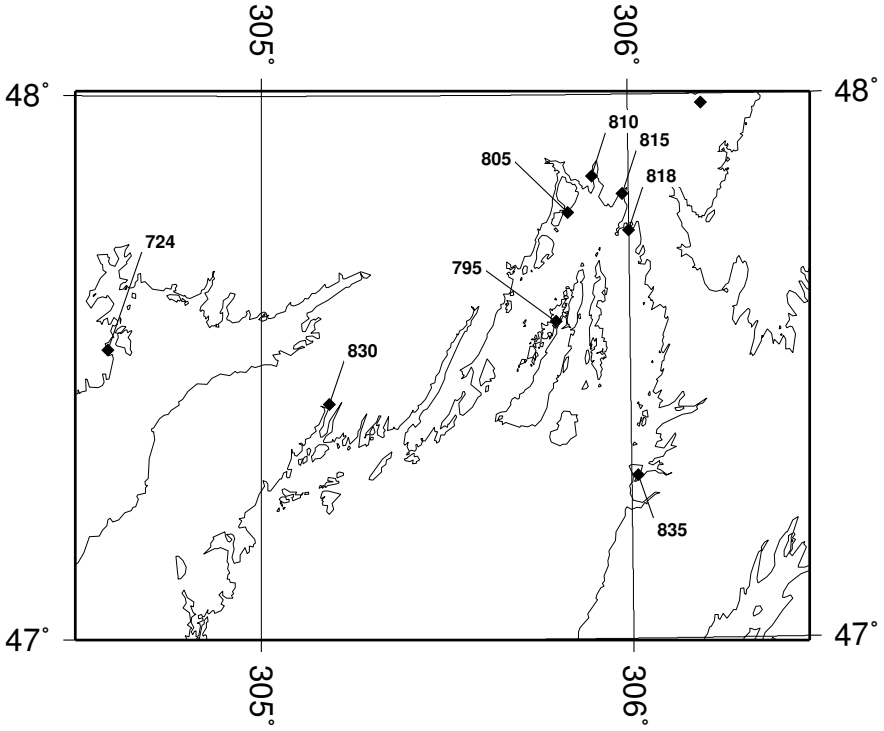

Figure 23: Newfoundland - South (close up)

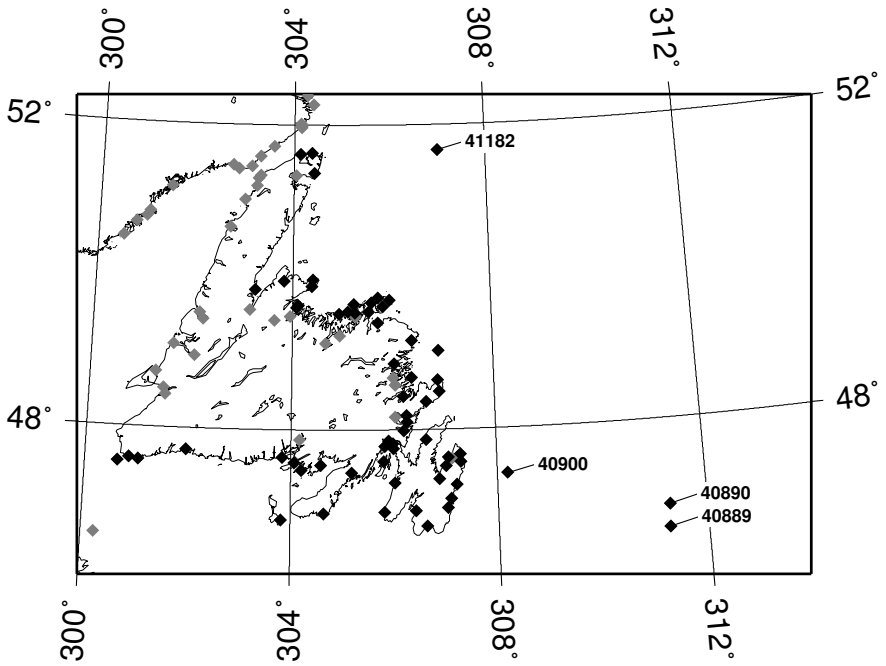

Figure 24: Newfoundland - Offshore

1030	-0.0	-2.2	-0.2	-16.3	-1.2	0.9	1.0	5.8	-1.0	2.6	2.0	3.5
1035	1.5	3.2	0.5	2.2	0.3	-1.6	0.9	8.5	-0.3	-7.8	2.1	5.7
1040	-1.4	0.3	0.2	-1.5	-1.4	-3.5	-0.3	3.0	-0.2	-7.5	1.7	5.0
1048	-3.6	-32.8	-0.6	-30.4	4.4	-7.8	-3.3	34.2	-1.2	-64.5	15.0	16.1
1049	-2.7	0.0	-0.4	0.2	-1.7	5.3	-0.4	3.4	-0.3	-8.1	2.6	6.1
1050	-0.0	-1.2	0.5	-4.5	-1.3	-0.6	-0.3	-0.5	-0.0	-6.2	1.3	5.0
1052	-7.8	4.7	5.1	1.2	-4.8	-10.2	-1.0	17.6	-0.4	-30.4	8.4	22.1
1053	-2.4	2.2	0.4	7.0	-1.6	-1.8	-1.0	0.5	-0.9	-7.2	2.6	7.2
1054	-0.3	16.6	0.1	23.7	0.2	16.0	-1.0	13.6	-0.4	-1.0	8.6	10.2
1060	-0.3	3.8	0.6	5.3	-0.9	1.8	0.3	4.3	0.1	-7.7	2.1	5.5
1065	-2.5	1.9	0.0	5.5	-2.4	-0.4	-0.3	1.2	-0.9	-5.9	2.8	6.2
1085	-0.3	1.4	0.5	5.7	-1.0	2.8	-2.6	13.0	0.3	-0.9	2.4	3.9
1095	-2.8	2.3	0.7	5.6	-1.4	0.7	0.6	4.6	0.2	-17.0	2.9	4.7
1097	-1.8	1.7	-0.5	14.2	-0.9	-1.4	0.1	13.5	0.2	-12.4	2.8	7.6
1102	1.1	5.5	4.0	-18.2	-0.2	3.0	-0.3	6.6	0.5	-12.8	4.7	5.5
1105	-2.6	-3.8	-0.6	-6.6	-2.5	3.0	-1.9	1.1	-1.1	-1.9	3.5	6.1
1110	-0.5	1.0	0.3	-8.8	-1.1	-3.1	-0.5	21.6	-1.7	-10.0	3.0	4.6
1135	-3.7	-2.1	-0.5	-0.9	-1.3	0.6	-1.5	12.2	1.0	5.0	3.5	5.0
1170	-1.0	-2.2	-0.2	3.8	0.1	-4.4	-1.1	2.9	-0.3	-7.3	1.8	5.0
1180	-2.1	-2.9	-0.3	4.3	-0.4	-3.7	-1.2	1.9	-1.1	-25.2	2.4	4.8
1181	-2.4	-5.0	-0.7	-1.5	-1.7	2.7	-1.7	-9.0	-0.9	-20.2	3.0	4.9

40889	0.3	-0.3	0.7	16.3	-0.5	-2.2	-1.3	8.3	-0.6	6.4	1.6	3.5
40890	-0.0	-0.9	0.7	3.8	-0.5	-1.3	-0.8	6.6	-0.1	6.3	1.1	3.3
40900	0.6	-1.0	1.0	0.9	-0.5	-1.6	0.0	0.7	0.7	-0.3	1.1	4.0
41182	-0.2	0.1	0.2	-0.1	-0.1	-1.6	-0.6	-0.2	-0.2	-1.4	0.5	4.5
Mean	-0.6	-0.3	0.2	2.4	-0.8	-1.4	-0.1	4.4	0.2	-3.0	3.6	7.1
Abs	1.7	3.4	0.9	7.1	1.5	4.4	0.8	7.0	0.7	8.3	3.6	7.1
rms	2.4	5.8	1.3	10.2	2.1	6.7	1.2	10.1	1.0	13.4	4.7	8.0

C.5 Gulf of Saint Lawrence

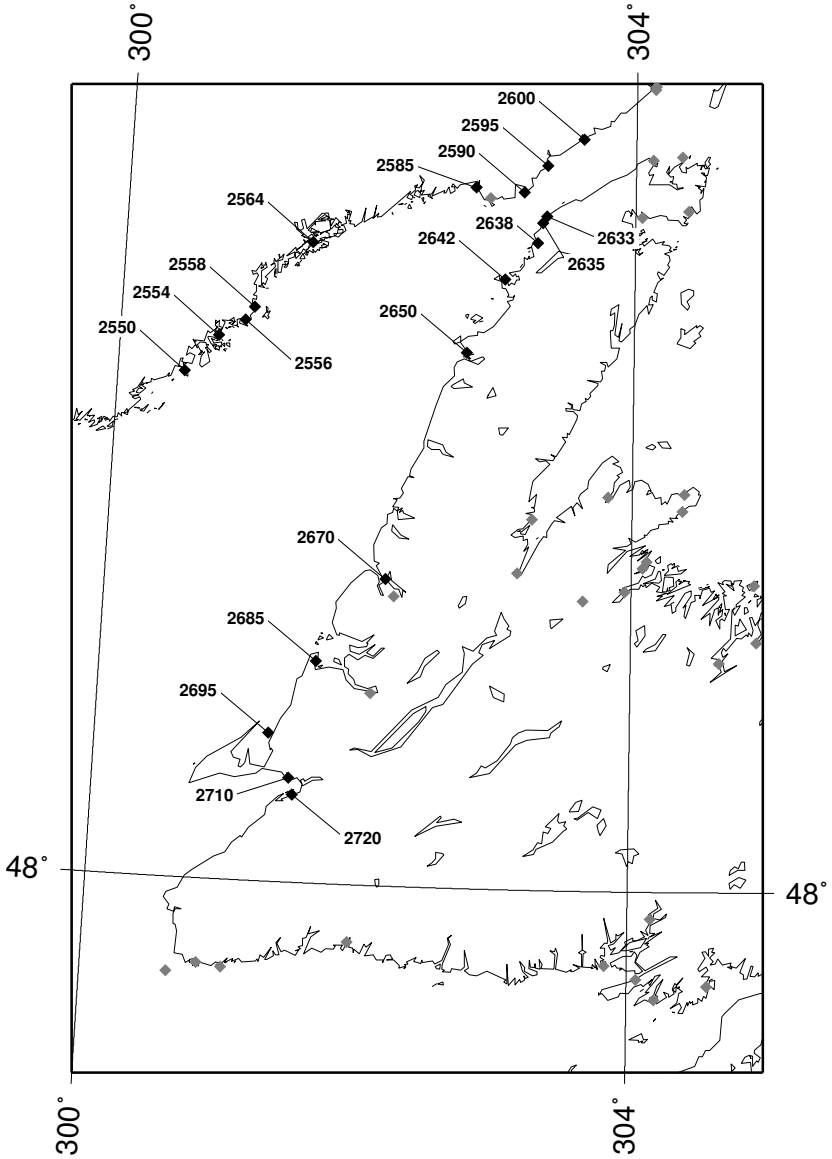

Figure 25: Gulf of Saint Lawrence - Western Newfoundland

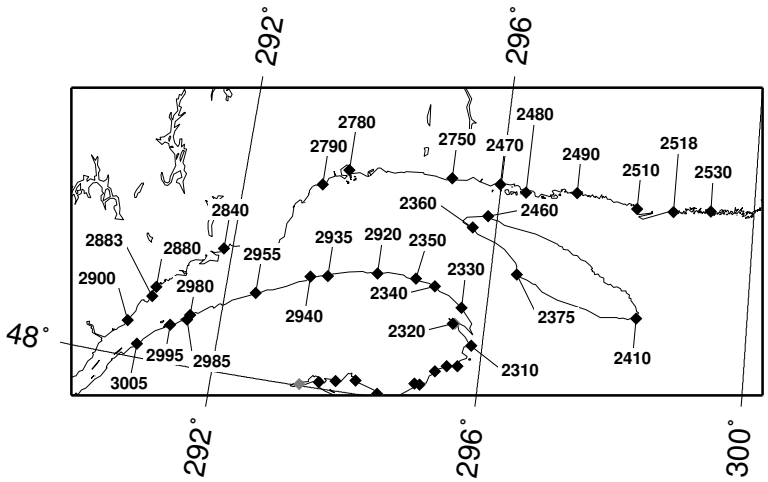

Figure 26: Gulf of Saint Lawrence - Estuary

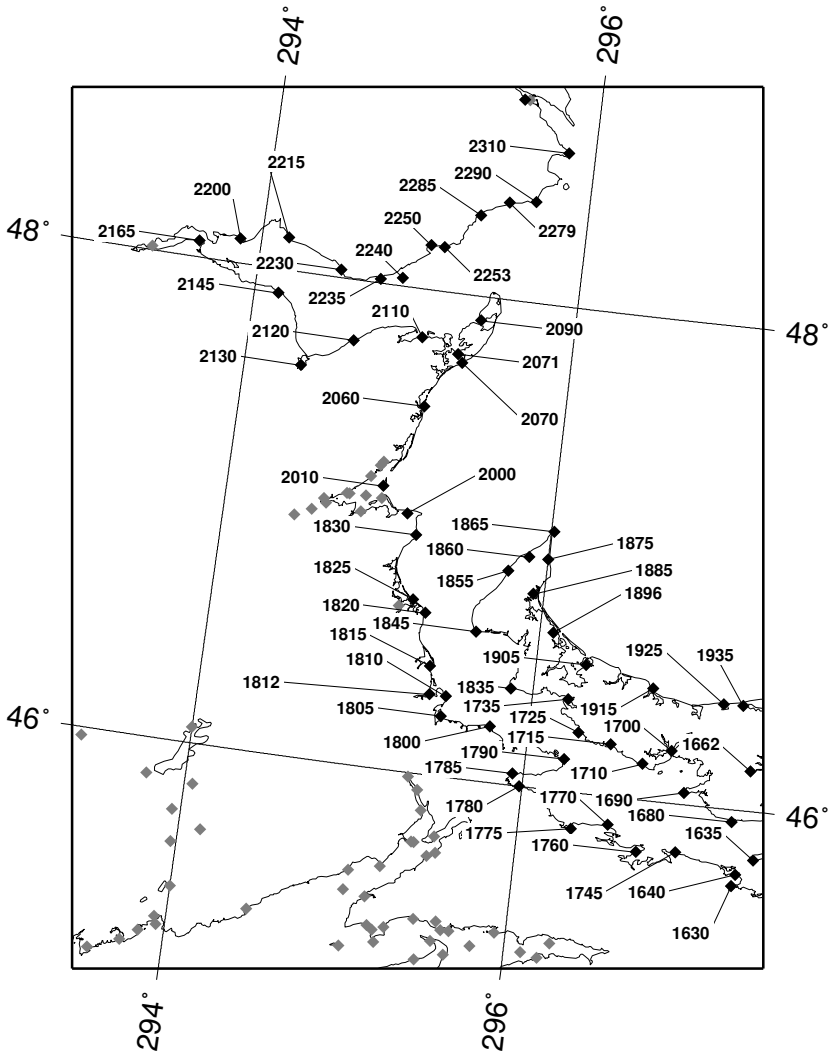

Figure 27: Gulf of Saint Lawrence - New-Brunswick - Western P.E.I.

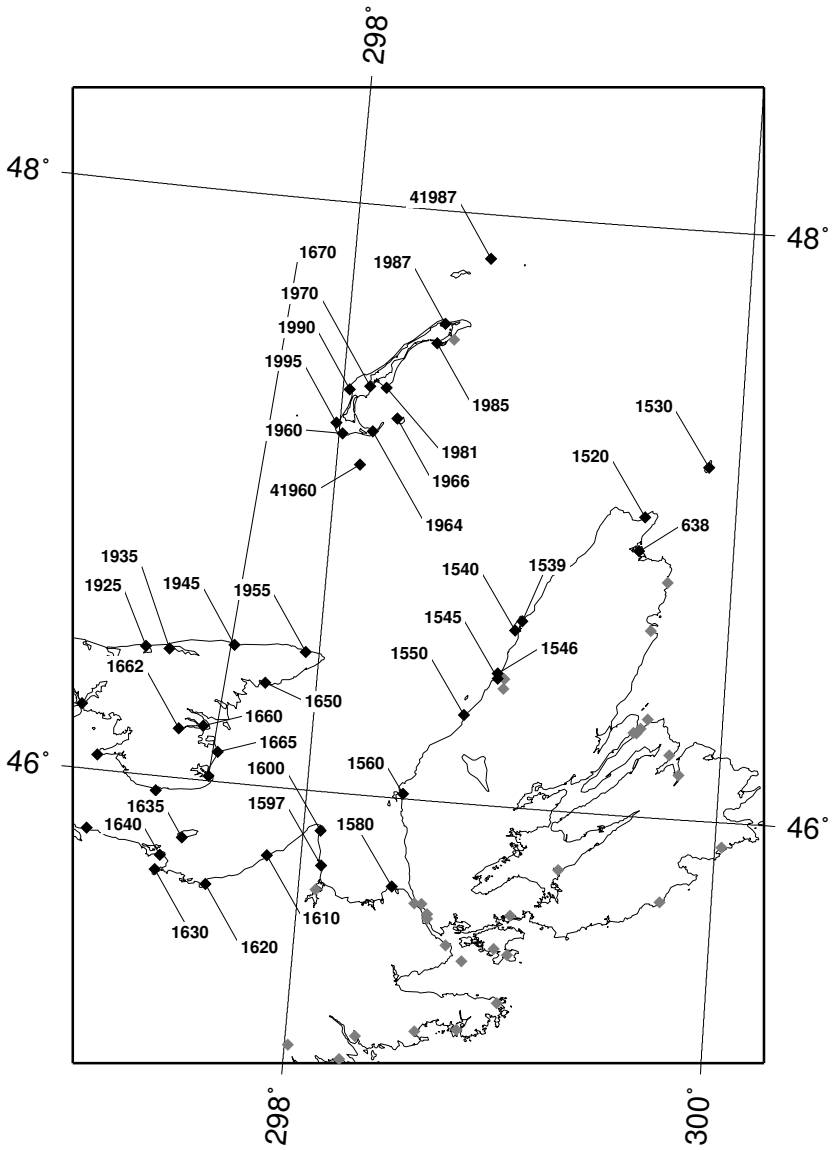

Figure 28: Gulf of Saint Lawrence - Magdalena I. - Cape Breton

Stat #	M2 error		N2 error		S2 error		K1 error		O1 error		time *rms*	
	cm	deg	cm	deg	cm	deg	cm	deg	cm	deg	cm	cm
638	-2.1	-0.3	-0.8	-25.3	0.1	12.0	1.5	-3.5	-0.1	-10.8	3.0	4.9
1520	0.4	7.5	0.5	3.8	0.9	3.7	1.9	19.4	2.3	-6.3	3.9	16.1
1530	0.1	-1.2	0.8	-2.6	1.1	0.2	1.1	-4.5	-0.7	-4.1	1.5	4.6
1539	0.4	-3.7	0.8	15.4	1.4	-4.3	-0.5	12.5	0.7	6.5	2.8	4.5
1540	-2.7	-0.5	1.0	40.5	-0.4	4.9	0.0	-4.6	0.4	-3.6	3.2	5.0
1545	-2.8	1.4	0.5	27.6	0.2	3.7	0.0	2.6	-0.8	2.2	2.7	5.6
1546	-2.1	-3.1	0.6	21.5	0.4	-2.6	0.4	-0.2	-0.2	-0.3	2.2	5.3

1550	-2.4	-2.1	1.8	25.5	-1.0	-2.1	1.1	1.4	1.0	1.0	3.0	5.5
1560	-3.3	1.6	0.9	22.0	-0.1	-3.2	-0.7	1.5	-1.8	0.2	3.3	5.5
1580	-4.4	-12.8	1.2	18.4	-0.5	-13.4	-1.7	-6.0	-0.9	-7.1	6.8	8.0
1597	-4.6	5.4	0.4	39.9	-1.1	-3.1	0.8	1.1	-0.5	-0.0	5.2	8.3
1600	-3.7	1.8	-0.1	31.6	-0.7	2.4	0.4	-2.3	-0.1	-8.6	4.1	6.4
1610	-2.9	4.3	1.1	43.7	-0.2	3.3	1.4	-5.2	1.0	-9.3	5.7	7.8
1620	-2.0	9.6	1.0	60.6	-0.9	23.3	-0.3	2.6	-2.4	1.7	8.8	10.0
1630	-8.4	2.7	0.9	36.2	-0.4	-1.6	0.3	-3.4	-1.8	-1.8	7.8	11.0
1635	-2.5	4.3	3.1	23.0	0.8	16.7	-0.7	-6.5	-1.1	-8.3	5.7	7.9
1640	-0.5	14.8	-1.3	50.1	-0.3	14.6	3.2	2.9	2.6	0.3	10.6	12.9
1650	-1.6	2.2	2.3	32.2	-0.4	5.7	1.6	-2.3	-0.2	-10.2	4.3	6.7
1660	-1.3	5.9	1.6	20.9	1.1	14.1	-0.3	3.5	-1.5	-4.4	4.6	6.7
1662	-2.0	10.5	2.1	36.8	0.1	8.4	0.5	0.3	0.3	0.0	6.9	11.0
1665	-3.3	2.9	1.1	21.6	-0.2	11.8	0.0	-4.3	-0.2	-10.1	4.3	6.6
1670	-3.5	15.6	1.0	52.6	0.0	27.0	-0.9	9.6	-1.2	10.0	11.4	12.7
1680	0.8	11.4	2.7	37.2	-0.5	17.5	0.4	-4.0	0.9	-2.7	10.0	11.5
1690	6.0	15.6	4.5	47.9	1.3	31.0	3.3	-1.3	3.1	-3.8	17.6	19.0
1700	4.3	20.0	4.9	55.0	2.8	24.3	3.2	-0.2	0.4	1.4	21.1	23.4
1710	0.7	20.2	3.2	51.4	1.4	28.1	2.7	-1.2	0.8	-4.6	20.2	21.5
1715	7.0	17.8	3.7	50.9	5.6	24.6	2.5	-4.7	-0.3	-5.2	19.6	21.1
1725	-5.5	24.4	3.9	65.0	2.2	27.5	1.3	4.3	0.1	4.2	19.9	22.2
1735	2.6	24.2	1.5	67.8	3.0	26.7	1.8	-2.5	-1.6	1.2	17.1	19.3
1745	-2.2	15.8	1.2	38.3	-0.6	30.5	0.2	-1.1	0.1	-1.4	13.5	14.8
1760	4.9	18.7	5.1	56.0	1.1	21.6	-0.1	-0.6	-1.6	1.2	19.0	20.1
1770	2.4	20.1	7.1	52.5	-1.7	30.4	1.4	-2.1	0.4	-2.3	20.3	24.9
1775	7.2	27.5	3.1	79.2	3.3	34.2	1.3	-0.4	0.5	-0.7	27.8	28.7
1780	9.5	20.1	5.6	53.5	2.5	27.8	2.4	-0.5	1.3	-2.9	21.9	23.2
1785	35.9	39.3	9.3	100.9	10.4	40.7	2.5	16.3	2.0	12.8	40.5	41.7
1790	-13.3	35.4	-0.4	59.4	-0.4	33.4	-0.6	13.0	-0.8	12.5	26.5	27.6
1800	-3.4	23.4	-1.0	77.9	0.7	26.9	1.7	-7.0	-0.8	-1.9	10.2	12.0
1805	-4.6	37.4	-2.2	85.6	2.4	43.7	2.3	-2.6	0.3	-0.2	10.6	13.3
1810	-3.7	36.7	-2.0	92.2	2.4	35.5	1.0	2.5	0.4	-6.6	9.9	13.1
1812	-1.0	76.9	-2.6	169.0	4.7	5.3	-0.6	10.7	1.9	11.8	15.7	16.8
1815	-5.9	64.0	-4.0	77.8	1.8	-63.3	1.2	5.3	-1.3	4.2	10.0	11.8
1820	-5.1	-15.4	-1.9	37.6	0.2	-12.8	-0.1	0.5	-0.6	3.1	5.6	8.5
1825	-5.3	-0.5	-3.5	44.0	-0.8	14.6	-0.3	6.7	-2.5	8.4	6.4	8.3
1830	-2.1	-3.9	-2.9	29.9	-0.4	5.5	1.0	-0.3	0.1	1.2	3.8	8.8
1835	-4.5	25.1	-0.7	91.2	0.5	39.3	2.7	8.7	-0.3	-4.1	10.8	12.7
1845	3.1	59.5	-3.5	159.3	1.7	-11.2	2.0	-5.1	1.7	0.1	7.8	11.8
1855	1.3	-2.0	-1.5	23.2	1.1	30.7	-1.0	0.8	-1.6	3.5	3.5	6.0
1860	-0.3	-4.2	-2.0	13.4	-0.5	17.5	-0.8	0.5	-1.0	4.8	2.6	7.1
1865	2.9	2.3	-0.3	2.8	1.7	22.1	-1.3	0.1	-3.9	-8.5	4.1	6.0

1875	2.1	-1.4	-1.0	23.0	0.1	11.8	2.0	5.8	-1.6	1.4	3.1	6.0
1885	-2.8	26.5	-0.4	38.0	-0.5	51.1	-1.5	17.7	-1.9	10.5	8.1	8.9
1896	-0.2	40.1	-0.9	85.3	-0.1	62.0	-0.9	18.6	-0.9	16.8	11.8	16.2
1905	1.2	39.6	-1.3	76.7	0.3	65.6	1.2	25.4	-1.4	18.3	12.4	13.2
1915	-1.0	11.7	-0.7	45.6	0.2	28.3	0.3	5.8	-1.4	6.7	4.3	8.4
1925	-4.6	22.4	-1.3	51.8	-0.3	45.9	-1.6	13.7	-3.9	12.8	7.4	9.8
1935	-4.2	5.0	-0.4	55.4	0.1	20.3	-2.3	6.8	-2.6	4.3	5.1	6.4
1945	-0.7	2.4	1.0	37.5	0.9	16.6	0.9	-0.7	-1.4	-0.8	2.8	8.9
1955	-4.1	-3.7	-0.4	33.7	-1.9	-6.2	-0.8	-4.0	0.4	-17.8	5.0	6.0
1960	-2.5	4.3	1.1	-5.7	-0.0	-3.5	1.2	6.7	0.2	3.0	2.5	5.3
1964	2.2	-4.3	2.2	-5.3	1.2	-7.5	0.1	-1.2	-1.3	-2.3	2.8	5.0
1966	-1.7	-2.8	1.2	-16.8	-0.2	8.1	1.9	0.3	1.4	-1.3	2.4	7.1
1970	-1.1	-2.9	1.3	-10.9	-0.1	-8.6	0.9	-0.5	-0.5	0.5	1.8	4.9
1981	-0.7	-0.1	1.2	-3.4	0.5	-1.6	0.6	4.5	0.7	-0.6	1.3	4.4
1985	-2.4	7.8	1.0	-6.0	-0.0	11.5	0.9	-0.0	-0.6	-1.9	2.9	8.9
1987	1.8	33.4	0.4	140.1	1.1	20.8	-2.1	5.0	-1.7	3.9	3.2	5.0
1990	-0.2	59.9	-1.1	38.7	0.5	-23.1	-0.4	0.7	0.0	2.0	1.4	7.6
1995	-1.9	1.4	0.1	-140.6	1.2	-12.6	3.5	10.5	0.0	-7.2	3.6	5.7
2000	0.8	-4.1	-1.5	26.1	0.2	8.2	0.9	-1.1	-1.1	0.0	3.2	7.3
2010	2.5	14.5	-0.9	44.4	0.5	33.4	1.3	3.0	0.2	4.8	7.6	10.1
2060	-5.1	11.4	-2.7	30.4	-1.5	18.9	-1.0	15.7	-3.1	11.4	7.5	8.9
2070	6.9	2.9	0.1	20.5	2.0	11.9	-0.6	4.5	-2.2	7.5	6.2	10.7
2071	16.7	1.8	6.9	13.3	6.9	10.5	0.4	7.2	-0.4	8.8	14.5	16.9
2090	3.6	6.5	-0.2	25.9	0.8	14.2	-0.6	1.0	-0.7	-0.4	6.0	8.3
2110	2.4	6.3	-0.4	18.1	0.7	9.4	1.0	-1.5	-0.1	1.0	5.1	8.1
2120	6.7	2.4	1.9	12.1	1.1	3.8	-0.1	-3.1	0.7	-3.2	5.9	7.9
2130	7.7	18.6	0.3	39.3	1.7	26.5	-0.4	0.9	-1.6	14.9	16.5	18.4
2145	8.2	1.2	1.9	24.6	2.9	5.0	0.3	-2.7	-0.5	-1.4	8.0	10.6
2165	17.3	4.9	4.0	25.8	2.9	12.8	1.7	-4.3	-0.5	-1.0	15.1	17.9
2200	12.3	2.8	3.8	17.4	3.5	9.4	2.0	-2.9	-0.4	-1.2	10.9	12.6
2215	7.3	2.8	2.2	31.8	-0.1	15.0	0.1	-4.5	-0.4	-2.7	8.8	11.7
2230	6.8	2.3	0.7	19.1	-1.0	6.8	-0.8	-2.5	0.0	0.1	6.3	10.1
2235	7.6	1.0	0.1	19.4	1.5	7.7	1.6	-0.6	-0.1	-3.6	6.6	9.4
2240	2.4	0.8	-1.1	-3.7	0.2	8.7	0.9	-5.1	-1.1	1.3	2.8	9.5
2250	2.7	6.6	-0.2	24.5	1.0	6.2	-0.4	-1.8	-2.1	1.8	5.4	7.6
2253	2.7	0.5	-1.0	11.6	-0.2	7.4	0.7	-1.9	-0.9	-0.7	2.9	7.0
2279	-0.1	1.1	-1.0	19.9	-1.3	13.9	-5.3	4.0	-3.0	-17.1	5.6	6.3
2285	-0.5	7.7	-1.0	25.5	-0.0	21.6	3.9	2.4	0.3	4.1	5.8	8.3
2290	1.7	0.9	-2.0	14.3	-0.0	1.6	-0.4	-0.2	0.4	1.3	2.4	7.1
2310	0.2	3.0	-0.1	17.9	0.4	3.7	1.6	-2.5	-0.6	-2.5	2.6	7.3
2320	-0.4	-2.5	2.5	7.7	1.8	3.6	1.6	-2.1	-1.1	-7.9	3.4	5.8
2330	0.5	-0.5	2.3	8.5	0.9	1.4	0.1	-3.1	-0.6	-5.7	2.6	7.4

2340	0.6	0.5	2.2	16.6	-0.1	-6.2	2.2	2.0	-0.4	-2.9	3.8	6.8
2350	-4.9	2.9	0.3	-1.5	1.4	13.3	-0.5	-5.7	-0.8	-3.6	5.7	8.7
2360	-2.4	6.7	3.8	23.0	1.9	6.5	-3.3	-4.0	-0.5	-2.5	8.3	16.2
2375	0.9	2.0	0.8	8.3	1.0	-0.1	-0.3	-6.1	-1.4	-7.3	2.9	7.5
2410	2.9	-9.0	0.3	-7.7	1.7	-3.9	-0.2	16.2	-3.2	-48.9	8.4	9.4
2460	1.9	0.6	0.1	-1.6	0.1	4.8	0.3	3.0	-3.3	-3.6	2.8	5.8
2470	0.2	-4.7	-0.8	-4.6	1.0	-10.1	-2.5	-2.7	-2.3	-1.5	5.1	7.4
2480	-2.4	2.2	-0.2	5.7	0.4	-1.0	1.7	11.0	0.4	3.2	3.6	6.8
2490	-4.7	3.5	-1.9	-4.5	0.3	-2.9	-0.7	2.2	-2.2	-4.3	4.6	6.7
2510	-0.7	1.0	-0.8	9.4	0.6	0.4	1.3	0.6	-1.6	-0.0	2.0	6.4
2518	-3.1	8.9	0.3	8.1	-0.8	6.0	-0.5	5.5	-1.1	3.8	5.9	9.8
2530	-9.8	7.8	1.5	-23.0	1.4	13.1	-0.5	-1.9	-4.8	3.9	9.6	10.6
2550	-1.3	-1.0	-0.2	-8.6	1.8	-4.0	0.9	2.4	-0.7	-2.1	2.4	7.2
2554	-5.1	1.8	-0.2	6.1	-0.6	-2.2	0.1	1.1	-1.6	-0.2	4.2	9.4
2556	-3.5	0.9	0.1	0.7	0.3	-6.9	0.2	-0.7	-1.6	2.9	3.2	7.5
2558	0.8	1.2	0.4	-9.4	2.6	10.0	1.2	3.6	-0.3	-8.9	3.7	5.9
2564	-4.8	18.7	-3.6	49.2	2.7	12.2	-2.8	6.8	-0.2	10.2	15.9	18.1
2585	-6.0	-4.8	-1.5	-9.3	2.0	3.2	0.7	0.3	-3.2	1.9	6.2	7.8
2590	-0.8	-1.2	-0.2	-9.9	1.5	3.2	0.4	6.6	-0.9	-3.6	2.1	7.1
2595	-3.1	10.9	0.4	9.0	-0.7	9.4	-1.4	12.5	-1.2	13.7	6.0	7.9
2600	-0.1	0.6	-1.0	-3.3	-2.9	9.4	-2.7	11.6	0.8	10.4	3.5	4.1
2633	1.6	-6.1	0.8	-20.2	2.2	-2.5	1.1	-9.9	-0.4	-12.0	4.2	7.7
2635	-3.2	-7.1	0.3	-23.0	0.4	-12.4	-0.0	-8.5	-2.3	-7.0	5.2	7.2
2638	-6.1	-4.2	-0.8	-16.6	-0.2	-11.2	-1.0	-7.4	-2.0	-0.2	5.8	8.0
2642	-3.7	-1.5	-0.2	-15.7	0.9	-9.0	-1.0	-1.2	-1.2	1.2	4.1	6.9
2650	-2.9	-9.4	0.6	-24.2	2.0	-12.6	1.3	-3.2	-1.4	-6.5	8.6	9.8
2670	-2.1	-4.1	-2.4	-15.9	0.9	-6.7	-0.6	-0.7	-2.8	-1.3	4.7	6.4
2685	-0.7	0.2	-0.4	-8.6	1.5	-3.1	0.5	0.1	-0.2	-0.1	1.8	7.7
2695	2.0	1.9	2.0	-12.7	0.4	4.2	-2.3	20.1	-1.2	-5.1	4.4	6.1
2710	-1.2	6.6	-0.3	16.3	0.8	2.3	0.9	10.7	-0.4	6.3	4.2	6.5
2720	-2.9	-8.1	-0.9	-18.9	0.3	-9.8	-2.0	-1.2	0.2	-3.8	5.3	8.1
2750	-1.7	0.3	2.6	15.3	-0.4	-3.3	1.7	5.9	-0.2	-3.7	4.4	7.5
2780	-1.3	1.7	3.3	3.0	2.0	1.2	-0.7	-1.7	-0.9	-2.1	3.7	10.4
2790	-0.9	1.5	6.4	-1.8	1.5	-1.5	0.1	5.6	0.2	-2.7	5.4	11.1
2840	-3.0	1.5	3.6	1.1	2.9	0.8	-1.9	-4.3	-0.8	-3.4	4.9	11.9
2880	0.2	0.4	-0.8	1.0	-0.2	-0.4	-3.1	-1.4	0.7	-1.3	2.3	14.3
2883	-9.7	5.8	3.1	14.7	-5.2	0.4	-5.3	2.6	-1.0	1.8	14.4	18.9
2900	-12.4	-1.3	0.1	-5.7	0.8	-5.1	-5.1	-6.0	-1.7	-4.4	10.7	14.7
2920	-0.4	-2.0	0.4	1.9	0.6	-4.0	-3.4	-9.3	-2.6	-6.1	4.3	8.7
2935	-1.7	0.9	3.1	1.7	1.7	0.6	-0.9	-5.5	-0.6	-3.4	3.5	10.7
2940	-5.7	0.7	3.7	3.7	-0.2	-3.2	-2.7	2.5	-1.3	-3.9	5.7	12.3
2955	0.1	-1.4	4.2	-0.4	-2.0	-2.8	-1.8	-17.4	-2.3	-5.9	6.3	9.3

2980	-5.1	0.7	5.9	-2.7	3.8	0.1	-2.1	-6.3	-0.7	-5.0	6.9	13.4
2985	-4.8	1.0	5.3	-4.8	2.6	0.5	-2.8	-8.4	-0.4	-5.5	6.7	13.9
2995	-9.8	-1.0	2.0	-4.2	0.6	-3.8	-5.2	-9.3	-3.0	-4.1	9.1	13.1
3005	-21.5	-2.0	2.2	-10.1	-2.8	-4.1	-6.9	-5.5	-3.7	-0.2	17.6	20.7
41960	-1.9	1.6	1.3	21.5	0.6	-3.9	0.4	1.6	-0.5	0.2	1.9	4.8
41987	-1.3	0.2	0.2	-23.0	0.6	-4.9	0.4	-2.7	-0.7	-1.8	1.4	3.8
Mean	-0.6	7.4	0.8	22.8	0.8	8.4	0.0	1.2	-0.8	-0.7	7.3	10.4
Abs	3.8	9.5	1.7	30.2	1.3	13.1	1.4	4.9	1.2	4.9	7.3	10.4
rms	5.8	16.5	2.4	43.2	1.9	18.7	1.8	6.8	1.5	7.4	9.5	11.9

C.6 Atlantic Nova Scotia

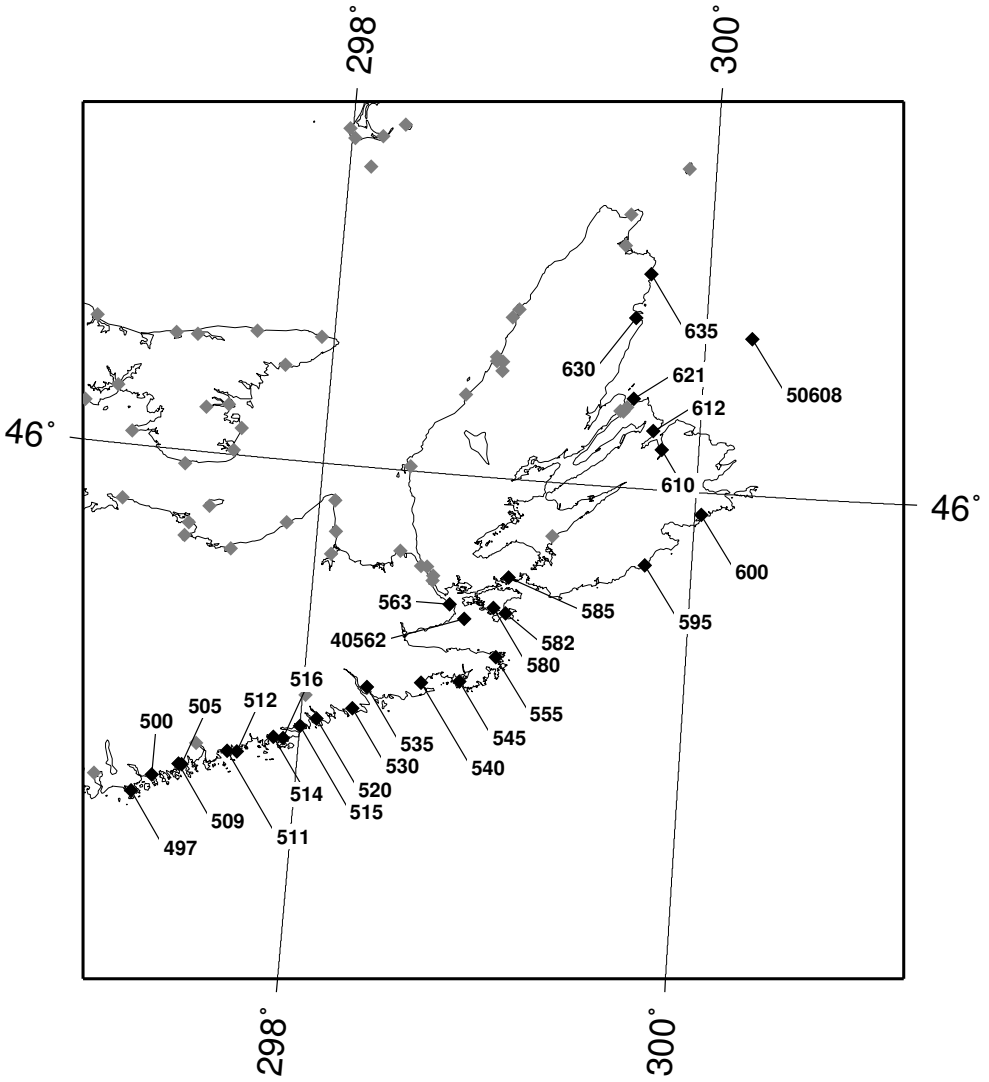

Figure 29: Nova Scotia - East

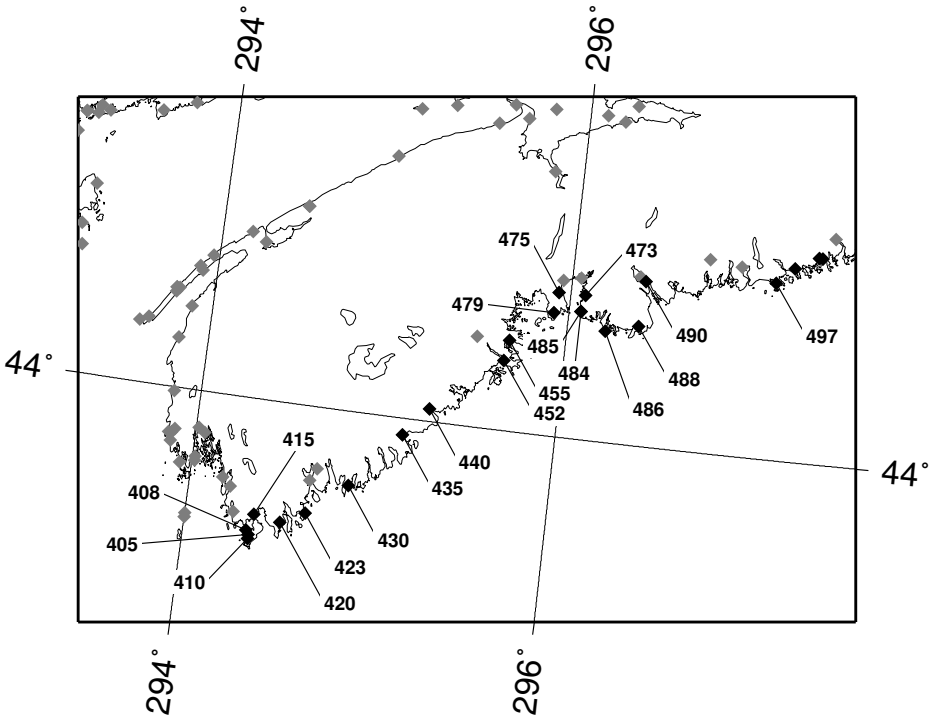

Figure 30: Nova Scotia - West

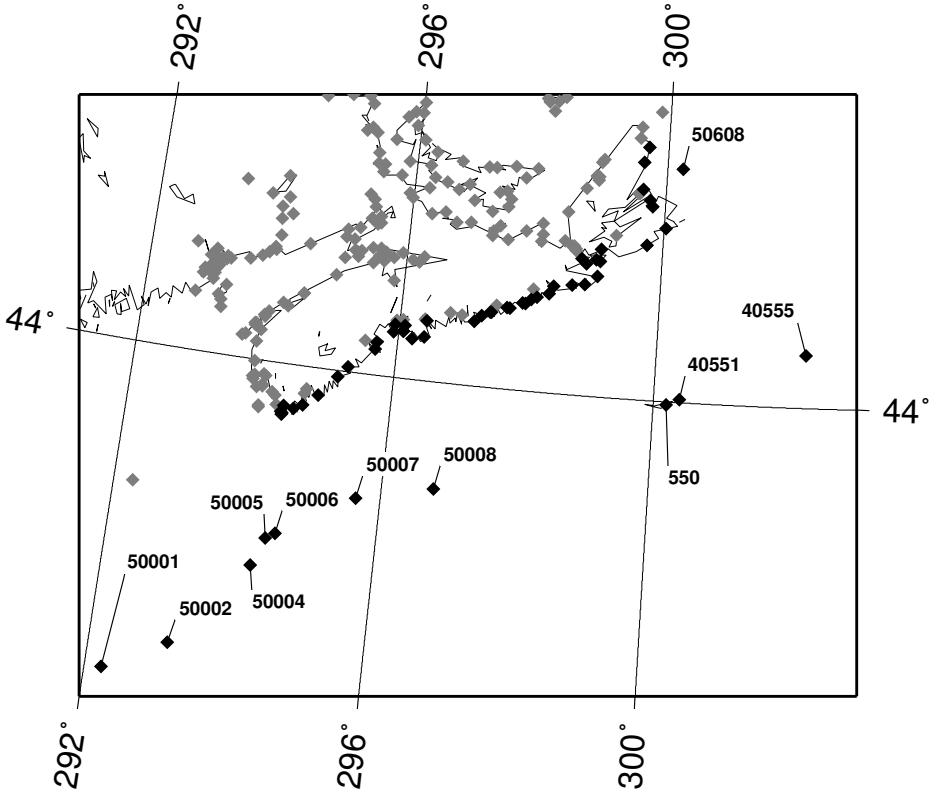

Figure 31: Nova Scotia - Offshore

Stat #	M2 error		N2 error		S2 error		K1 error		O1 error		time *rms*	
	cm	deg	cm	deg	cm	deg	cm	deg	cm	deg	cm	cm
405	5.6	3.4	-1.0	-4.6	-1.3	4.4	0.7	4.7	1.2	7.1	6.6	10.1
408	5.5	2.7	2.6	-1.8	3.2	1.7	-0.6	4.9	1.4	5.0	6.3	11.2
410	4.8	9.5	2.7	2.4	0.4	9.6	0.5	11.8	-0.9	8.6	13.2	14.6
415	-7.9	6.3	-2.8	12.7	-4.8	6.5	-0.8	-0.9	-2.2	-1.1	10.3	11.1
420	-6.6	4.5	-0.1	3.9	-1.2	5.6	-1.0	2.2	-0.7	17.8	6.9	7.9
423	-6.5	4.4	-3.7	2.1	0.7	-1.4	-2.8	4.5	-1.0	2.9	7.1	13.0
430	-1.9	-1.6	0.8	-1.0	-0.9	-3.4	-1.3	-2.1	-0.7	-6.8	2.5	4.6
435	-5.2	1.4	0.9	4.4	-2.7	2.3	-1.5	2.6	-0.6	-3.6	4.6	5.9
440	-1.7	-0.9	-0.5	-0.4	-0.5	-1.1	2.5	-6.5	0.5	36.7	3.6	7.8
452	0.4	0.9	1.0	0.3	1.6	0.5	-2.2	5.2	0.2	4.4	2.3	7.9
455	-0.5	-3.3	0.3	-3.0	-0.5	-8.1	-1.2	-2.3	-0.0	11.3	3.3	8.0
473	-2.3	-2.0	-1.8	-0.5	-2.3	-3.8	-0.8	-1.1	0.0	2.0	3.3	6.3
475	-0.5	-3.9	-0.9	-5.8	-0.5	-6.0	-1.3	1.7	-0.1	2.3	3.8	13.0
479	-2.0	3.6	-0.4	3.8	2.2	14.0	0.2	-10.5	-2.0	22.7	5.0	9.6
484	-0.1	0.7	-0.8	2.2	-1.2	-1.6	-0.6	0.8	-0.1	-1.7	1.3	6.5
485	-2.9	1.9	-4.7	-18.5	-3.8	21.8	-0.7	1.7	-1.4	19.2	6.8	7.9
486	-4.2	-1.1	-0.4	-5.3	-0.4	2.6	-0.6	0.5	1.2	7.7	3.5	8.2
488	-0.1	-2.5	-2.4	-4.1	-1.2	-7.2	-0.1	-0.9	-0.2	-5.2	3.1	5.8
490	0.7	0.2	0.0	0.1	-0.0	-0.4	-1.1	0.9	-0.6	5.2	1.0	6.9
497	-6.0	-2.4	1.3	6.1	-6.7	5.0	-2.9	-5.7	-1.4	-34.9	7.2	15.4
500	-0.6	-0.5	0.7	0.5	1.6	-0.4	-2.7	4.8	-0.6	2.5	2.2	7.6
505	1.3	-2.4	-1.5	-2.9	-3.3	4.3	0.2	-0.0	-0.5	0.8	3.4	6.8
509	-0.8	2.8	-0.1	2.6	-2.3	7.7	-0.4	15.1	-1.6	3.8	3.6	6.5
511	0.1	-0.9	0.6	1.2	-0.9	1.3	-0.8	-3.7	-1.3	-12.4	1.5	4.7
512	0.2	-0.8	3.3	1.4	2.7	3.8	-1.1	-8.3	-0.0	-4.5	3.4	6.4
514	-0.9	1.0	0.4	0.3	-1.3	0.3	-1.1	-1.1	-1.3	-11.7	1.8	7.5
515	-0.5	0.5	-1.1	-1.2	-1.9	-1.1	-1.1	-7.4	-1.0	-22.0	2.2	6.3
516	-9.9	0.1	-3.3	-6.4	-3.9	-8.4	-1.2	-1.2	-0.2	-7.0	8.3	10.6
520	0.2	2.5	-0.6	1.9	-1.5	0.6	-1.5	-4.3	-0.4	-12.3	2.6	6.8
530	0.1	-2.2	2.1	4.4	-1.5	-9.5	1.6	-4.4	-1.5	-18.8	3.4	6.7
535	0.2	-1.4	0.4	-0.6	3.6	3.7	0.1	-13.2	-0.4	-17.0	3.3	6.3
540	1.7	-0.3	0.1	5.5	-0.6	-1.5	-2.6	3.8	-0.5	-21.6	2.5	5.2
545	0.6	0.6	1.1	2.2	1.9	1.2	-2.6	-3.7	-0.6	-12.0	2.5	7.5
550	-0.5	2.4	0.0	5.2	0.7	2.1	-0.1	42.0	0.6	-63.8	2.7	6.0
555	3.2	2.6	-2.1	22.8	0.5	-2.4	-1.3	-15.2	-2.2	-25.6	5.1	6.8
563	2.4	-0.1	-0.5	-4.3	-0.4	5.8	-0.3	-11.3	-0.5	-16.1	2.5	8.2
580	1.0	-2.8	-0.3	5.4	-0.2	11.3	-0.4	-11.4	-1.4	-29.5	3.4	5.6
582	4.2	2.2	1.7	2.4	-2.4	18.4	0.2	-13.1	0.1	-12.9	5.1	8.0
585	1.2	7.2	-0.4	14.4	-1.3	15.4	-1.7	-14.7	-1.0	-33.4	6.5	7.8
595	-4.3	-3.8	-0.5	-3.6	-4.8	-5.2	0.7	-5.7	-0.4	-23.8	5.4	7.7

600	0.5	0.9	1.0	2.3	1.6	1.7	-0.8	-18.4	0.4	-9.7	2.1	7.1
610	-0.4	0.5	0.4	11.9	-0.4	11.8	0.9	0.2	-0.5	-3.6	2.0	3.2
612	1.5	1.7	1.0	3.0	0.8	3.3	0.9	-5.1	-0.1	-2.9	1.8	6.2
621	-0.9	0.3	-0.1	-6.4	-1.9	5.6	-0.0	-5.9	0.3	-4.1	1.8	5.3
630	3.0	5.5	0.4	8.2	0.5	11.4	0.7	-6.1	0.6	-1.9	3.8	4.4
635	-1.5	5.5	0.3	0.2	-1.0	9.3	0.6	6.3	-0.4	-7.7	2.9	5.0
40551	-0.2	-4.1	0.5	-13.0	-0.9	0.2	-0.2	16.1	0.9	-32.5	3.2	5.1
40555	1.1	0.5	-1.2	7.3	-2.4	10.4	1.3	10.5	0.7	-2.6	2.8	3.5
40562	-0.7	160.9	0.8	-166.7	1.1	143.1	0.7	159.0	-0.2	145.9	86.1	87.8
50001	4.1	2.2	-0.2	5.3	1.3	0.3	-1.3	-1.3	-2.2	-27.6	4.2	6.0
50002	4.3	-2.1	-0.3	-13.4	-2.0	0.7	1.5	-12.0	-2.4	-7.2	4.5	5.1
50004	0.5	-3.1	-1.6	-6.8	-1.4	6.1	0.1	9.6	-0.3	12.8	2.7	3.2
50005	2.1	-2.3	-0.5	7.3	1.6	-2.6	-3.5	13.6	-0.5	15.0	3.6	5.0
50006	2.0	-4.6	-0.6	6.6	1.8	-4.1	-3.6	14.6	-0.3	15.2	4.4	5.9
50007	2.0	-1.5	-0.2	8.4	1.9	-2.6	-2.4	20.1	0.7	14.6	3.4	4.7
50008	1.6	-2.7	-0.9	-12.6	-2.1	2.6	1.6	6.4	0.9	9.9	3.4	4.2
50608	0.7	0.5	1.1	4.1	1.0	1.9	1.6	-8.1	0.0	-8.6	1.8	3.3
Mean	-0.2	3.3	-0.2	-1.9	-0.6	5.0	-0.6	2.8	-0.4	-2.3	5.4	8.5
Abs	2.2	5.1	1.1	8.0	1.7	7.5	1.2	10.0	0.8	15.4	5.4	8.5
rms	3.1	21.5	1.5	23.1	2.1	20.2	1.5	23.3	1.0	26.0	12.3	13.9

C.7 Gulf of Maine

Stat #	M2 error		N2 error		S2 error		K1 error		O1 error		time *rms*	
	cm	deg	cm	deg	cm	deg	cm	deg	cm	deg	cm	cm
1	-21.7	-5.9	-21.0	4.3	5.5	13.7	-1.8	-9.9	-1.3	-22.2	28.5	29.3
4	-2.5	2.1	1.2	-2.4	-4.5	-1.3	0.4	3.9	0.9	-1.8	6.6	13.0
5	-17.0	3.0	1.6	-6.3	-5.9	-2.9	0.0	8.6	0.3	2.2	15.9	20.6
6	-10.4	7.8	-2.7	5.5	-1.4	4.0	-1.0	12.2	-0.8	7.7	15.2	16.8
7	2.0	4.5	2.7	-1.2	-3.6	-3.4	-0.0	5.2	0.7	0.4	12.7	16.8
10	-0.1	3.5	-17.0	-0.4	1.4	-5.1	1.9	9.4	-1.7	0.1	17.2	23.4
11	-17.6	3.3	1.8	-3.9	-3.8	2.0	-0.5	2.2	0.4	-5.4	16.4	24.4
15	10.9	6.6	1.4	2.0	-5.4	2.7	-0.1	7.6	0.5	0.2	23.7	28.7
20	-10.8	1.4	4.9	-8.2	-0.4	2.4	-1.9	1.1	0.5	-3.9	11.4	23.4
21	-7.2	2.6	3.9	-4.0	-6.9	-3.2	-0.5	6.1	-1.0	-3.0	11.9	21.2
24	7.8	4.3	6.4	-10.4	1.0	4.7	-0.6	6.7	0.4	5.9	17.6	27.1
28	8.3	11.7	3.5	11.4	-3.0	8.7	0.8	6.9	-1.7	12.9	40.7	44.6
29	8.8	7.8	0.2	1.9	-1.2	0.3	1.8	8.5	1.3	2.0	26.8	31.8
30	-2.9	3.2	7.5	-4.3	2.8	-3.7	-2.3	8.9	-2.2	7.4	12.8	15.0
33	3.2	5.1	-1.3	-2.4	-6.0	2.6	0.9	2.7	0.4	1.7	17.9	23.8
42	-5.3	3.6	-1.8	1.2	-3.0	-4.7	0.5	9.9	1.4	5.7	13.2	19.5
44	0.6	1.8	-5.2	-4.2	-5.7	3.3	0.1	1.3	2.6	-6.1	8.8	20.8
333	16.4	19.1	0.2	14.2	33.3	13.0	2.3	7.0	2.0	12.0	61.2	62.5

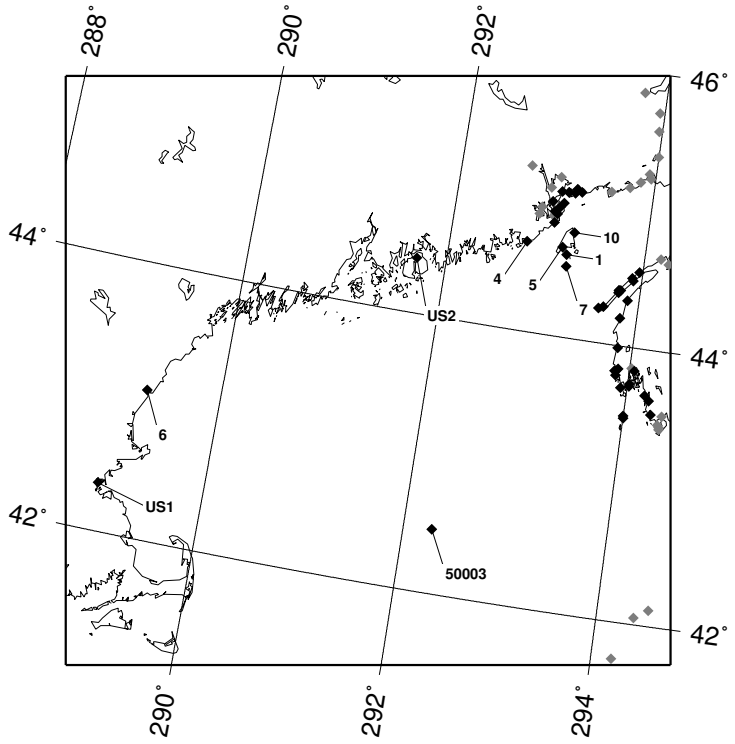

Figure 32: Gulf of Maine - Global

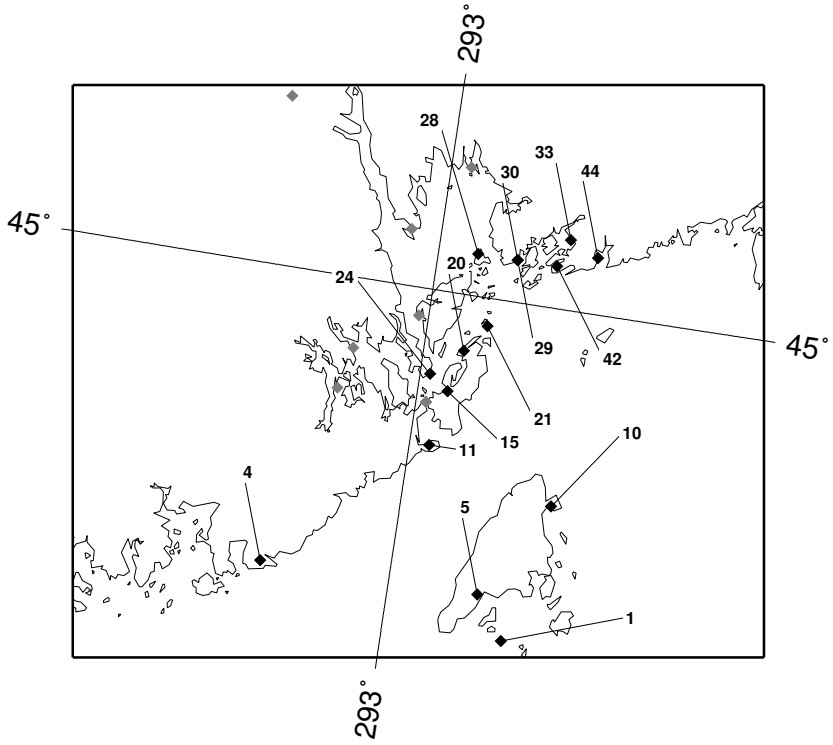

Figure 33: Gulf of Maine - Northeast

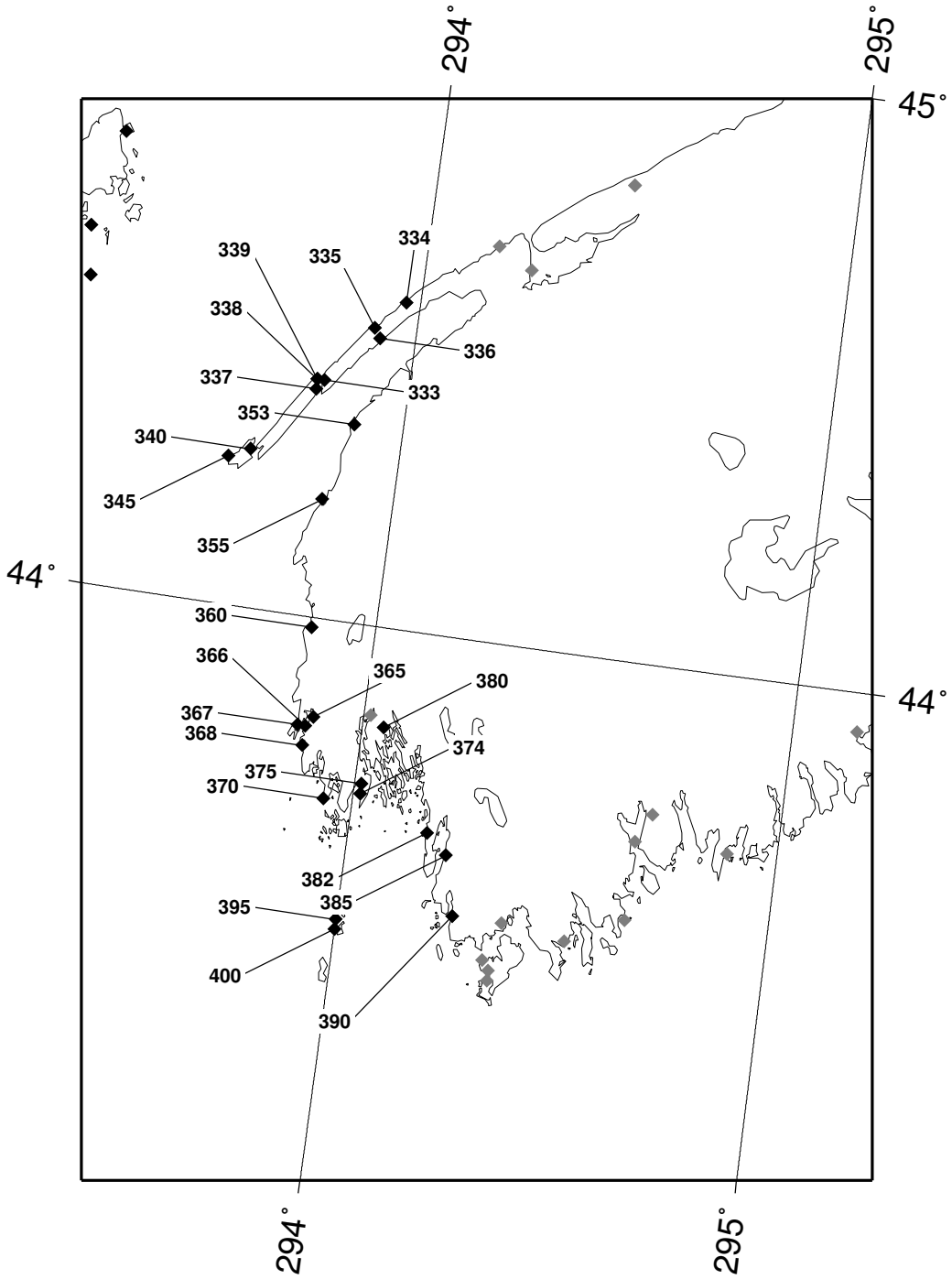

Figure 34: Gulf of Maine - East

334	-4.9	7.7	9.5	10.8	-3.6	7.7	0.4	7.0	0.5	-0.3	29.0	34.5
335	-34.4	-8.5	-15.6	-15.3	-6.8	-12.2	-0.7	0.6	0.0	-3.8	39.6	42.2
336	-6.2	3.5	-0.4	-9.0	-5.1	-1.2	0.6	2.8	0.5	3.1	12.6	20.8
337	-6.1	5.0	1.0	-4.1	-2.0	-2.6	-0.7	5.9	0.1	5.6	14.5	16.1
338	-4.6	-2.9	5.5	-13.2	-2.6	-11.1	0.7	0.6	0.4	-7.8	14.7	24.6
339	-14.8	-2.5	-6.0	-11.7	-6.1	-1.3	-0.1	7.4	0.5	-4.0	16.2	26.0
340	-1.3	1.4	1.6	-8.6	-3.2	-2.1	0.9	2.0	0.8	-1.6	7.1	16.6
345	2.2	4.7	0.1	-2.7	-1.0	-0.7	2.4	2.9	-0.2	1.2	13.2	15.5
353	1.7	1.7	-3.0	-2.5	4.3	-10.1	0.4	4.1	1.5	2.8	8.0	10.5
355	-3.2	2.5	-1.1	8.2	-2.2	-9.8	1.3	2.8	1.1	3.3	9.5	11.3
360	2.1	0.6	-0.4	5.0	-0.7	-3.3	1.5	4.8	0.7	3.0	3.8	7.4
365	-2.1	1.6	-0.5	-4.4	-0.9	-2.0	0.5	7.1	0.7	2.8	4.6	12.0
366	-7.6	3.3	2.7	-6.2	-0.7	-3.2	0.8	9.3	0.4	-5.6	9.5	17.0
367	-14.2	1.5	2.2	-6.3	-2.1	-4.2	1.1	8.3	-0.1	-5.2	11.6	19.5
368	-2.4	-4.7	-9.4	-12.5	0.8	1.3	0.6	-1.8	0.7	1.6	13.0	15.0
370	-0.8	5.5	2.2	2.1	-1.5	0.9	0.6	8.3	0.6	0.5	10.7	14.7
374	-9.0	-9.9	-2.3	-17.7	-1.2	-24.5	2.1	6.3	0.4	-9.9	21.4	22.8
375	-5.0	-8.4	-2.2	-12.5	-4.9	-11.4	1.3	-1.0	0.6	-5.3	17.0	19.0
380	-24.6	-5.6	-6.8	2.0	-7.5	-4.9	0.1	8.2	0.0	4.4	21.5	24.0
382	-3.8	-12.0	-2.9	-30.1	-8.9	-18.7	0.4	-5.8	0.7	-10.2	24.7	27.2
385	-7.3	-3.6	-1.2	-14.6	-0.6	-7.3	1.6	3.8	1.4	-5.2	10.1	11.7
390	-5.6	-5.8	-0.9	-6.1	-2.6	-10.1	0.3	5.1	-0.4	7.5	10.2	14.2
395	2.7	0.3	-2.5	-10.7	-2.8	1.4	0.8	2.2	0.6	1.4	5.0	10.1
400	-6.1	3.5	-2.6	-1.4	-0.3	1.9	0.5	7.4	0.7	7.6	7.6	8.9
50003	1.1	0.8	-1.7	-13.8	-2.8	1.6	3.6	5.9	0.7	-5.6	4.9	6.6
US1	0.1	4.6	0.3	2.4	0.8	1.6	-0.1	9.6	-0.4	5.3	8.1	11.3
US2	-3.2	2.9	1.7	-4.7	0.5	-2.4	0.3	8.1	0.5	0.6	6.9	11.5
Mean	-4.3	1.6	-1.0	-4.1	-1.6	-2.1	0.5	4.9	0.4	0.1	15.9	20.7
Abs	7.3	4.7	3.7	7.3	3.7	5.4	0.9	5.7	0.8	4.8	15.9	20.7
rms	10.1	5.9	5.8	9.2	6.1	7.4	1.2	6.4	1.0	6.3	19.1	23.2

C.8 Bay of Fundy

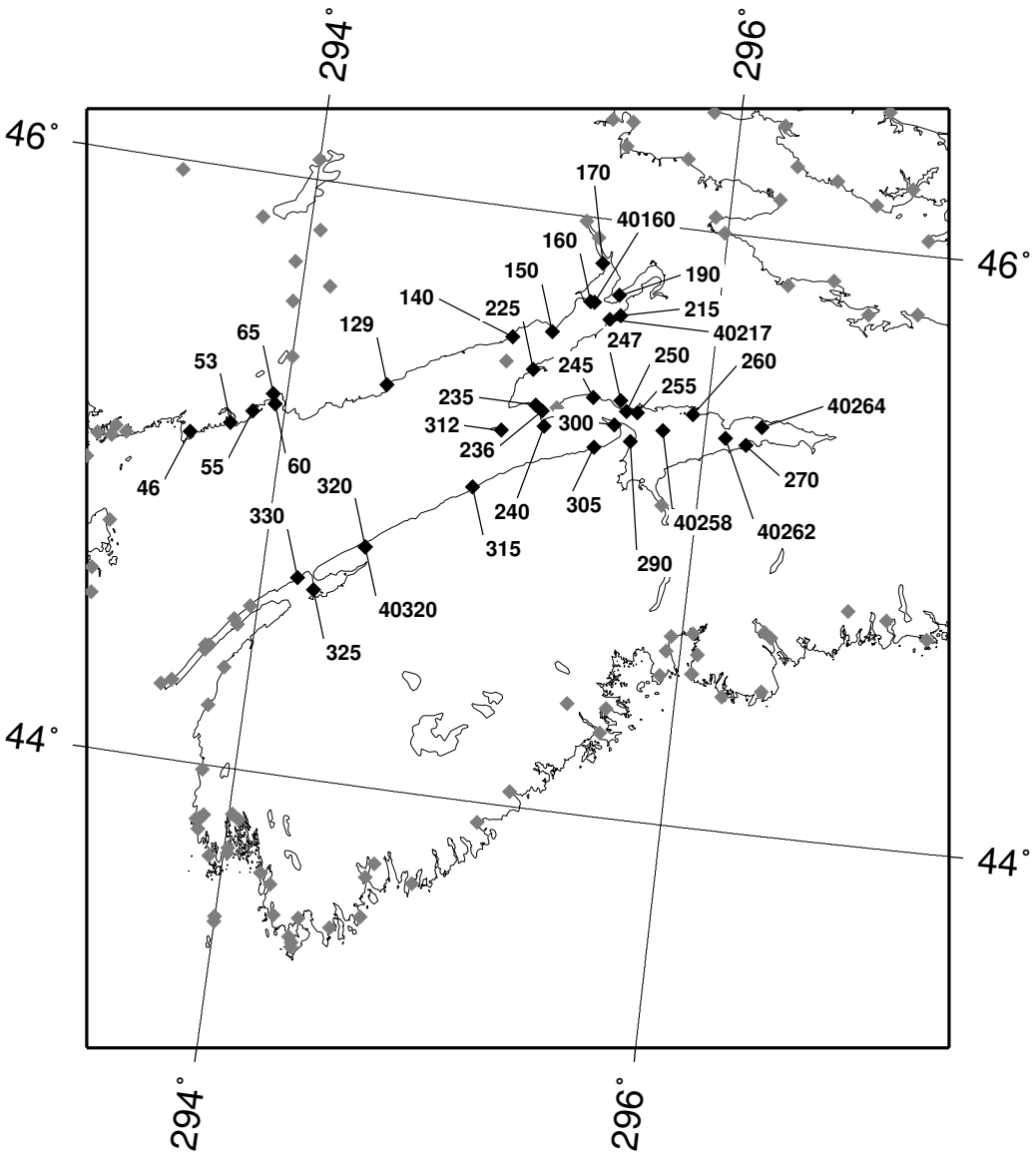

Figure 35: Bay of Fundy stations

Stat #	M2 error		N2 error		S2 error		K1 error		O1 error		time *rms*	
	cm	deg	cm	deg	cm	deg	cm	deg	cm	deg	cm	cm
46	-5.0	3.5	-0.4	-5.7	-4.4	-4.9	2.7	12.7	0.2	0.5	14.1	26.6
53	7.3	4.9	1.2	-0.7	0.7	-5.1	0.9	4.1	1.1	-10.6	19.1	21.1
55	16.6	4.0	3.2	-1.7	-7.9	-9.2	-2.0	-5.7	3.1	-14.5	21.4	24.2
60	8.5	-1.1	-2.3	-10.3	1.2	-10.1	1.1	3.4	-0.5	-0.9	12.7	15.6
65	3.3	3.9	-0.4	-4.7	-0.6	-1.5	0.3	6.7	0.5	0.9	15.8	26.3
129	8.4	4.5	16.3	-7.7	-1.9	4.4	0.6	5.9	0.7	1.5	26.3	28.2
140	-4.6	5.7	-3.1	-29.6	-10.5	2.6	6.5	8.3	-0.9	15.0	44.1	56.0
150	14.1	7.6	9.2	-11.2	5.7	1.8	2.3	4.6	1.0	-2.5	45.5	49.6
160	30.8	7.6	24.3	-10.7	-1.1	7.0	1.6	7.8	2.8	0.1	54.7	57.4
170	45.8	6.5	14.0	-8.9	4.0	5.4	1.5	8.7	2.3	4.2	53.8	58.7
190	21.7	6.4	29.1	-3.4	2.1	3.5	0.4	5.1	0.6	1.3	46.2	48.9
215	41.9	7.4	-15.1	-5.1	-4.9	2.7	-0.1	3.0	1.7	-1.7	55.0	58.8
225	3.1	6.1	-6.2	-4.7	-3.5	-2.5	2.9	5.0	-1.4	5.9	33.0	35.3
235	-1.9	0.4	3.9	-12.6	-1.8	0.3	2.0	-6.4	-1.2	-14.3	14.6	19.1
236	1.3	1.1	-1.3	-7.2	0.8	-0.3	10.6	6.2	-1.0	-13.8	12.1	20.5
240	13.0	4.3	4.7	-4.6	-3.1	-4.5	1.0	8.0	1.3	-3.2	26.5	43.6
245	-1.3	9.0	-8.4	-6.4	-9.8	3.7	1.0	4.4	4.6	10.2	54.3	55.9
247	7.5	6.7	4.5	-6.0	-10.1	-1.0	2.4	1.0	1.5	2.9	43.3	55.6
250	-10.5	13.1	-10.6	9.1	-12.0	15.9	-0.7	6.1	0.1	21.5	84.4	85.8
255	4.8	13.0	-18.4	0.4	-10.8	8.6	2.6	9.0	0.8	13.3	85.4	86.6
260	9.6	13.8	11.0	11.3	-14.6	9.5	-0.2	11.2	0.4	8.6	97.6	104.3
270	14.7	18.9	-4.3	10.4	-12.8	14.2	-2.7	17.6	-0.1	14.2	136.3	137.2
290	-10.9	12.1	-5.6	-0.7	-15.6	3.5	-0.6	15.9	-0.6	12.1	80.1	81.1
300	-17.0	-1.5	-4.0	-13.7	-15.4	-6.2	-0.3	6.5	0.0	-13.6	26.3	28.8
305	11.6	5.2	10.4	-11.8	-3.9	3.9	4.0	4.4	2.2	-2.2	35.6	38.2
312	16.7	4.1	-7.4	-13.9	-14.5	3.1	2.2	9.3	0.7	1.1	30.6	44.6
315	7.5	2.0	28.9	-10.6	-22.5	5.1	-0.0	1.6	1.6	-1.7	31.3	48.2
320	16.7	3.2	-1.8	-4.4	-3.3	-3.1	1.6	5.8	0.4	0.6	18.9	28.5
325	19.7	5.1	0.9	-0.6	1.2	1.1	0.0	8.1	0.6	4.8	24.6	31.8
330	17.0	1.9	-3.9	-5.8	1.6	-3.1	2.4	3.7	0.1	-4.6	15.4	24.2
40160	44.5	5.0	-1.2	-3.8	-4.4	4.0	0.6	5.7	1.4	0.9	44.5	61.5
40217	31.3	5.8	8.5	6.0	10.5	-7.4	-1.9	7.4	1.8	-0.2	43.4	55.7
40258	32.9	11.5	-9.9	3.2	-12.3	12.2	0.2	11.3	1.6	4.8	84.2	99.5
40262	47.5	14.3	-12.4	-3.8	-22.1	14.1	5.3	11.4	1.3	9.1	112.0	125.2
40264	57.2	17.7	-8.9	10.2	-10.9	21.1	0.8	16.7	1.3	10.3	140.8	155.4
40320	-216.1	3.3	-45.1	-3.5	-37.5	-3.9	-9.9	7.8	-7.2	2.4	164.3	164.4
Mean	8.0	6.6	-0.0	-4.5	-6.8	2.4	1.1	6.7	0.6	1.7	51.3	58.4
Abs	22.4	6.7	9.2	7.3	8.3	5.9	2.1	7.4	1.3	6.4	51.3	58.4
rms	41.5	8.2	13.2	9.1	11.2	7.5	3.2	8.3	1.9	8.6	64.2	69.8